

**SANDIA REPORT**

SAND2022-0952

Printed January 2022

Sandia  
National  
Laboratories

# Improbability of Nuclear Criticality in Compacted Criticality Control Overpacks after Room Closure by Salt Creep at Waste Isolation Pilot Plant

Rob P. Rechard, Brad A. Day, Benjamin Reedlunn, James E. Bean, Jr.

Prepared by  
Sandia National Laboratories  
Albuquerque, New Mexico  
87185 and Livermore,  
California 94550

Issued by Sandia National Laboratories, operated for the United States Department of Energy by National Technology & Engineering Solutions of Sandia, LLC.

**NOTICE:** This report was prepared as an account of work sponsored by an agency of the United States Government. Neither the United States Government, nor any agency thereof, nor any of their employees, nor any of their contractors, subcontractors, or their employees, make any warranty, express or implied, or assume any legal liability or responsibility for the accuracy, completeness, or usefulness of any information, apparatus, product, or process disclosed, or represent that its use would not infringe privately owned rights. Reference herein to any specific commercial product, process, or service by trade name, trademark, manufacturer, or otherwise, does not necessarily constitute or imply its endorsement, recommendation, or favoring by the United States Government, any agency thereof, or any of their contractors or subcontractors. The views and opinions expressed herein do not necessarily state or reflect those of the United States Government, any agency thereof, or any of their contractors.

Printed in the United States of America. This report has been reproduced directly from the best available copy.

Available to DOE and DOE contractors from

U.S. Department of Energy  
Office of Scientific and Technical Information  
P.O. Box 62  
Oak Ridge, TN 37831

Telephone: (865) 576-8401  
Facsimile: (865) 576-5728  
E-Mail: [reports@osti.gov](mailto:reports@osti.gov)  
Online ordering: <http://www.osti.gov/scitech>

Available to the public from

U.S. Department of Commerce  
National Technical Information Service  
5301 Shawnee Rd  
Alexandria, VA 22312

Telephone: (800) 553-6847  
Facsimile: (703) 605-6900  
E-Mail: [orders@ntis.gov](mailto:orders@ntis.gov)  
Online order: <https://classic.ntis.gov/help/order-methods/>



# **Improbability of Nuclear Criticality in Compacted Criticality Control Overpacks after Room Closure by Salt Creep at Waste Isolation Pilot Plant**

Rob P. Rechard

Nuclear Waste Disposal Research and Analysis Department 8842

Sandia National Laboratories,

Albuquerque, New Mexico 87185-0747

Brad A. Day

Nuclear Waste Partnership

Carlsbad, New Mexico

Benjamin Reedlunn

Materials and Failure Modeling Department 1558

Sandia National Laboratories

Albuquerque, New Mexico 87185-0840

James E. Bean, Jr.

Solid Mechanics Department 1554

Sandia National Laboratories

Albuquerque, New Mexico 87185-0840

## **ABSTRACT**

Based on the rationale presented, nuclear criticality is improbable after salt creep causes compaction of criticality control overpacks (CCOs) disposed at the Waste Isolation Pilot Plant, an operating repository in bedded salt for the disposal of transuranic (TRU) waste from atomic energy defense activities. For most TRU waste, the possibility of post-closure criticality is exceedingly small either because the salt neutronically isolates TRU waste canisters or because closure of a disposal room from salt creep does not sufficiently compact the low mass of fissile material. The criticality potential has been updated here because of the introduction of CCOs, which may dispose up to 380 fissile gram equivalent plutonium-239 in each container. The criticality potential is evaluated through high-fidelity geomechanical modeling of a disposal room filled with CCOs during two representative conditions: (1) large salt block fall, and (2) gradual salt compaction (without brine seepage and subsequent gas generation to permit maximum room closure). Geomechanical models of rock fall demonstrate three tiers of CCOs are not greatly disrupted. Geomechanical models of gradual room closure from salt creep predict irregular arrays of closely packed CCOs after 1000 years, when room closure has asymptotically approached maximum compaction. Criticality models of spheres and cylinders of 380 fissile gram equivalent of plutonium (as oxide) at the predicted irregular spacing demonstrate that an array of CCOs is not critical when surrounded by salt and magnesium oxide, provided the amount of hydrogenous material shipped in the CCO (usually water and plastics) is controlled or boron carbide (a neutron poison) is mixed with the fissile contents.

## **ACKNOWLEDGEMENTS**

The authors gratefully acknowledge the weekly guidance and review provided by Ronald Livingston, Omega Technical Services, and Paul E. Shoemaker, Sandia National Laboratories, as this report developed over 2½ years. Bret Brickner and his team from Oak Ridge National Laboratory, talked weekly with the authors to provide hundreds of thousands of criticality calculations from which the final report figures were created. Ross Kirkes, Sandia National Laboratories, provided helpful insight on evaluating and screening the post-closure criticality scenario. Finally, Sandi Larson, 21Consulting Group, provided an overall technical/programmatic review of the approach.

## EXECUTIVE SUMMARY

Salt creep causes disposal rooms to close after transuranic (TRU) radioactive waste is disposed at the Waste Isolation Pilot Plant (WIPP), an operating repository in bedded salt in southern New Mexico. The room closure beneficially encapsulates and isolates the TRU waste generated by atomic energy defense activities; however, the compaction influences the potential for criticality because spacing between containers is not maintained and containers lose structural integrity. For most TRU waste disposed at WIPP, the likelihood of post-closure criticality is negligible because remote-handled canisters are neutronically isolated by the salt and because contact-handled containers do not have sufficient fissile mass and concentration to be compacted sufficiently to form a critical array. As discussed here, the likelihood of criticality is also negligible after compacting TRU waste disposed in criticality control overpacks, provided the hydrogenous content is constrained or a neutron poison is included.

### ES.A. Criticality Control Overpack

The criticality control overpack (CCO) consists of a standard 55-gal carbon-steel drum that overpacks a criticality control container (CCC), composed of 304L stainless steel. The CCC is held in place by plywood spacers on the top and bottom. Nothing else is placed in the radial space between the CCC and CCO (e.g., no impact-absorbing fiberboard, and no polyethylene liner). Various convenience handling containers may be used inside the CCC to facilitate waste packaging operations.

The maximum fissile content for a CCO is 380 fissile gram equivalent  $^{239}\text{Pu}$ , almost double the amount of fissile mass allowed in pipe overpack containers used for the 3.2 metric tons of  $^{239}\text{Pu}$  bearing residues already disposed at WIPP.<sup>1</sup> Hence, CCOs are an efficient method for shipping surplus Pu and possibly other waste to WIPP. As demonstrated, a shipped array of CCOs maintains fissile separation during a transportation accident; thus, each CCO can be at the maximum 380 g  $^{239}\text{Pu}$  when shipped in TRUPACT-II and HalfPACT packages with a total of 5320 g  $^{239}\text{Pu}$  (two 7-packs of CCOs) and 2660 g  $^{239}\text{Pu}$  (one 7-pack of CCOs), respectively.<sup>2</sup>

### ES.B. Screening Criticality Scenario

In the *Waste Isolation Pilot Plant Land Withdrawal Act*,<sup>3</sup> Congress designates the US Environmental Protection Agency (EPA) as responsible for implementing its radioactive waste disposal standard at WIPP (in Title 40 Code of Federal Regulations Part 191—40 CFR 191). Thus, after WIPP closure, a criticality evaluation occurs within the probabilistic

regulatory framework defined in 40 CFR 191<sup>4, 5</sup> and EPA's implementing regulation 40 CFR 194.<sup>6, 7</sup> In 40 CFR §194.32, EPA provides three criteria for excluding features, events, and processes (FEP) and scenarios, such as criticality, from the WIPP assessment of performance: (1) regulatory fiat; (2) low consequence; and (3) low probability of occurring.

The approach here develops a qualitative low-probability rationale that compaction cannot sufficiently form a critical assembly of 380 fissile gram equivalent  $^{239}\text{Pu}$  emplaced within CCOs provided (a) sufficient neutron poison boron carbide (B<sub>4</sub>C) is mixed with the fissile material, or (b) a constraint is placed on the mass of hydrogenous material present (primarily water and plastics), which, in turn, depends upon the mass of non-hydrogenous filler mixed with the fissile material.

### ES.C. Compaction of CCOs

Support for a low-probability rationale in the closed WIPP repository depends upon constraints developed from two types of quantitative modeling: geomechanical phenomenological modeling<sup>8, 9</sup> and neutron transport modeling.

#### ES.C.1. Conceptual Model of CCO Compaction

For the situation here, Sandia National Laboratories conducted geomechanical modeling, using the Sierra/Solid Mechanics finite-element code system,<sup>10</sup> to establish a reasonable configuration of CCOs during two representative repository phases:<sup>11</sup> (1) early large salt block fall onto CCOs, and (2) later gradual salt compaction of a room filled with CCOs (without brine seepage and subsequent gas generation to allow maximum room closure). Rock fall in the first phase does not greatly disrupt three tiers of CCOs.

For gradual salt compaction in the second phase, the model represents a segment in disposal Room 4 (middle of a panel of 7 rooms) halfway down the 91-m room axis where the ratio of horizontal to vertical compaction is likely the greatest (ES-1). The room is modeled at both horizons (elevations) of geologic strata in the Salado Formation bedded salt (designated simply as upper and lower horizons) to consider the influence of differing arrangements of geologic strata, particularly the interspersed clay seams where slippage occurs.

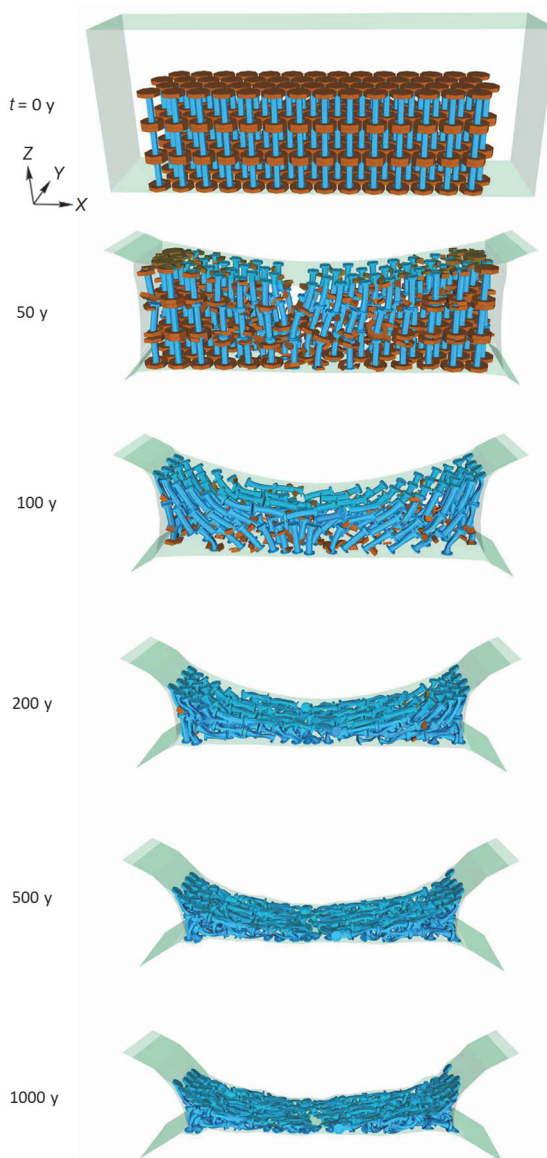


Fig. ES-1. CCO compaction in WIPP disposal room in upper salt horizon in southern portion of WIPP repository with most CCCs on their side by 200 years, where blue is flanged CCCs, and brown is top and bottom stabilizing plywood spacers; outer 55-gallon CCO drum and salt strata are present in analysis but removed in the visualization.<sup>12, Fig. 9</sup>

Although a room full of 7-packs of CCOs would initially be placed in a hexagon configuration, the 7-packs are held together with plastic wrapping that will allow CCOs to readily shift once the walls contact the emplaced containers. Hence, the salt compaction analysis includes results both where the CCOs start as a hexagonal array and where the CCOs start as a more compact triangular array.

### ES.C.2. CCO Compaction Results

The compaction simulations predict the CCO carbon-steel drum shells crumple and the plywood spacers rapidly fail shortly after the room ceiling contacts CCOs (in the room center by ~35 years and along the entire length after ~60 years) (Fig. ES-1). By 100 years, CCOs begin to topple over on their sides. By 200 years, most CCOs are on their side, which allows for substantial compaction.

Most room closure occurs by 300 years; yet, the room continues to consolidate and approaches a maximum at ~1000 years (Fig. ES-2). For CCOs, the horizontal closure at the mid-height of the disposal room at 1000 years is between 39.0% and 42.4% of the original 10.06 m width (depending on the arrangement of strata, in the two different room horizons). The vertical closure at mid-width is between 94.0% and 97.3% of the original 3.96 m height (Fig. ES-2). That is, the change in disposal room horizon (and, thereby, clay strata sequence) only causes small changes in final room closure. Furthermore, comparing results of room full of CCOs and an empty room shows that weak CCO containers (e.g., those degraded by corrosion) will only somewhat increase room closure beyond that already modeled.

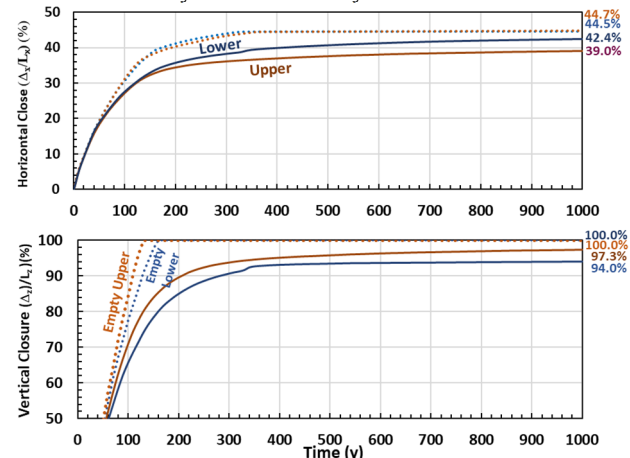
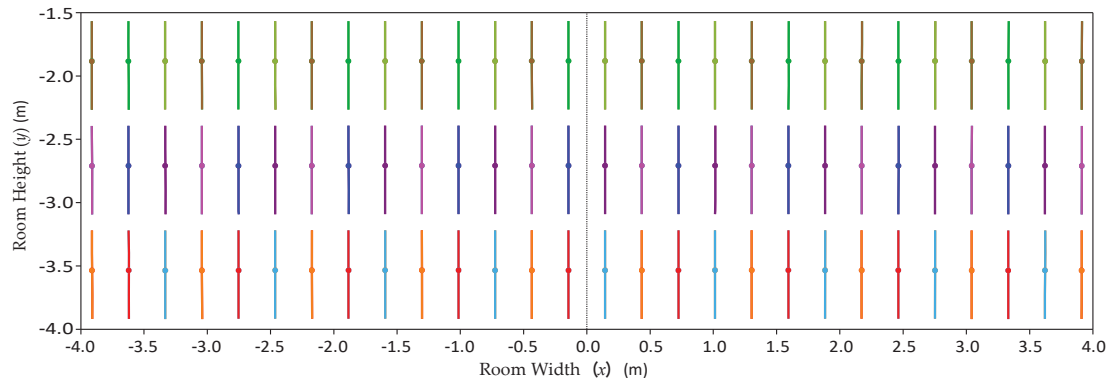
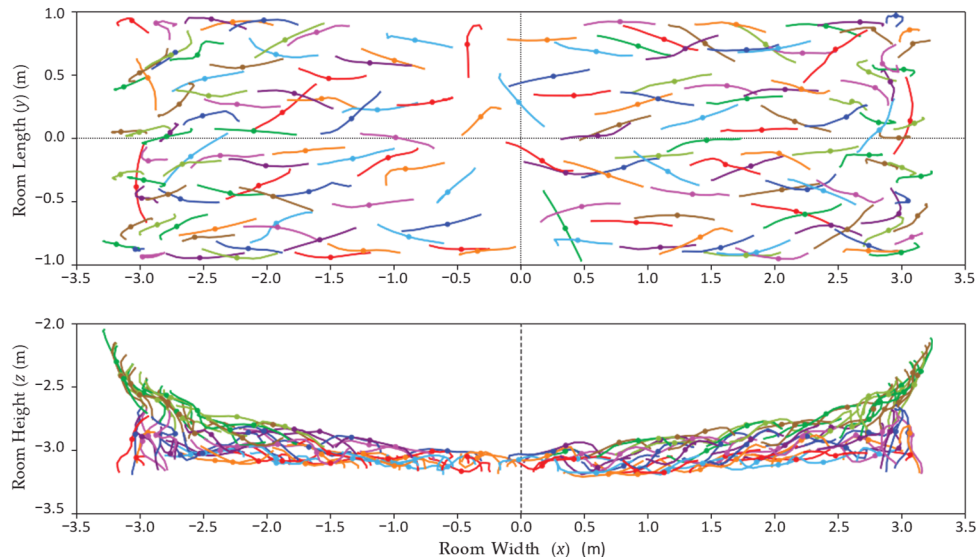


Fig. ES-2. Horizontal and vertical room closure at mid-height and mid-width, respectively, mostly complete by 300 years but continues to 1000 years for CCOs initially emplaced in triangular array in upper and lower salt horizons.<sup>12, Fig. 10</sup>

The plan and side views of CCC centerlines at 1000 years provide revealing perspectives of CCO compaction (Fig. ES-3). The greater closure at the room center displaces much of the top tier of CCCs (green, yellow-green, and brown centerlines) toward the room sides. The second tier (dark blue, burgundy, and pink) is also displaced toward the room sides but not nearly as much. The center is mostly a single layer, which consists primarily of the bottom tier of CCCs (orange, light blue and red). CCCs are not clumped or bunched together down the axis of the room in the y-direction.



(a) Side view of three tiers of CCCs in triangular array at 0 years (~1 m gap to room wall omitted on each side)



(b) Plan and side view of compacted CCCs at 1000 years (roof initially at  $z=0.0$ ; floor initially at  $z=-3.96$  m)

Fig. ES-3. Centerlines of CCCs at 0 and 1000 years located in upper repository horizon.<sup>12</sup>

In addition to room closure, another measure of CCO compaction is the number of CCOs in a specified volume (i.e., the CCO concentration—Fig. ES-4). Salt rapidly attenuates the neutron flux from CCOs and is reduced by 2 orders of magnitude in 75 cm from an ideal point source.<sup>12</sup> At 1000 years, CCO concentration in a 75 cm radius about each CCO center has a mean between 10.9 and 11.9 CCO/m<sup>3</sup> and maximum between 15.3 and 18.1 CCO/m<sup>3</sup>.

The distribution of CCO concentrations demonstrates that the geomechanical analysis has

produced a wide variety of deformed spacing between CCOs. Additional cases are also studied with (1) larger coefficient of friction for two nearby clay layers, (2) stronger CCC in CCO, and (3) similar sized pipe overpack containers. For all these variations, the distribution range and shape of CCO concentration is similar (Fig. ES-4). That is, the geomechanical analysis provides reasonably consistent behavior across a range of conditions, and thus, the 4 cases provide representative conditions of CCO compaction for criticality analysis.

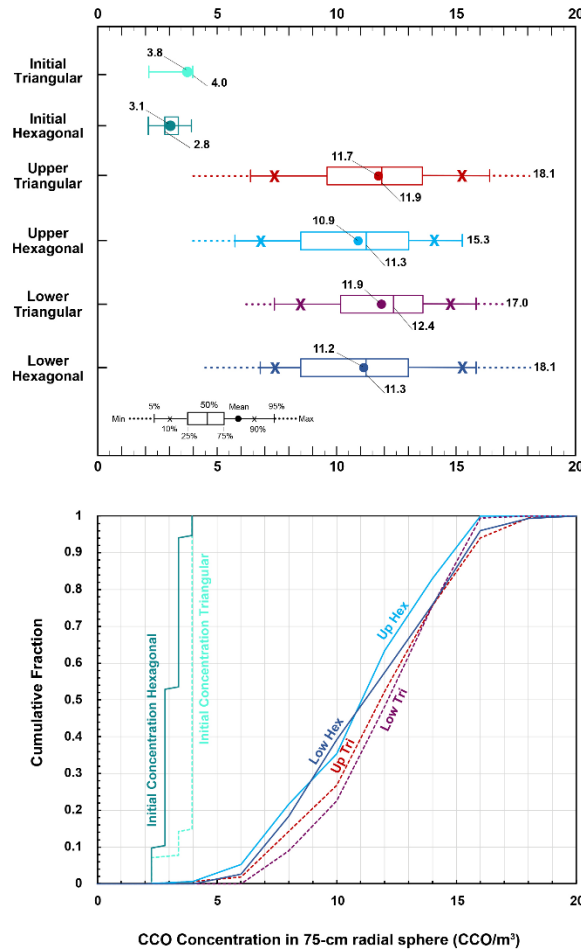


Fig. ES-4. Distributions of CCO concentration in a 75-cm radial sphere about CCO centers at 1000 y are similar when initially arranged as triangular or hexagonal arrays in upper or lower repository horizon.<sup>12</sup>, Fig. 11

## ES.D. Criticality Analysis of Compacted Arrays without Boron Carbide

Two general types of criticality analysis are performed: (1) analysis without  $B_4C$ , as described here, and (2) analysis of  $B_4C$  mixed with CCO fissile contents, described below in §ES.E.<sup>13;14</sup> For the criticality analysis, Oak Ridge National Laboratory (ORNL) uses the final compacted coordinate positions of the centers of each CCC in the SCALE neutron transport code system<sup>15</sup> to determine whether the compaction is sufficient to promote criticality, and, if so, what constraints on moderating hydrogenous material are necessary.<sup>a</sup> ORNL also conducts a criticality analysis of an idealized bounding regular, uniformly compacted array to show that the behavior of the CCO arrays do not dramatically change at extreme conditions and that observed trends are properly understood but the uniform analysis is not discussed here in this summary.

### ES.D.1. Conceptual Model without $B_4C$

The criticality analysis examines the potential for criticality with generic waste forms and, thereby, expands the usefulness of CCOs beyond surplus Pu waste. The criticality analysis models 380-g  $^{239}\text{Pu}$  spheres and cylinders (Region 1) at the calculated irregular, non-uniform spacing surrounded by salt and magnesium oxide (Region 2). Region 2 is surrounded by 10 m of salt (Region 3—Fig. ES-5). The straight room segment is about 2-m long down the room axis ( $y$ -direction) with mirror boundary conditions on the edges to represent the full WIPP room.

The CCO criticality analysis focuses on dry conditions in the disposal room during salt compaction with hydrogenous material present only within the fissile region. Previous analysis with pipe overpack containers showed that the influx of brine greatly reduces room reactivity.<sup>1;16</sup>

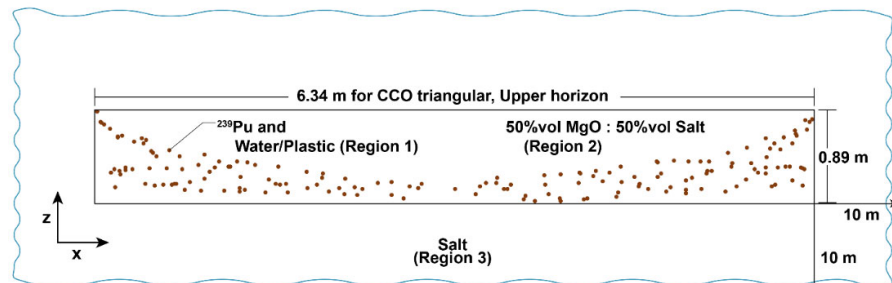


Fig. ES-5. Three material regions of criticality model in ~2-m wide room segment, where dimensions of Region 2 defined by maximum extent of CCO center coordinates, which change somewhat per simulation (Region 2 dimensions shown for CCOs in upper horizon initially in triangular array).

<sup>a</sup> Those materials that moderate the neutron energy (i.e., reduce the neutron energy to the thermal range—about 0.025 eV—through elastic and inelastic impact with material nuclei)

without a propensity to absorb the neutron themselves promote nuclear chain reactions. Material with much hydrogen, such as water or organic material, are excellent moderators.

Whether a fissile region (or assembly of fissile regions) is critical depends upon the generation and interaction of neutrons with matter within and outside the assembly, which for a finite heterogenous system, depends upon four general categories of parameters (1) type, mass, and form of fissile material (i.e., 380 g FGE  $^{239}\text{Pu}$  as  $\text{PuO}_2$ ); (2) material mixed with the fissile material and its overall concentration; (3) nearby material and its concentration outside the fissile array; and (4) shape of individual CCOs and array configuration of fissile regions and, thereby, neutron leakage. In the criticality analysis here, the parameters in the first category are fixed and parameters in the latter three categories are varied to determine relative importance.

#### ES.D.2. Results with and without Filler in Fissile Region

The modeled system remains subcritical (i.e.,  $k_{\text{eff}} \leq 1$ )<sup>b</sup> when the allowable hydrogenous moderator mass in the fissile Region 1 is  $\leq 1690$  g per CCO for the representative irregular, non-uniformly compacted array without boron carbide.

Including a non-hydrogenous filler material in the fissile Region 1 reduces the reactivity of the CCO array, whether the filler material is conservatively modeled as graphite or represented as a cement-like mixture of silicon dioxide, magnesium oxide, and aluminum oxide as ORNL evaluated previously for surplus plutonium disposition (Fig. ES-6).<sup>13</sup> In particular, adding 2000 g of graphite increases the maximum mass of allowed moderator by 11% (factor of 1.11 greater) from 1690 g to 1880 g.

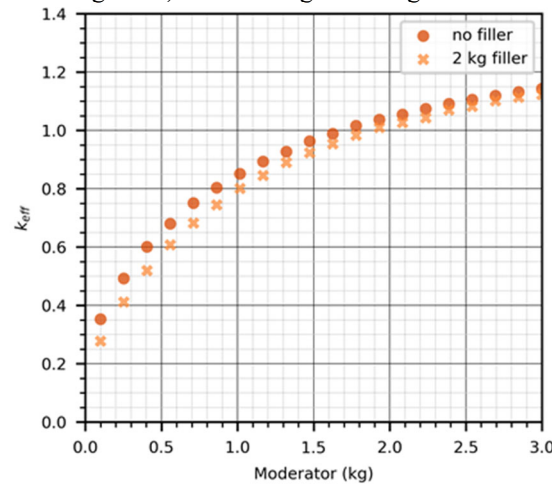


Fig. ES-6. Adding 2000-g graphite or non-hydrogenous generic filler per CCO in fissile region moderately reduces reactivity of irregular, non-uniformly compacted CCO array.

<sup>b</sup> The neutron multiplication factor ( $k_{\text{eff}}$ ) is conceptually the ratio of the number of neutrons in one generation to the

The results with a graphite filler or generic cement-like filler are similar (3.4% increase in allowable moderator mass with generic cement-like filler) because the influence of the two filler types is primarily in changing the volume of the fissile region and the corresponding change in neutron leakage from the system rather than reflecting or absorbing neutrons.

#### ES.D.3. Other Material in Fissile Region

Based on varying other parameters, additional factors are not necessary to control to ensure improbability of post-closure criticality. Specifically, including 585-g beryllium (Be) or beryllium oxide (BeO) special reflector material in the fissile region (7% more than allowed in WIPP Waste Acceptance Criteria) has little influence on reactivity ( $k_{\text{eff}}$  decreases by  $<0.01$  near  $k_{\text{eff}}$  of unity) for irregular array.<sup>14</sup>

The influence of excess MgO surrounding individual CCOs (which may act as a reflector) is small; specifically, the model includes  $\sim 3.7$  times the amount of MgO that would be necessary in the room full of CCOs, yet, the reactivity with 100% salt is only slightly less ( $k_{\text{eff}}$  decreases by 0.025).

As expected, using water as the sole moderator in the fissile region is much less reactive than polyethylene:  $k_{\text{eff}}$  is reduced by 0.125 and the allowable moderator mass increases by  $\sim 50\%$  for the irregular, non-uniformly compacted CCOs.

Finally, the introduction of brine around the fissile region reduces reactivity, as occurred when analyzing the behavior of pipe overpack containers. The presence of brine in Region 2 reduces room  $k_{\text{eff}}$  by 0.15 such that 3000 g of moderator per CCO is allowable.

#### ES.D.6. Minor Influence of CCO Configuration and Boundary Conditions

The room reactivity is only slightly influenced by the CCO configuration and boundary conditions. Specifically, the allowable moderator mass only increases 3% from 1690 g to 1740 g without filler and 3% from 2020 g to 2080 g with filler with a change from a hexagonal array with mirror boundary conditions to a triangular array with periodic boundary conditions.

#### ES.D.5. Uncertainty from Geologic Strata

As noted in §ES.B.1, the geomechanical analysis analyzes compaction of a room located in either the upper or lower horizon, each with different positions of clay layers. For CCOs emplaced in a hexagonal array in the lower horizon, the allowable moderator mass for the irregular compacted array is 1850 g/CCO.

number of neutrons present in the previous generation and indicates a system is subcritical when less than unity.

For CCOs emplaced in the upper horizon, the allowable moderator mass is 1690 g per CCO (9% decrease in moderator mass for upper horizon) (Fig. ES-7).

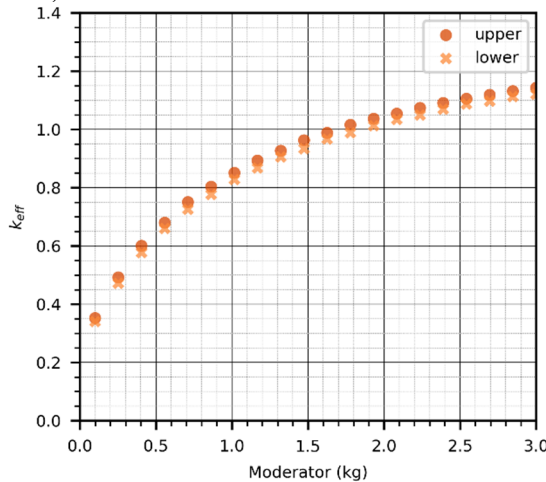


Fig. ES-7. Reactivity of final irregular array in upper horizon greater than in lower horizon of repository when CCOs emplaced as hexagonal array.

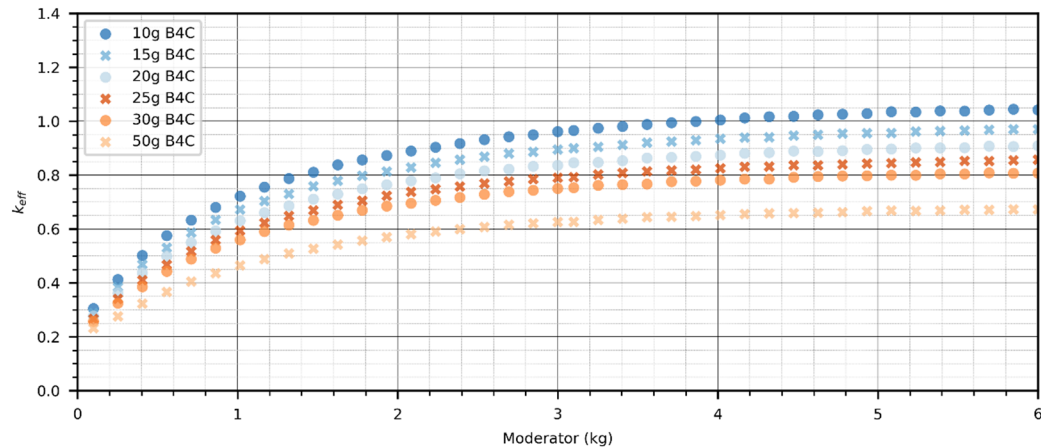


Fig. ES-8. Compacted irregular array is subcritical with 10-g B<sub>4</sub>C and moderator mass less than 3900 g for subcriticality limit of unity.

### ES.F. Supplemental Waste Acceptance Criteria for CCO Contents

EPA invoked “reasonable expectation” as the standard of proof for evaluating compliance with the Containment Requirements in 40 CFR §191.13(a). Reasonable expectation connotes a flexible standard of proof and use of central estimates or representative values when encountering unknowns that considers both positive and negative uncertainty. Consistent with reasonable expectation and the use of mean results to evaluate compliance, EPA guidance implies a mean estimate of the probability of criticality

### ES.D.4. Stainless Steel Around Fissile Region

Increasing the reflecting thickness of the stainless steel CCC has only a small influence. For the irregular array, a 0.71-cm discrete stainless-steel reflector is set around the fissile Region 1, which is the thickness of the CCC. A 1.41-cm thick discrete stainless-steel reflector, which is twice the thickness of the CCC, only slightly increases  $k_{eff}$  by 0.03 near  $k_{eff}$  of unity.

### ES.E. Criticality Analysis with Boron Carbide

A criticality analysis of compacted CCOs containing B<sub>4</sub>C neutron poison establishes the fact that 10 g of B<sub>4</sub>C mixed with the contents prevents criticality if the moderator mass is less than 3900 g per CCO (Fig. ES-8). The criticality analysis uses the previous assumptions and the same irregular array configuration, based on the salt-creep calculation, but includes B<sub>4</sub>C where natural boron is considered (19.9 wt. % <sup>10</sup>B and 80.1 wt. % <sup>11</sup>B).

provides an adequate estimate for screening a FEP such as criticality. EPA does not expect nor does the WIPP Project use worse-case scenarios that may combine numerous unrealistic combinations of imagined events to assemble fissile material.

Consequently, we use a representative dry irregular, non-uniformly compacted array and corresponding representative criticality analysis to define three options for WIPP Waste Acceptance Criteria (WAC) and screen out the criticality scenario for disposal of TRU waste. However, a subcriticality limit of 0.95 rather than 1.0 is used, to account for

additional uncertainty in CCO configuration and geology beyond the analyzed influence of clay-seam positions in the upper and lower repository horizon. With the conservative bias, the allowable moderator is 1300 g per CCO without miscellaneous, non-hydrogenous filler and is 1500 g per CCO when crediting the presence of miscellaneous filler mass that is at least 6 times the amount of FGE (Table ES-1). With the same conservative bias, the required mass of B<sub>4</sub>C is 10 g per CCO if the moderator mass is less than 2800 g.

The general conditions of the TRU waste packaged in a CCC are as follows: (1) waste shall adhere to Table 1 of WAC (e.g., less than or equal to 380 <sup>239</sup>Pu fissile gram equivalent in CCC); (2) optional 10-g B<sub>4</sub>C shall be well mixed with the fissile contents; (3) mass of hydrogenous material in a CCC shall include mass of all organic material (e.g., mass of polyethylene plastic wrap) and mass of water associated with all inorganic material (e.g., mass of adsorbed water on zeolite); and (4) only non-hydrogenous filler mass well-mixed with <sup>239</sup>Pu fissile gram equivalent shall be credited.

Acceptable knowledge includes (a) any information about the process that generated the waste, (b) any material added in the process, (c) period of waste generation, and (d) waste analysis that is available through, for example, procurement specifications and records of assembly. Acceptable knowledge may be used to determine presence of B<sub>4</sub>C, graphite/generic filler, and allowable hydrogenous material (primarily water and plastic) present in CCCs to determine compliance with requirements in Table ES-1. As a point of reference, compliance with WAC limits for many TRU waste characteristics are established via acceptable knowledge.<sup>17</sup>

Option A in Table ES-1 (placing 10 g of B<sub>4</sub>C in each CCC) may be useful for TRU waste that can be well mixed with B<sub>4</sub>C and has high plastic and water content, or contains hydroscopic salts that may theoretically increase water content.

Option B assesses only the mass of hydrogenous material in the CCO, which may be useful for TRU waste that cannot be well mixed with B<sub>4</sub>C (or miscellaneous filler material in Option C) and/or has existing limits on water and plastic content, such as planned surplus Pu disposal at WIPP.

For surplus Pu disposal, for example, the starting content of the stabilized plutonium-bearing oxide or other fissile material used as feedstock have a known moisture content based on acceptable knowledge of the process. The adulterant filler used to dilute <sup>239</sup>PuO<sub>2</sub> is either non-hygroscopic or has defined moisture based on process controls. The plastic content may be assessed through procurement and process controls on mass of plastic bags used for packaging and

contamination control. Thus, the total moderator is the sum of plastic packaging and total estimate of moisture contents. Adherence to process controls (i.e., verification of packaging configuration) could be verified by routine radiography, if required.

Option C assesses both the mass of non-hydrogenous, well-mixed filler and mass of hydrogenous material in the CCC. Option C may be useful for waste forms with defined amounts of miscellaneous filler that could benefit from the marginal increase in allowable moderator.

Table ES-1. Supplemental WIPP Waste Acceptance Criteria for a CCO

Option <sup>(1)</sup>	Boron Carbide (B <sub>4</sub> C) <sup>(2)</sup> (g)	Hydrogenous Content <sup>(3)</sup> (g)	Miscellaneous Filler <sup>(4)</sup> (g)
A	≥10	≤2800	—
B	—	≤1300	—
C	—	≤1500	≥6×FGE

- (1) Waste packaged in each CCO shall adhere to limits in Table 1 of WIPP Waste Acceptance Criteria in addition to limits specified under Options A, B, or C.
- (2) The B<sub>4</sub>C shall be well mixed with the <sup>239</sup>Pu fissile gram equivalent (FGE) and remain so during transportation, storage, and handling operations. The B<sub>4</sub>C mass is based on the natural abundance of <sup>10</sup>B (i.e., 19.9 wt. % <sup>10</sup>B). The B<sub>4</sub>C mass requirement shall apply to (a) each CCC that contains directly loaded TRU waste with <sup>239</sup>Pu FGE, or (b) any convenience containers used to load a CCC that contain <sup>239</sup>Pu FGE. For example, if a CCC is directly loaded with TRU waste containing <sup>239</sup>Pu FGE and also loaded with two convenience containers containing <sup>239</sup>Pu FGE, the directly-loaded TRU waste in the CCC and each convenience container in the CCC shall include at least 10-g of well mixed B<sub>4</sub>C.
- (3) Mass of hydrogenous content shall include mass of any organic material (e.g., mass of plastic, cellulose, foam) and mass of water associated with any inorganic material (e.g., mass of adsorbed water on zeolite, water of hydration in concrete and clay, or water in hydrate such as hydrated metal ion).
- (4) Only the non-hydrogenous portion of miscellaneous filler mass well mixed with <sup>239</sup>Pu fissile gram equivalent (FGE) shall meet the miscellaneous filler mass requirement. The miscellaneous filler shall remain well mixed with <sup>239</sup>Pu FGE during transportation, storage, and handling operations. If several convenience containers are used to load a CCC, then each convenience container shall independently meet the miscellaneous filler criteria. For example, if a CCC is loaded with two convenience containers, where the first contains 100 <sup>239</sup>Pu FGE and the second contains 280 <sup>239</sup>Pu FGE, at least 600 g and 1680 g of miscellaneous filler shall be present within each respective convenience container.



## CONTENTS

Executive Summary.....	5
Figures .....	15
Tables .....	16
Acronyms and Initialisms.....	17
I. Introduction .....	19
I.A. Criticality Control Overpack .....	19
I.B. Approach for Screening Post-Closure Criticality in CCOs .....	19
II. Screening Criticality Scenario .....	20
II.A. Low Probability Criteria for Screening.....	20
II.B. Studies of Post-Closure Criticality Applicable to WIPP .....	21
III. Modeling of Rock Fall.....	23
III.A. Conceptual Model of Rock Fall.....	23
III.B. Rock Fall Results.....	23
IV. Modeling of Room Closure From Salt Creep.....	23
IV.A. Conceptual Model of Room Closure.....	23
IV.A.1. Salt Stratigraphy .....	25
IV.A.2. CCO Configuration.....	25
IV.B. Deformed Irregular Array.....	26
IV.C. Room Closure Measure .....	29
IV.C.1. Room Closure at 1000 years .....	29
IV.C.2. Room Closure in Previous CCO and POC Simulations.....	30
IV.C.3. Closure of Room Filled with Mix of CCOs and other Containers .....	31
IV.D. CCO Concentration Measure .....	32
IV.D.1. Concentration of CCOs at 1000 years .....	32
IV.D.2. Relative Weighted Concentration.....	32
IV.D.3. Concentration at 1000 years for Containers with Different Strengths .....	33
IV.E. Room Closure and CCO Concentration Stability .....	35
V. Criticality Analysis of Compacted Arrays Without Boron Carbide.....	35
V.A. Computational Tool.....	35
V.B. Upper Subcriticality Limit in Nuclear Criticality Modeling.....	35
V.C. Conceptual Model for Criticality .....	36
V.C.1 Plutonium, Waste Form, Volume, and Mass.....	36
V.C.2. Material Mixed with Pu Waste.....	37
V.C.3. Material Surrounding Individual CCCs.....	37
V.C.4. Geometry: Irregular CCO Array Configuration .....	38
V.C.5. Geometry: Idealized Uniform Array .....	38
V.C.6. Geometry: Fissile Shape.....	39
V.D. Room Reactivity with and without Filler Material in Fissile Region .....	39
V.D.1. Generic and Carbon Filler.....	39
V.D.4. Influence of Spherical and Cylindrical Fissile Region on Reactivity.....	41
VI. Influence of other Parameters on Room Reactivity without B <sub>4</sub> C .....	44
VI.A. Room Reactivity with Material in Fissile Region .....	44
VI.A.1. Water and Polyethylene Moderator .....	44
VI.A.2. Density and Salt/MgO Proportion .....	44
VI.A.3. Beryllium Influence .....	45
VI.B. CCC Stainless Steel Around Fissile Region .....	45
VI.C. Uncertainty from Geologic Strata Arrangement.....	47
VI.D. Minor Reactivity Differences between Hexagonal and Triangular Arrays .....	47
VI.E. Reduced Reactivity when Brine Enters Room.....	48
VI.F. Reactivity as Room Creeps Closed.....	48
VI.G. Correlation of CCO Concentration with Neutron Flux .....	49

VII. Criticality Analysis of Compacted Arrays with Boron Carbide.....	52
VII.A. Similar Conceptual Model of CCO Compaction with B <sub>4</sub> C.....	52
VII.B. Results with B <sub>4</sub> C .....	52
VII.C. Longevity of B <sub>4</sub> C in Disposal Room.....	53
VII.C.1 Insolubility of B <sub>4</sub> C .....	53
VII.C.2. B <sub>4</sub> C Consumption in Radiation Field .....	53
VIII. WIPP Waste Acceptance Criteria .....	53
VIII.A. Approximation of Mean Probability of Criticality .....	53
VIII.B. Supplemental WAC Limits for CCOs .....	54
VIII.C. Use of Acceptable Knowledge.....	55
IX. Rationale of Low-Probability of Criticality in CCO at WIPP .....	56
IX.A. Rock Fall in Room Filled with CCOs .....	56
IX.B. Compaction of CCOs from Salt Creep .....	56
IX.C. Criticality Analysis of Compacted Arrays without Boron Carbide .....	57
IX.C.1. Allowable Hydrogenous Moderator with and without Filler in Fissile Region .....	57
IX.C.2. Other Material in Fissile Region .....	57
IX.C.3. CCC Stainless Steel Around Fissile Region .....	57
IX.C.4 Uncertainty from Geologic Strata .....	58
IX.C.5. Minor Influence of Initial CCO Configuration and Boundary Conditions .....	58
IX.C.6. Reduced Reactivity from Brine around Fissile Region .....	58
IX.D. Criticality Analysis of Compacted Arrays with Boron Carbide .....	58
IX.E. Uniform Array Analysis Provides Additional Understanding .....	58
References .....	61
Distribution.....	65

## FIGURES

1. Criticality control container (CCC), and criticality control overpack (CCO); various handling canisters may be used inside the CCC; two convenience containers proposed for surplus Pu (dimensions in cm).<sup>8, App. C; 22, Figs. 2-7,2-8&Table 2-1; 23,pp. 8,30</sup> .....19
2. Conceptual model of large trapezoidal-shaped salt block that detaches at Clay G seam and falls onto CCOs...23
3. Roof fall onto CCOs emplaced in a hexagonal array in the lower repository horizon (a) mostly flat roof fall; (b) rotating roof fall. Brown discs represent the top and bottom plywood stabilizer for the blue stainless steel CCCs inside the 55-gallon CCO shell (which is hidden for visualization).<sup>9, Fig. 5</sup> .....24
4. Idealized stratigraphy near WIPP disposal rooms in the lower and upper horizon. Elevations are referenced to Clay G , which is at elevation 386 m, 652 m below surface at exploratory well ERDA-9.<sup>12, Fig. 1; 64</sup> .....25
5. Emplacement of CCOs in WIPP disposal room (a) ideal hexagon array with 51 whole and 12 half CCOs in a tier or 171 total CCOs in 2.15-m room segment of 3 tiers ( $3.52 \text{ kg }^{239}\text{Pu}/\text{m}^2$ ); modeled hexagonal array with 12 half CCOs in a tier deleted for a total of 153 CCOs in 3 tiers ( $3.15 \text{ kg }^{239}\text{Pu}/\text{m}^2$ ); and (c) modeled triangular array of 56 whole CCOs in a tier or 168 total CCOs in a 2.08-m room segment ( $3.57 \text{ kg }^{239}\text{Pu}/\text{m}^2$ ).<sup>12, Figs. 4&6</sup> ..26
6. Salt compaction in room segment with CCOs emplaced in triangular array; most inner CCCs are on their side by 200 years; the outer CCO drums and bedded salt stratigraphy are included in the analysis but removed in the visualization; the brown elements represent the plywood stabilizing the CCC, which are deleted when splintered and failed.<sup>9, Fig. 9</sup> .....27
7. Deformed centerlines of CCCs at 1000 years when initially emplaced as triangular array. .....28
8. Plan and side view of deformed coordinated positions of CCC centers in upper horizon (orange circles) used in criticality analysis relative to undeformed coordinate positions (blue squares) as triangular array in 10.06 m wide, 3.96 m tall, and 2.08 m thick room segment. .....29
9. Horizontal and vertical closure at room mid-height and mid-width, respectively, for CCOs initially emplaced as triangular and hexagonal arrays in upper and lower repository horizons.<sup>9, Fig. 7; 12, Fig. 10; 62</sup> .....30
10. CCO compaction in hexagonal array in upper horizon has more column buckling when friction coefficient set at 0.5 for Clay F and Clay G layers.<sup>12, Fig. 21</sup> .....30
11. Horizontal and vertical closure of upper and lower horizon rooms filled with CCOs and POCs initially emplaced in triangular and hexagonal arrays from previous analysis, where room closure for current analysis and empty rooms in Fig. 9 shown in gray.<sup>12, Fig. 18</sup> .....31
12. Distribution of CCO concentration about each CCC center at 1000 years. .....32
13. Weighting in sphere of influence for uniformly weighted (simple) and relative-weighted concentration<sup>12, Fig. 8</sup> 33
14. Change in distribution of container concentration at 1000 years with change in clay friction coefficient, change in CCC stainless-steel strength, and change in POC container; unlabeled curves same as Fig. 12.<sup>12, Fig. 19</sup> .....34
15. Three material regions of criticality model where dimensions of Region 2 defined by maximum extent of the coordinates for CCC centers, which change somewhat per simulation (Region 2 dimensions shown for CCOs in upper horizon initially as triangular array).....38
16. Room closure of uniform array of CCOs.<sup>12</sup> .....38
17. Range of horizontal room closure in modeled irregular and idealized uniformly compacted CCO arrays initially emplaced as triangular and hexagonal arrays in upper and lower repository horizons.<sup>12, Fig. 10</sup> .....39
18. Adding 2 kg graphite or non-hydrogenous generic filler to fissile region moderately reduces reactivity of irregular, non-uniformly compacted CCO array; similar trend observed for more reactive regular, uniformly compacted CCO array.....40
19. Adding 4 kg graphite and generic/cement-like filler have similar influence on maximum reactivity and allowable moderator for irregular, non-uniformly compacted and regular, uniformly compacted CCO arrays. V.D.2. Metallic Filler .....41
20. Stainless steel material from handling canisters in fissile region substantially reduces reactivity of uniform array and moderately reduces reactivity of irregular CCO array.V.D.3. Mixing of Pu, Moderator, and Filler ..41
21. Cylindrical representation most reactive if fissile region constrained by 7.7 cm radius of CCC in both irregular, non-uniformly compacted and regular, uniformly compacted CCO array.....42
22. Unconstrained spherical fissile region slightly more reactive than cylindrical fissile region for irregular, non-uniformly compacted CCO array. .....42
23. Cylindrical representation of fissile region for 50% and 25% uniformly compacted array remains more reactive than unconstrained sphere. .....43

24. Largest reactivity of irregular, non-uniformly compacted CCO array with cylindrical fissile region changes from smallest radius at low moderation to largest radius at high moderation; behavior is similar for uniformly compacted CCO array but the transition to the largest radius occurs at lower moderation.....	43
25. CCO array with water moderator less reactive than polyethylene moderator for irregular array; the uniform array follows a similar trend. ....	44
26. Influence of MgO in Region 2 on system reactivity is small. <sup>14, App. L</sup> .....	45
27. Adding 0.585 kg Be/BeO has little influence on reactivity for $k_{eff}$ near unity but does slightly reduce reactivity below and above $k_{eff}$ of unity.....	45
28. Stainless-steel reflector, twice thickness of CCC, slightly changes the reactivity of irregular and uniformly compacted CCO arrays. ....	46
29. Reactivity of irregular CCO array in upper horizon greater than in lower horizon of repository when initially emplaced in hexagonal array.....	47
30. Reactivity of irregular compacted array initially emplaced in a hexagonal configuration is similar to an irregular compacted array initially emplaced in a triangular configuration. ....	48
31. Presence of brine in Region 2 greatly reduces room reactivity filled with CCOs.....	48
32. General monotonic increase of reactivity as room creeps closed in upper repository horizon filled with CCOs using polyethylene CCC, 100% polyethylene moderator, and without any filler or beryllium. ....	49
33. Plan and side view of the spatial distribution of simple concentration at 1000 years for CCOs emplaced in a hexagonal array in the lower repository horizon; maximum neutron flux overlays maximum simple concentration.....	50
34. Plan and side view of the spatial distribution of relative weighted concentration at 1000 years for CCOs emplaced in a hexagonal array in the lower repository horizon; maximum neutron flux overlays maximum relative weighted concentration. <sup>12, Fig. 27</sup> .....	50
35. Plan and side view of the spatial distribution of simple concentration at 1000 years for CCOs emplaced in a hexagonal array in the upper repository horizon; maximum neutron flux at edge of region with highest simple concentration.....	51
36. Plan and side view of the spatial distribution of relative weighted concentration at 1000 years for CCOs emplaced in a hexagonal array in the upper repository horizon; maximum neutron flux at edge of region with high relative weighted concentration. <sup>12, Fig. 29</sup> .....	51
37. Reactivity of irregular array with between 10 g and 50 g B <sub>4</sub> C and up to 6 kg moderator.....	52

## TABLES

I. Studies of Post-Closure Criticality at WIPP and Related Events .....	22
II. Allowable Moderator Mass per CCO with Non-Hydrogenous Filler and Metal Mixed in Fissile Region with Subcriticality Limit of Unity.....	40
III. Supplemental WIPP Waste Acceptance Criteria for a CCO .....	54
IV. Low Probability of Criticality Caused by Salt Creep Compacting CCOs in WIPP Repository.....	59

## ACRONYMS AND INITIALISMS

ANS	American Nuclear Society
ANSI	American National Standards Institute
CCA	Compliance Certification Application
CCC	criticality control container (inside CCO)
CCDF	complementary cumulative distribution function (measure for evaluating WIPP compliance)
CCO	criticality control overpack container
CFR	US Code of Federal Regulations
CH	contact-handled (transuranic waste)
CRA	Compliance Recertification Application
DOE	US Department of Energy
EIS	Environmental Impact Statement to satisfy requirements in Nuclear Waste Policy Act of 1969
EPA	US Environmental Protection Agency
FEP	feature, event, process
FGE	fissile gram equivalent
HalfPACT	half transuranic package transporter
NNSA	DOE National Nuclear Security Administration
NRC	US Nuclear Regulatory Commission
ORNL	Oak Ridge National Laboratory
PA	performance assessment (for evaluating compliance with EPA post-closure standards)
POC	pipe overpack container
RH	remote-handled (transuranic waste)
SCALE	standardized computer analysis for licensing evaluation neutron transport code system
SPD	surplus plutonium disposition
SRS	Savannah River Site in South Carolina
TRU	transuranic (radioactive waste)
TRUPACT-II	transuranic package transporter model 2
USL	upper subcriticality limit
WAC	waste acceptance criteria (for WIPP)
WIPP	Waste Isolation Pilot Plant (repository in southeastern New Mexico)



## I. INTRODUCTION

To certify the compliance of a geologic repository for disposing of radioactive waste, the US Environmental Protection Agency (EPA) requires estimates of the range of future behavior through models that capture essential features, events, and processes (FEPs) of the disposal system as it naturally evolves after closure. One potential FEP is the possibility of sufficient fissile mass and concentration causing a self-sustained neutron chain reaction (hereafter, succinctly referred to as criticality). Concern about criticality in waste disposed at the Waste Isolation Pilot Plant (WIPP), an operating repository in bedded salt for disposal of wastes containing transuranic (TRU) radioisotopes from atomic energy defense activities, is generally negligible because of (1) the low initial concentration and mass of fissile material (mostly plutonium) in contact-handled containers (e.g., 325 FGE  $^{239}\text{Pu}$  in each bundle of seven (7-pack) of standard drums trucked to WIPP), (2) the neutronic isolation of remote-handled containers by salt, and (3) the natural tendency of fissile solute to disperse after release from degraded containers.<sup>18, 19</sup>

However, waste destined for WIPP has expanded to include surplus plutonium disposition (SPD). Specifically, the US Department of Energy (DOE) decided (in 2010 SPD Supplemental Environmental Impact Statement—EIS—and 2016 Record of Decision) to dispose 6 metric tons of surplus non-pit plutonium waste at WIPP,<sup>20</sup> and 6 metric tons was added to the WIPP inventory for the 2019 Compliance Re-certification Application for WIPP (CRA-2019). DOE has also proposed to dispose an additional 34 metric tons of surplus Pu waste at WIPP.<sup>21</sup> Hence, a renewed evaluation has been undertaken of the likelihood of assembling critical arrays of TRU waste disposed at WIPP to support DOE management of surplus plutonium.

The surplus Pu waste destined for WIPP will be shipped and disposed in criticality control overpacks (CCOs). Thus, the analysis here directly supports development of supplemental criteria for CCOs in the WIPP Waste Acceptance Criteria. The analysis also demonstrates WIPP compliance with EPA Standards and will support the WIPP Compliance Re-certification Application to EPA in 2024, which will include planned increases in the surplus plutonium planned for disposal at WIPP.

### I.A. Criticality Control Overpack

The CCO consists of a standard 55-gal carbon-steel drum shell that overpacks a criticality control container (CCC), composed of 304L stainless steel (Fig. 1). The CCC, with a flange on the top and bottom, is held in place by plywood spacers on the top and bottom. Nothing is placed in the space between the CCC and

CCO (i.e., no impact absorbing fiberboard, and no polyethylene liner).<sup>1, Fig. 6</sup> Various handling canisters (typically called convenience cans within the DOE complex) may be used inside the CCC to facilitate loading of the TRU waste.

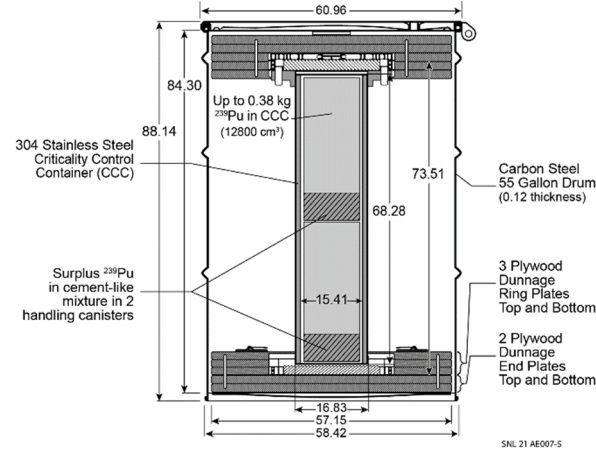


Fig. 1. Criticality control container (CCC), and criticality control overpack (CCO); various handling canisters may be used inside the CCC; two convenience containers proposed for surplus Pu (dimensions in cm).<sup>8, App. C; 22, Figs. 2-7,2-8&Table 2-1; 23,pp. 8,30</sup>

The maximum fissile content for a CCO is 380  $^{239}\text{Pu}$  fissile gram equivalent (FGE) (Table V), almost double the amount of fissile mass allowed in pipe overpack containers (POCs) previously used to ship 3.2 metric tons of Pu residues and scraps already disposed at WIPP.<sup>1</sup> Hence, CCOs provide a significant cost advantage for shipping surplus Pu and improved space utilization for disposal.

A CCO can maintain fissile separation during a transportation accident; thus, each CCO in the TRUPACT-II and HalfPACT shipping containers can be at the maximum 380 FGE  $^{239}\text{Pu}$  (i.e., 2660 FGE  $^{239}\text{Pu}$  in each 7-pack of CCOs).<sup>2</sup> To account for measurement uncertainty, however, DOE plans to use a nominal loading of 330 FGE per CCO. Thus, about 121 000 CCOs would be used to ship 6.0 metric tons of the non-pit Pu currently part of the WIPP inventory and the additional proposed 34 metric tons. In comparison, 176 200 containers have already been shipped and emplaced in 7 Panels at WIPP.<sup>1, Table V</sup>

### I.B. Approach for Screening Post-Closure Criticality in CCOs

To support the screening out of post-closure criticality in CCOs, two types of criticality analysis are performed: (1) criticality analysis with B<sub>4</sub>C mixed with CCO fissile contents, and (2) criticality analysis without B<sub>4</sub>C but with several options for managing moderator mass in CCO contents. The analysis without B<sub>4</sub>C examines the potential for criticality in CCOs disposing

TRU wastes defined by (1) mass limits on hydrogenous material (primarily water and plastics) and miscellaneous filler material, and (2) general conditions of transport (e.g., 380 fissile gram equivalent Pu compacted waste). The materials mixed with the Pu are varied over a wide range, and the findings are translated into constraints for the 2022 WIPP Waste Acceptance Criteria (WAC) document.

A manufactured waste form, such as surplus Pu readily defines the conditions for criticality analysis. However, an unspecified, generic waste form is evaluated here to support authorizing use of CCOs for a broader range of contents.

The criticality analysis follows the methodology used for evaluating the improbability of criticality in POCs for CRA-2019.<sup>1</sup> To elaborate, support for a low-probability rationale in the closed WIPP repository depends upon constraints developed from two types of quantitative modeling: geophysical phenomenological modeling and neutron/photon transport modeling. For the evaluation, Sandia National Laboratories (Sandia) has conducted geomechanical modeling, using the Sierra/Solid Mechanics finite-element code system,<sup>10</sup> to predict coordinate positions of CCOs after compaction from salt creep closure of the disposal room.<sup>11</sup>

In turn, Oak Ridge National Laboratory (ORNL) has conducted criticality modeling using the SCALE (Standardized Computer Analysis for Licensing Evaluation) neutron transport code system.<sup>15</sup> The final coordinate positions of each CCO in the compacted irregular array (or an bounding regular uniformly compacted array) are used to determine whether CCO compaction is sufficient to promote criticality, and, if so, what constraints on moderating hydrogenous material are necessary, including constraints coupled with the presence of filler materials or B<sub>4</sub>C neutron poison.<sup>14</sup>

The WIPP Project uses administrative controls for (a) the safe movement of TRU waste within the WIPP facility, (b) positioning of TRU waste containers in the disposal room, (c) placement of the magnesium oxide (MgO) engineered barrier above the waste containers, and (d) recording the emplacement location of TRU containers for auditing and potential retrieval. The administrative controls on positioning TRU packages relate to the stability of waste packages types when stacked on top of each other to promote operation safety. For example, 4-packs of 85-gallon drums can only be stacked on top of each other or placed on the top tier of other container stacks).<sup>24</sup> Also, 3-pack 100-gallon drums containing super-compacted waste cannot be placed next to each other, and 3-pack shielded containers containing RH-TRU must be placed near a room wall.<sup>1, Fig. 9</sup>

The proximity of other types of packages to each other is not specified. Thus, any number of CCOs can be placed next to each other in a disposal room. Placing administrative controls on CCO proximity could

complicate CCO disposal if a large campaign of CCOs must be stored while waiting for other waste streams to mix within a room. Hence, the geomechanical analysis and subsequent criticality analysis evaluates the possibility of a room filled entirely with CCOs.

## II. SCREENING CRITICALITY SCENARIO

Steps taken to ensure the impossibility of critical event during transport, such as required spacing between fissile material as controlled by TRU waste containers, do not necessarily remain applicable after repository closure when room closure from salt creep compacts containers tightly together. Rather, screening the post-closure criticality scenario introduces additional constraints.

### II.A. Low Probability Criteria for Screening

A post-closure criticality scenario evaluation occurs within the probabilistic regulatory framework for radioactive waste disposal defined by EPA.<sup>4,5</sup>

In the *Nuclear Waste Policy Act of 1982*,<sup>25</sup> §121 Congress designated EPA as responsible for setting standards for nuclear waste disposal. In response, EPA promulgated radiation protection standards for spent nuclear fuel, high-level waste, and TRU waste disposal in 1985 under Title 40 Code of Federal Regulations part 191 (40 CFR 191).<sup>7,26</sup> In 1993, EPA revised 40 CFR 191, in response to court remand.<sup>5</sup> In 40 CFR 191, EPA defines the process of assessing whether the WIPP radioactive waste disposal system meets its regulatory performance criteria as a performance assessment (PA). Specifically,<sup>26, §191.12 (q)</sup>

“Performance assessment” means an analysis that: (1) Identifies the processes and events that might affect the disposal; (2) examines the effects of these processes and events on the performance of the disposal system; and (3) estimates the cumulative releases of radionuclides, considering the associated uncertainties, caused by all significant processes and events.

To elaborate, a PA answers three basic questions:<sup>27</sup> What features, events, and processes (FEPs) and scenarios formed from these FEPs may occur in the disposal system? What is the probability of each FEP or scenario? What are the consequences in terms of the performance criteria of each FEP or scenario? The formal selection and screening of FEPs and scenarios for inclusion in modeling is an important step in PA and one aspect that sets PA apart from typical scientific modeling or engineering analysis.

In the *Waste Isolation Pilot Plant Land Withdrawal Act*,<sup>3</sup> Congress designates EPA as responsible for implementing its 40 CFR 191 standard at WIPP. In response, EPA promulgated implementing regulation 40 CFR 194.<sup>6,7</sup> In 40 CFR part 191 and 40 CFR §194.32, EPA set the guiding philosophy for FEP selection and

provides three criteria for excluding FEPs and scenarios, such as criticality, from the performance assessment: (1) regulatory fiat; (2) low consequence; and (3) low probability of occurring.

The approach here develops a low-probability rationale to exclude criticality in the closed, underground facility based on arguments that compaction cannot sufficiently concentrate fissile  $^{239}\text{Pu}$ .<sup>c</sup> Regarding the probability criterion, EPA explicitly states "...performance assessments need not consider categories of events or processes that are estimated to have less than one chance in 10,000 of occurring over 10,000 years." Yet, direct estimation of a numerical probability (e.g., based on past frequency data) is not required; EPA also accepts reasoned qualitative discussion that argues against the likelihood of a FEP, as done here.

## II.B. Studies of Post-Closure Criticality Applicable to WIPP

Like other nuclear facilities, the possibility of criticality has been considered since inception of WIPP. In preparation for the first EIS of the WIPP facility in 1976, FEPs, which had not been eliminated through WIPP site selection, were listed (Table I).<sup>7</sup> The list included post-closure criticality,<sup>30;31</sup> but it was dismissed in supporting documentation.<sup>32</sup> When the option to place high-level waste and spent nuclear fuel at WIPP was blocked by Congress in 1979, concern for criticality greatly diminished because of the low initial concentrations in typical TRU waste. Nevertheless, FEP screening efforts retained criticality for more thorough investigation in 1989, 1992, and 1996.<sup>33-35</sup> The criticality scenario was formally evaluated and screened out for the compliance certification application to EPA in 1996 (CCA-1996).<sup>18;36</sup> The emphasis was on the geochemical deposition outside disposal region but compaction of standard drums inside the disposal region was considered (Table I).

In 2007, DOE began construction of a mixed oxide Fuel Fabrication Facility for processing 34 metric tons at Savannah River Site, but it encountered substantial schedule delays and cost overruns.<sup>37, p.4</sup> In 2014, DOE reassessed disposition options and proposed to dilute the 34 metric tons of surplus Pu, and dispose it at WIPP,<sup>38</sup> using a process like that for the 6.0 metric tons already being evaluated for disposal at WIPP in the SPD Supplemental EIS.<sup>39;40</sup> However, the safety of the option was challenged.<sup>41, p.11</sup> For FY17, Congress authorized \$15 million for planning, which was completed in

2018,<sup>37, p.5; 42</sup> and mandated that the National Academies examine the option's viability, which was completed in 2020.<sup>43</sup> An important aspect was the need to re-evaluate the potential occurrence of post-closure criticality in compacted CCOs. DOE asked Sandia to coordinate the post-criticality safety effort, with ORNL providing criticality modeling support. In the initial 2018 evaluation, ORNL concluded that criticality was highly unlikely in CCOs when limiting hydrogenous material (primarily, moisture and plastics) and following Sandia's suggestion to add boron carbide (B<sub>4</sub>C—a highly water insoluble, nonhazardous, long-lived neutron poison) to the mixture of surplus Pu and adulterant. The final report from the National Academies also acknowledged this approach for CCOs.<sup>43</sup> The adulterant, which is added to the surplus plutonium to reduce the level of attractiveness to adversaries, was bounded using cement-like components such as MgO, silicon dioxide (SiO<sub>2</sub>), and aluminum oxide (Al<sub>2</sub>O<sub>3</sub>).<sup>44</sup> In 2020, ORNL showed that limiting hydrogenous materials in CCOs was unnecessary if 50-g B<sub>4</sub>C was included in each CCO.<sup>13</sup>

As part of WIPP's fourth compliance re-certification application to EPA in 2019 (CRA-2019), Sandia updated the rationale excluding criticality from the performance assessment.<sup>1; 45-47</sup> One focus of the criticality screening was the criticality potential of 3.2 metric tons of surplus Pu in POCs already disposed at WIPP. High-fidelity salt-creep modeling in combination criticality analysis showed nuclear criticality in POCs, each with 0.2 kg  $^{239}\text{Pu}$ , was improbable.<sup>1</sup> For the CCOs disposing 6.0 metric tons of surplus non-pit Pu, the rationale excluded criticality in CRA-2019 by adopting an option to add 50-g B<sub>4</sub>C to the mixture of Pu and adulterant (Table I).<sup>1</sup>

Conceivably, administrative controls could also have been placed on CCO placement in the repository. However, these administrative and engineering controls can have operational impacts in comparison to small hypothetical consequences of criticality once the repository is closed. Instead, this paper reports on several waste form disposal options that ensure criticality does not occur in CCOs after WIPP is closed, including the previously evaluated option of mixing B<sub>4</sub>C with the waste form, and, thereby, provides additional flexibility when using CCOs.

<sup>c</sup>EPA does not designate post-closure criticality for special consideration in 40 CFR 191. In the later 2008 site-specific standard for the Yucca Mountain repository (40 CFR 197),<sup>28;29</sup> EPA again did not set apart criticality when evaluating the post-

closure behavior even though EPA had the opportunity to do so when EPA used criticality as a FEP screening example in the preamble.

Table I. Studies of Post-Closure Criticality at WIPP and Related Events

Date	Study	Description
1973	Operational Safety Analysis at Hanford	Hanford evaluates and dismisses the potential for criticality in radioactive waste disposed in trenches on Hanford Reservation. <sup>48</sup>
1979	WIPP Environmental Impact Statement (EIS)	Post-closure criticality scenario listed in documents supporting draft and final WIPP EIS; emphasis on mobilization in disposal room and potential deposition throughout disposal system (3 <sup>rd</sup> summation in Eq. (2)), <sup>30; 31</sup> geochemical constraints on accumulating fissile material used to dismiss scenario. <sup>32</sup>
1980	Operational Safety Assessment at WIPP	First safety assessment for operations dismisses potential for criticality event in array of CH-TRU standard drums on surface and in disposal room; <sup>49; 50</sup> Updates to the safety assessment occur periodically.
1983	Nuclear explosion in waste trenches dismissed	Stratton (of Los Alamos National Laboratory—LANL) dismisses speculation that explosion in waste trenches in the Russia Ural Mountains was nuclear. <sup>51</sup>
1989	FEP construction for 1989 WIPP PA	Criticality scenario listed when constructing FEPs and scenarios for the first WIPP PA. <sup>33</sup>
1992	FEP construction for 1995 preliminary CCA	Criticality scenario listed and retained for more thorough investigation for 1992 WIPP PA and 1995 preliminary CCA. <sup>34</sup>
1995	Autocatalytic critical event in fractures at Yucca Mt speculated	News articles draw attention to Bowman and Venneri (of LANL) speculation that autocatalytic critical event possible in <sup>239</sup> Pu deposited in fractured tuff below proposed repository for commercial spent nuclear fuel at Yucca Mountain. <sup>52; 53</sup>
1996	Conditions for autocatalytic assembly dismissed	Numerous articles argue geochemical constraints on deposition prevent assembling sufficient <sup>239</sup> Pu in condition necessary for autocatalytic behavior in tuff fractures (and, by analogy, fractures throughout WIPP disposal system). <sup>54-58</sup>
1996	FEP construction and screening for CCA submission	Criticality scenario dismissed in 1996-CCA; qualitative reasoning emphasizes lack of geochemical processes capable of causing deposition of sufficient quantities of fissile material throughout disposal system; modeling of salt creep for evaluating room porosity shows maximum fissile density inside drum far below asymptotic critical concentration for water. <sup>18</sup> A low consequence rationale is also developed. <sup>36; 59</sup>
2005	Supplemental analysis for CRA-2005	Sandia conducts supplemental evaluation of compaction of other containers, such as POCs and super compacted waste in ten-drum overpacks, on room porosity. <sup>60</sup>
2014	Operational Safety Assessment at WIPP	WIPP Project shows a uniform array of CCOs in disposal room is not critical when initially placed in disposal room. <sup>22</sup>
2015	Stakeholder challenges criticality screening of surplus Pu disposal	Stakeholder scoping analysis shows a uniform array of 21 CCOs compacted 30% with MgO reflector on top has potential for criticality; <sup>37; 43</sup> analysis demonstrates a post-closure criticality screening update is needed that includes CCO compaction.
2017-2018	Efficacy of B <sub>4</sub> C in preventing criticality in CCO demonstrated	Oak Ridge National Laboratory (ORNL) concludes criticality is highly unlikely in an extremely uniformly compacted array of CCCs with flanges touching when hydrogenous material limited and 50-g boron carbide (B <sub>4</sub> C) added to dilute-and-dispose waste form of the Surplus Plutonium Disposition Program (i.e., Pu mixed with diluting adulterant). <sup>44</sup>
2018-2019	Geomechanics studies of empty and CCO filled rooms	With advances in computational geomechanics of salt creep, <sup>61</sup> Sandia improves modeling of disposal room closure when empty <sup>62</sup> and when filled with individual CCOs emplaced as hexagonal array in ~2-m room segment. <sup>8</sup>
2019	CRA-2019	Sandia updates post-closure criticality screening for 4 <sup>th</sup> compliance recertification application (CRA-2019) that includes updated geochemical constraints on <sup>239</sup> Pu mobilization in disposal room and deposition elsewhere in WIPP disposal system. <sup>47</sup> Sandia models compaction of individual 6-inch and 12-inch POCs emplaced as a hexagonal array after roof fall and while gradually closing from salt creep. <sup>11</sup> ORNL places 0.2-kg Pu spheres at centroids of deformed POC array in three different hydrologic regimes to show compacted assembly not critical. <sup>1; 16</sup> The screening rationale excludes CCO criticality by requiring 50-g B <sub>4</sub> C in container. <sup>1; 44</sup>
2020	Efficacy of B <sub>4</sub> C in CCOs updated	ORNL updates criticality analysis of extremely uniformly compacted CCCs with 50-g B <sub>4</sub> C and shows limits on hydrogenous material unnecessary. <sup>13</sup>
2021	Updated criticality FEP evaluation and WAC revision for CCOs	Herein, Sandia expands CCO disposal options for the 2022 WAC revision, in addition to the B <sub>4</sub> C option. The geomechanical analysis examines CCO movement from rock fall and when compacted from salt creep when initially emplaced as hexagonal and triangular arrays. <sup>9; 12</sup> In the criticality analysis, ORNL places cylinders and spheres of generic wastes at various positions along the centerline of deformed CCCs in a dry hydrologic regime to define constraints on water/plastic to ensure subcriticality after WIPP closure. <sup>14</sup>

### III. MODELING OF ROCK FALL

To establish a reasonable CCO configuration after compaction, high-fidelity geomechanical simulations were conducted for a slice of a room segment filled with discrete CCOs.<sup>8,9</sup> Two phases of post-closure repository conditions are envisioned: (1) rock fall in the first 20 years or so, and (2) gradual compaction of containers from salt creep to the maximum extent up to 1000 years without brine present (thus, avoiding gas generation by metal corrosion and cellulose degradation and subsequent room pressurization which impedes room compaction). The geomechanical modeling of CCOs for these two phases is similar to the geomechanical modeling of POCs conducted for CRA-2019.<sup>11</sup>

#### III.A. Conceptual Model of Rock Fall

During the first 20 years or so after sealing a panel of disposal rooms, salt rock fall and room closure from salt creep mostly fills the room void space (Fig. 2). Discrete rock fall models were constructed to evaluate the potential of rock fall scattering and clustering CCOs and, thereby, potentially producing a reactive CCO configuration prior to full compaction from salt creep. A trapezoidal-shaped salt block was chosen to match the Panel 7, Room 4 roof fall, which is the biggest roof fall that has occurred in a disposal room at WIPP.<sup>1</sup> The WIPP disposal panels are located in two different horizons (elevations) of the geologic strata of the Salado Formation. Panel 7 is in the lower horizon such that 2-m distance to Clay G seam, from where the salt block separated, is the largest observed. Larger salt blocks are not anticipated (Fig. 2).

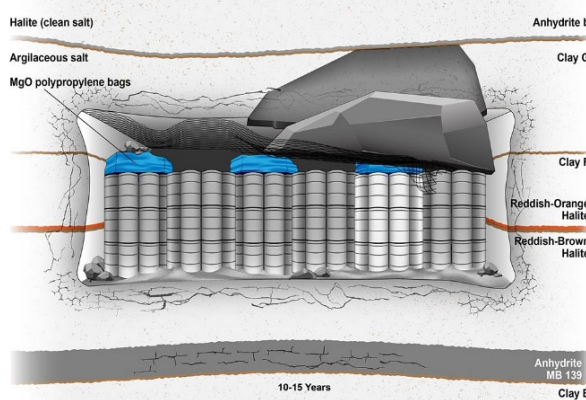


Fig. 2. Conceptual model of large trapezoidal-shaped salt block that detaches at Clay G seam and falls onto CCOs.

Several conservative assumptions are made to produce bounding conditions: (a) one large trapezoidal-shaped block with one thick side is used to promote some moment and uneven impact, (b) the large block is not allowed to break into pieces, (c) each layer of CCOs is

laterally offset by 2.54 cm to promote minor instability; and (c) the rock fall occurs immediately after CCO emplacement so that the block fell as far as possible. Also, the polypropylene bags of MgO are omitted to increase the free-fall distance and avoid dissipating the rock fall impact. Furthermore, the plywood strength is reduced 80% to promote greater inner CCC movement, and the minimum yield strength of stainless and carbon-steel is used. Finally, the stainless steel, carbon-steel, and plywood strengths are based on slow strain rate experiments and treated as strain-rate independent. Defining container strength as a function of strain rate would more accurately model impact conditions but also would increase the stability of the CCO array.

Two rock fall models are developed. In the first roof-fall simulation, the entire length of the trapezoidal salt block detaches from the roof. In the second roof-fall simulation, the salt block progressively detaches from the roof, to impart more rotation.

#### III.B. Rock Fall Results

When the entire block length detaches simultaneously (Fig. 3a) the trapezoidal shape imparts some rotation, but the salt block lands almost flat, and settles on top of the drum ensemble. The impact breaks the top plywood layers (in brown), dents some of the outer 55-gallon drums (not shown), and causes the CCCs to sway back and forth slightly (blue pipes); but CCOs mostly return to the initial configuration.

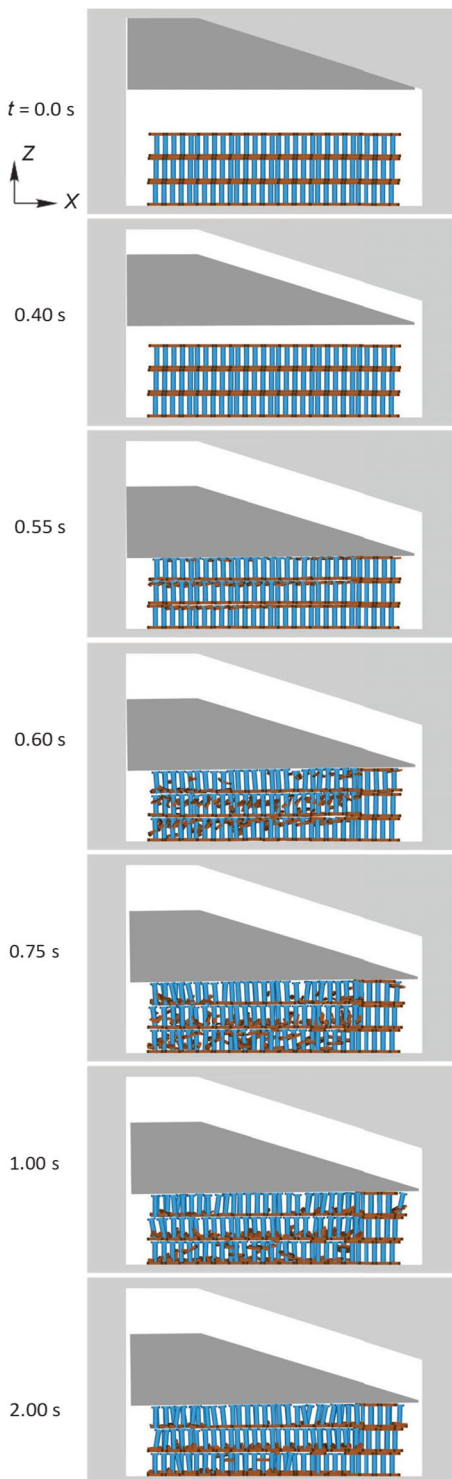
When the salt block progressively detaches (Fig. 3b), the CCOs are jostled more such that not all the CCOs return to a neat arrangement, but still no clustering or noticeable deformation of CCOs occurs.

Because of the bounding conditions selected for the rock fall analysis, salt block falls shortly after disposal are not likely to cause extensive deformation, collapse, or clustering and, thereby, produce a critical assembly of CCOs prior to later room closure from salt creep.

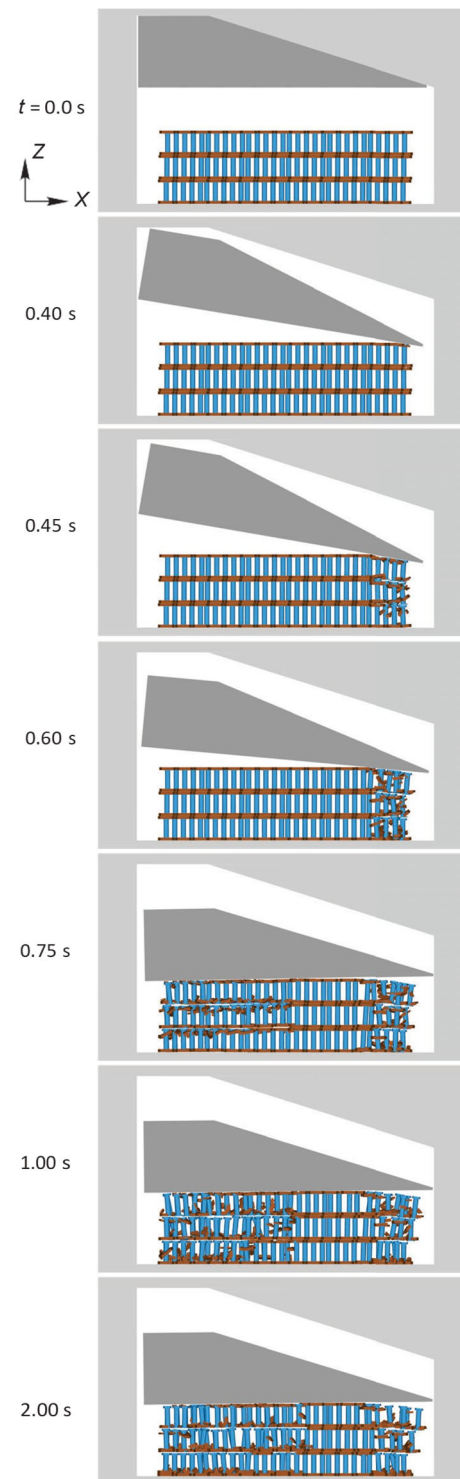
### IV. MODELING OF ROOM CLOSURE FROM SALT CREEP

#### IV.A. Conceptual Model of Room Closure

An array of CCOs compacts as the disposal room in the bedded salt naturally closes and beneficially encapsulates the CCOs. The driving force for room closure is shear stresses in the salt surrounding the room. Salt creeps in the presence of shear stress, and a large void space within a geologic salt formation, such as a room, causes significant shear stresses. As the salt creeps into the room, it gradually compacts the containers. The containers provide little crushing resistance at first, but they slowly become stiffer and stronger. Eventually, the container resistance balances the salt crushing pressure, the salt shear stresses become negligible, and the room closure asymptotically comes to a halt.



(a) Mostly flat roof fall



(b) Rotating roof fall

Fig. 3. Roof fall onto CCOs emplaced in a hexagonal array in the lower repository horizon (a) mostly flat roof fall; (b) rotating roof fall. Brown discs represent the top and bottom plywood stabilizer for the blue stainless steel CCOs inside the 55-gallon CCO shell (which is hidden for visualization).<sup>9, Fig. 5</sup>

#### IV.A.1. Salt Stratigraphy

The geomechanical model adopted an idealized stratigraphy of the salt formation, that included salt, anhydrite, and clay seams. A portion of this stratigraphy is shown in Fig. 4.<sup>63</sup> The adopted idealized stratigraphy is the same as used for POC analysis.<sup>1</sup>

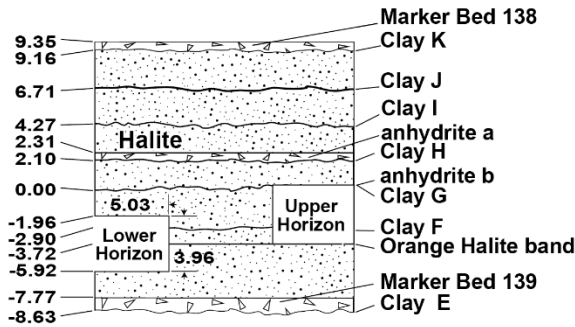


Fig. 4. Idealized stratigraphy near WIPP disposal rooms in the lower and upper horizon. Elevations are referenced to Clay G, which is at elevation 386 m, 652 m below surface at exploratory well ERDA-9.<sup>12</sup> Fig. 1; 64

The salt and anhydrite material models were based on laboratory measurements of their mechanical behavior. Sliding along the clay seams was modeled using Coulomb friction with a friction coefficient of 0.2. This friction coefficient has not been directly measured, but 0.2 produces reasonable amounts of sliding and room closure rates that agree with underground measurements.<sup>63</sup>

The model represents the 10.06-m wide (*x*-direction), 4-m high (*z*-direction), and  $\sim$  2-m slice (*y*-direction) of Room 4 (middle of a panel of 7 rooms) halfway down the 91-m room segment axis where the ratio of horizontal to vertical room closure is likely the greatest. The most vertical closure is likely to occur at the intersection of straight room segment with an end drift.<sup>d</sup> The location of the greatest horizontal closure might also be of interest, but the location cannot be discerned without detailed studies. The room closure analysis models the disposal rooms in both repository salt horizons to estimate the influence of differing arrangements of geologic strata (Fig. 4).<sup>8,9</sup>

The finite element mesh of the salt is like past models with empty rooms, whose results have compared favorably with international codes and grid convergence studies.<sup>62</sup> The empty room closure model was recently

<sup>d</sup> A panel is divided into 7 disposal rooms. A disposal room consists of a straight 91.4-m long segment and a portion of the drift on either end to form a square bracket. Although this definition is important for tracking disposal room contents, much analysis for gas generation and salt creep models only the straight 91.4 m segment of a disposal room to avoid three-

validated against horizontal and vertical closure rate measurements.<sup>63</sup> These measurements were collected from three different empty rooms at the WIPP, at least 5.7 years after room excavation.

Rock fall could occur as the room closes. In general, rockfall would tend to make the rectangular room more circular and retard the closure rate, but rock fall also enlarges the room, which would have the opposite effect and somewhat increase the closure rate.<sup>62, Ch 6, 65</sup> Rock fall may also produce some salt blocks that wedge in between containers and have a minor influence on the CCO distribution. However, numerical difficulties thwarted efforts to demonstrate the competing phenomenon by combining rock fall and gradual compaction analyses.<sup>11</sup>

#### IV.A.2. CCO Configuration

The geomechanical analysis examined CCOs arrays starting in two different configurations: (1) hexagonal array, and (2) triangular array. A hexagonal array is the approximate emplacement scheme for CCOs (Fig. 5). However, 18 CCOs must be eliminated when modeling a hexagonal array with mirror boundary conditions. With a disposal room filled with 7-pack hexagon CCO bundles, any room slice cuts 6 CCOs in half. Half CCOs cannot buckle in direction of the mirror boundary and can cause numerical difficulties with shell elements, as considered here for the CCCs in the CCOs. Hence, 36 one-half CCOs are eliminated in the analysis for a total of 153 CCOs in the room segment. Reducing the material in the room permits slightly more room closure.

In addition, 168 discrete CCOs are modeled in a more compact, triangular array with mirror boundary condition.<sup>e</sup> The 7-packs are held together with plastic wrapping, which could allow CCOs to readily shift into an approximate triangular array once the walls contact CCOs. In the triangular array, 14 CCOs are modeled per row over 8.607-m width and 2.08-m segment. The triangular array with 168 CCOs has a slightly higher maximum fissile areal density of 3.57 kg  $^{239}\text{Pu}/\text{m}^2$  compared to the ideal hexagon configuration areal density of 3.52 kg  $^{239}\text{Pu}/\text{m}^2$  when including all 171 CCOs at 380 FGE per CCO (Fig. 5).

In the analysis (and like the rock fall simulations), three discrete CCO components (CCC stainless-steel pipe, its plywood stabilizer on the top and bottom, and outer 55-gallon carbon-steel CCO shell—Fig. 1) use individual elastic-plastic-failure material constitutive equations.

dimensional effects. Herein, we almost exclusively refer to the straight room segment rather than an entire disposal room.

<sup>e</sup> A mirror boundary condition implements a plane strain solution. A mirror boundary is slightly stiffer than a periodic boundary. Although a periodic boundary may converge faster with increasing room length, a periodic boundary is difficult to implement.

A grid convergence study has not been conducted on the container mesh. Too coarse a finite mesh for the containers could reduce compaction somewhat, but the influence is expected to be minor.

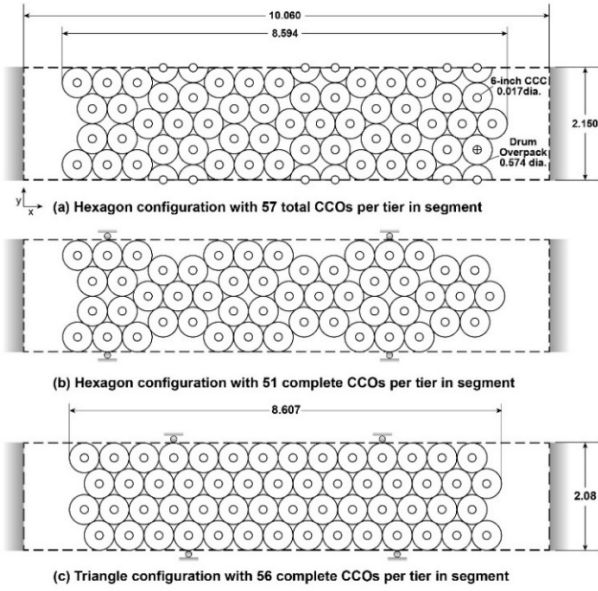


Fig. 5. Emplacement of CCOs in WIPP disposal room (a) ideal hexagon array with 51 whole and 12 half CCOs in a tier or 171 total CCOs in 2.15-m room segment of 3 tiers ( $3.52 \text{ kg } ^{239}\text{Pu}/\text{m}^2$ ); modeled hexagonal array with 12 half CCOs in a tier deleted for a total of 153 CCOs in 3 tiers ( $3.15 \text{ kg } ^{239}\text{Pu}/\text{m}^2$ ); and (c) modeled triangular array of 56 whole CCOs in a tier or 168 total CCOs in a 2.08-m room segment ( $3.57 \text{ kg } ^{239}\text{Pu}/\text{m}^2$ ).<sup>12</sup> Figs. 4&6

Although the model is reasonably realistic, two conditions could conceivably cause slightly more actual compaction than calculated (besides the remote possibility of too coarse of container mesh mentioned above): (a) the CCC strength is treated as independent of strain rate, but stainless steel could be weaker at the slow strain rates of gradual compaction, and (b) container corrosion would weaken the containers.

However, several conservative assumptions are employed that promote more calculated compaction than actual compaction: (a) any gas pressure from cellulose degradation and metal corrosion that would normally arrest compaction is not included; (b) container elements are deleted from the analysis once they become severely distorted or the material fractured thereby reduced material volume in a room (e.g., plywood quickly splintered and thus not much of the plywood elements remain at 1000 years); (c) plywood failure strength is reduced 80%; (d) the stainless steel pipes are empty; thus, structural stiffening from TRU waste is omitted; and (e) MgO bags are omitted thereby reducing material volume in a room by ~5%.

#### IV.B. Deformed Irregular Array

The salt-creep simulations predict the outer CCO shell crumples and the plywood rapidly fails shortly after the room ceiling contacts the CCO drums (in the room center by ~35 years and along the entire length after ~60 years—Fig. 6). By 100 years, the CCCs have begun to topple over on their sides. By 200 years, most CCOs are on their side, which allows for substantial compaction.

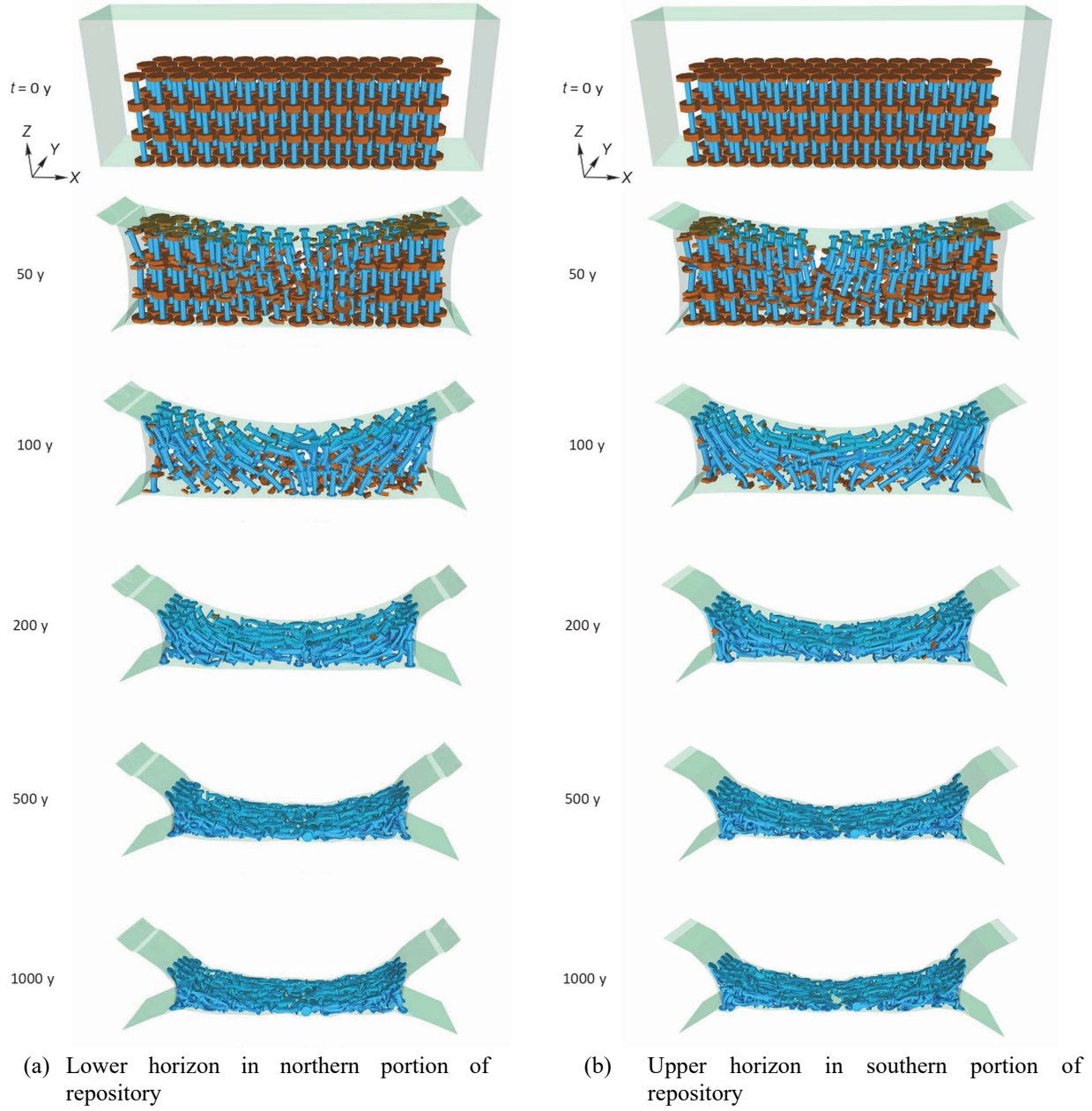
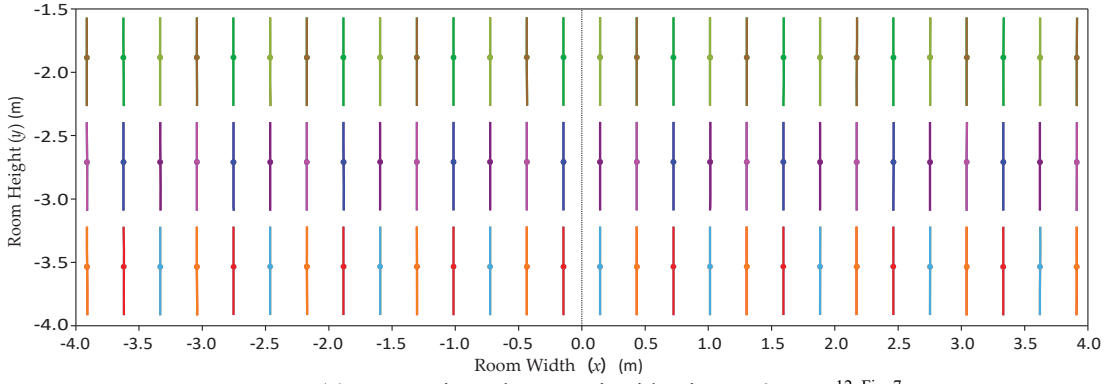


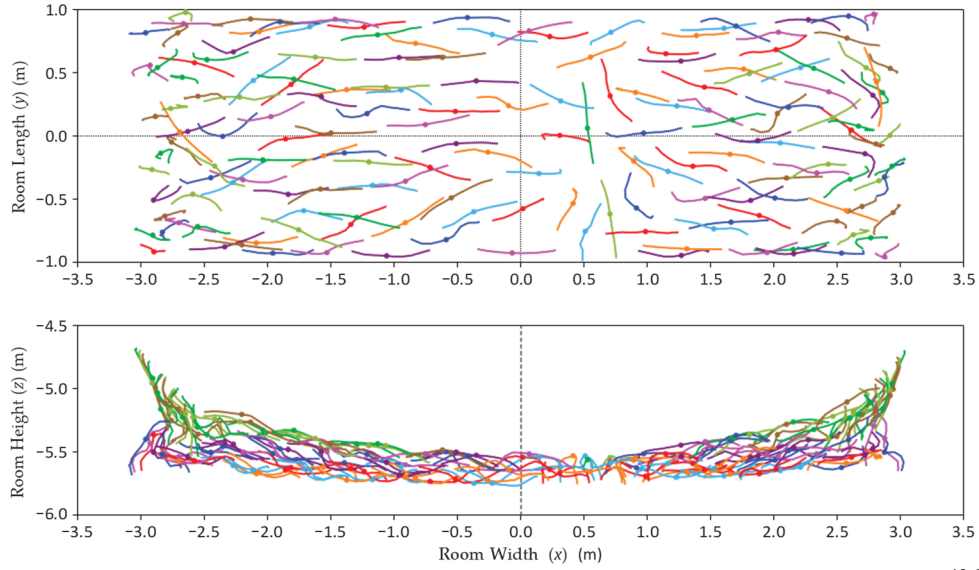
Fig. 6. Salt compaction in room segment with CCOs emplaced in triangular array; most inner CCCs are on their side by 200 years; the outer CCO drums and bedded salt stratigraphy are included in the analysis but removed in the visualization; the brown elements represent the plywood stabilizing the CCC, which are deleted when splintered and failed.<sup>9, Fig. 9</sup>

A more revealing perspective of CCO compaction is the plan and side view of CCC centerlines at 1000 years (Fig. 7). Clearly, most CCOs are on their side. The greater closure at the room center displaces much of the top tier of CCOs (green, yellow-green, and brown centerlines) toward the room sides (while the room sides are moving toward the center). The second tier (deep

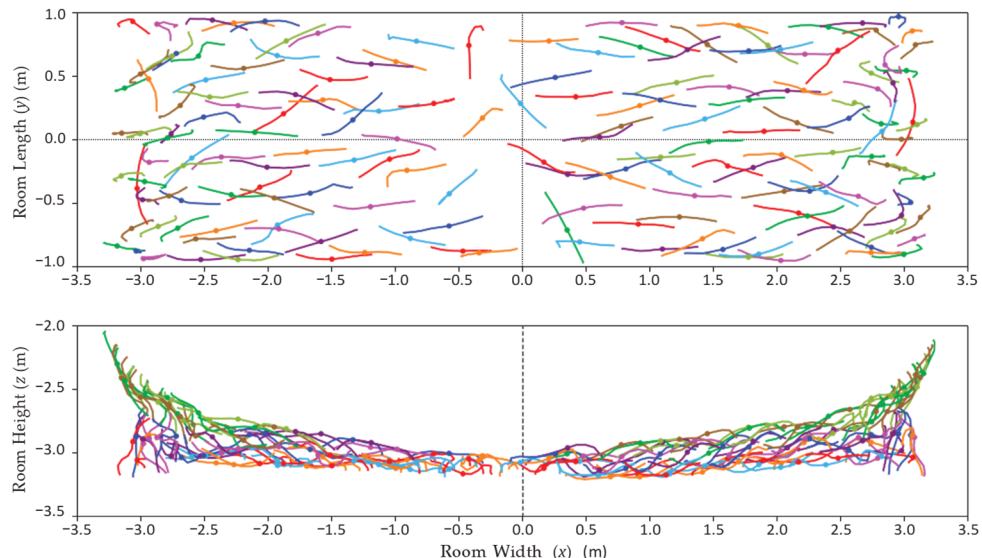
blue, burgundy, and pink) is also displaced toward the room sides but not nearly as much. The center is mostly a single layer, which consists primarily of the bottom tier of CCOs (orange, light blue, and red). The CCOs are not noticeably clumped or bunched together down the axis of the room segment in the  $y$ -direction.



(a) CCC triangular array in side view at 0 years<sup>12, Fig. 7</sup>



(b) Lower horizon plan (x-y direction) and side view (x-z direction) at 1000 years<sup>12, Fig. 31</sup>



(c) Upper horizon plan and side view at 1000 years<sup>12, Fig. 33</sup>

Fig. 7. Deformed centerlines of CCCs at 1000 years when initially emplaced as triangular array.

The final coordinate positions of the CCC centers are used in subsequent criticality calculations (Fig. 8). The initial emplacement coordinate positions of the CCC centerlines shown are when the CCOs touch each other. Hence, a 1.12 m gap exists between the CCC centerline

and the room wall (or gap of 0.83-m between the CCO drum and room wall). Normally, the pallets and plastic wrap for the 7-pack CCO bundles prevent such a tight spacing. The typical minimum distance to the wall during emplacement is 20 cm.<sup>1</sup>

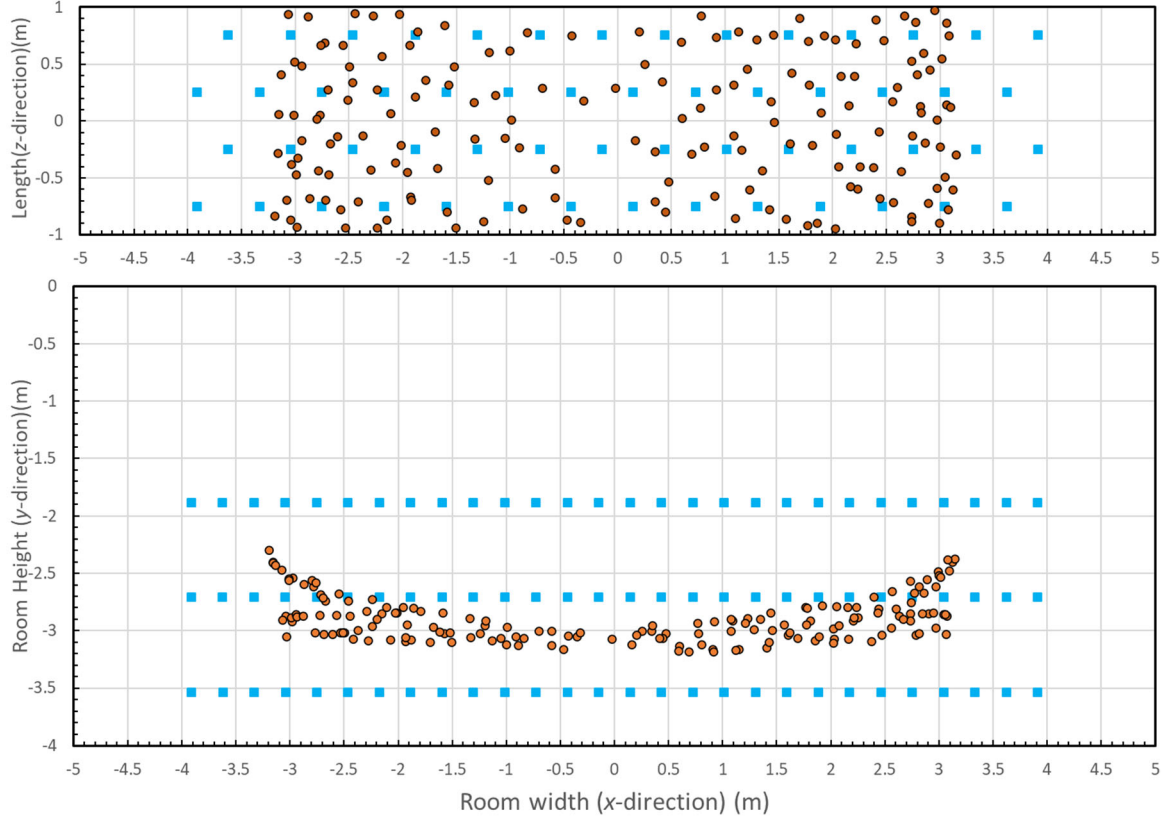


Fig. 8. Plan and side view of deformed coordinated positions of CCC centers in upper horizon (orange circles) used in criticality analysis relative to undeformed coordinate positions (blue squares) as triangular array in 10.06 m wide, 3.96 m tall, and 2.08 m thick room segment.

#### IV.C. Room Closure Measure

Although illustrations of deformed CCO arrays are qualitatively instructive, summary measures of the deformed CCO arrays are necessary to quantitatively compare geomechanical model results in order to determine the influence of input parameters and starting conditions. Two measures are considered (1) room closure at the disposal room mid-height and mid-width, and (2) the distribution CCO concentration within the room to determine the extent of CCO clustering.

##### IV.C.1. Room Closure at 1000 years

Most room closure occurs by 300 years; but, the room continues to close and approaches a maximum at ~1000 years (Fig. 9). The smallest horizontal closure at the room mid-height at 1000-years occurs for the triangular array in the upper repository horizon: 39.0% of the original 10.06 m width. The largest horizontal

room closure occurs in the lower horizon for the hexagonal array: 42.5%.

The smallest vertical room closure at the room mid-width occurs for the hexagonal array in the lower horizon 93.9% of the original 3.96 m height (Fig. 9). The largest vertical compaction occurs for the hexagonal array in the upper horizon: 97.3%. Understandably, a room filled with 168 CCOs for the triangular array generally closures less than 153 CCOs for the hexagonal array, but the difference is not great. That is, changes in the initial emplacement configuration influence the progression of room closure between 100 and 400 years, but cause only minor changes in final room closure at 1000 years.

Comparing closure results of a room full of CCOs and an empty room shows that CCO containers weaker than modeled (e.g., CCOs degraded by corrosion or CCOs with weaker strength parameters) will only somewhat increase room closure beyond that already modeled.

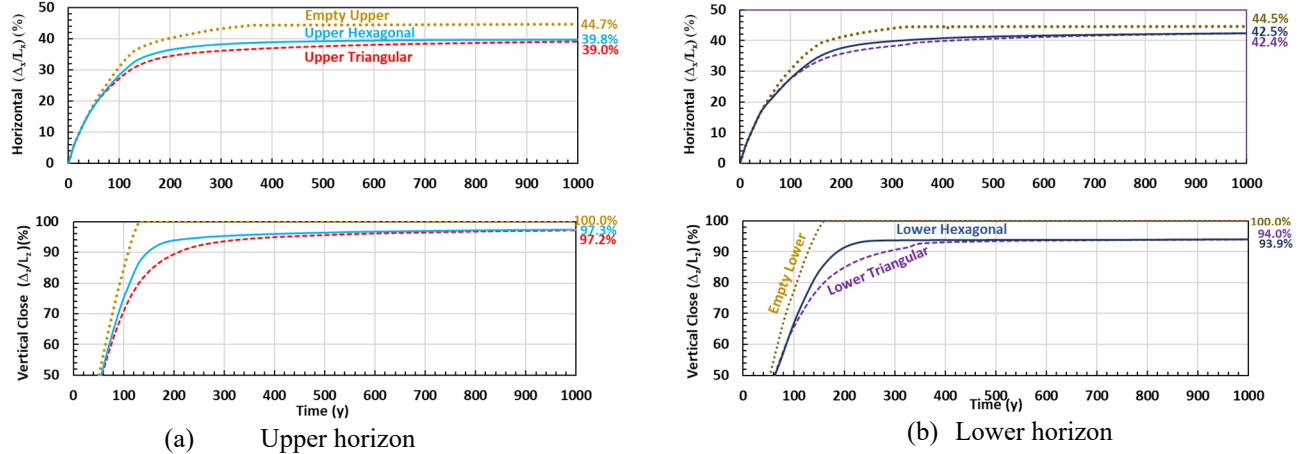


Fig. 9. Horizontal and vertical closure at room mid-height and mid-width, respectively, for CCOs initially emplaced as triangular and hexagonal arrays in upper and lower repository horizons.<sup>9, Fig. 7; 12, Fig. 10; 62</sup>

#### IV.C.2. Room Closure in Previous CCO and POC Simulations

In 2018, several simulations of room closure preliminary calculations were conducted of CCOs in a hexagonal array the upper horizon in a with a friction coefficient of 0.5 for Clay F and Clay G seams (Fig. 4). A friction coefficient ( $\mu$ ) of 0.5 reduces clay slippage

such that the room closes slightly slower. In turn, more CCCs are pinned first and then column buckle. Because the CCCs are pinned in place, the CCCs are not segregated into layers as before (Fig. 10 versus Fig. 7). A friction coefficient ( $\mu$ ) of 0.2 allows slightly faster closure such that more CCCs toppled over with the top tier shoved to the sides.<sup>12; 66</sup>

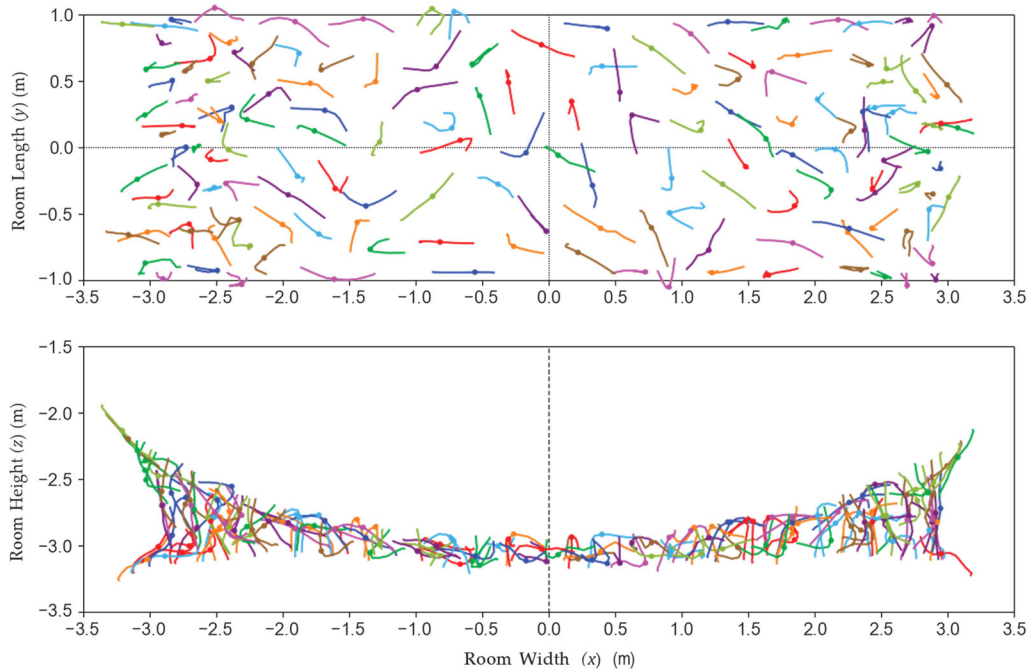


Fig. 10. CCO compaction in hexagonal array in upper horizon has more column buckling when friction coefficient set at 0.5 for Clay F and Clay G layers.<sup>12, Fig. 21</sup>

To make additional comparisons, a 6-inch and 12-inch POC simulation was repeated with the CCO modeling assumptions.<sup>9</sup> Although the progression of room closure changes somewhat, the influence of the

friction coefficient on the final horizontal and vertical closure of a room filled with 6-inch POCs initially emplaced in hexagonal arrays with a friction coefficient of 0.05 are similar to room closure of CCOs (Fig. 11).

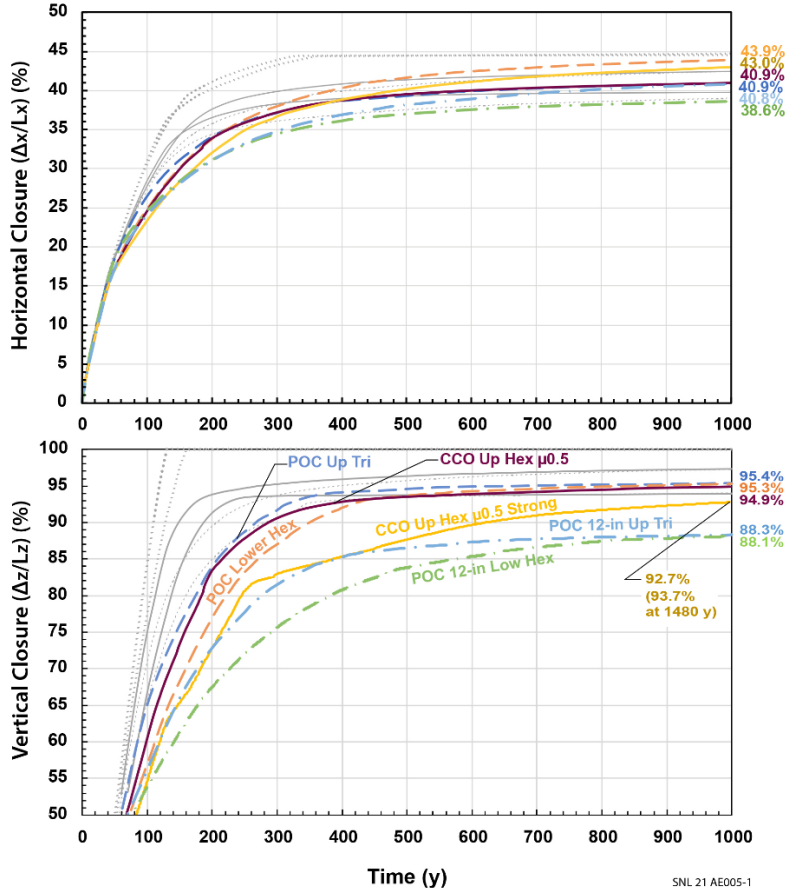


Fig. 11. Horizontal and vertical closure of upper and lower horizon rooms filled with CCOs and POCs initially emplaced in triangular and hexagonal arrays with different clay friction coefficients ( $\mu$ ), where room closure for current analysis and empty rooms in Fig. 9 shown in gray.<sup>12, Fig. 18</sup>

#### IV.C.3. Closure of Room Filled with Mix of CCOs and other Containers

All the CCO simulations assume the disposal room is filled with CCOs, which will be reasonable for large shipment campaigns. However, WIPP disposal rooms are typically filled with a mixture of mostly standard 55-gallon TRU drums (54% global average), standard 12-inch POCs (15%), 100-gallon drums (20%), some TRU waste boxes (8%), and miscellaneous other containers, usually stacked 3 high.<sup>1, Table V</sup> Mixing the most common types of containers in a disposal room mostly filled with CCOs would not likely substantially change the final extent of compaction. For example, the initial yield strength of the stainless steel CCCs has been varied between zero (like empty room) to a factor of 4 greater than nominal strength; yet, the final vertical room closure is similar (Fig. 11).<sup>8</sup> Only the time to reach asymptotic closure varies. An empty room vertically closes by 150 years, a room with CCOs initially emplaced in hexagonal array closes by 250 years, CCOs and 6-inch POCs initially emplaced in triangular array close by 350 years, 6-inch POCs initially emplaced in

hexagonal array close by 450 years, and a CCO with 4 times nominal strength in 1480 years (Fig. 11). For most containers, the initial container strength is too small to provide enough resistance to the lithostatic pressure (~15 MPa).<sup>9</sup> Only when the containers become significantly compacted are they able to resist the overburden pressure.

The container strength of 100-gallon drums filled with super-compacted waste (compressed with ~60 MPa) could resist the lithostatic pressure and a cluster would prop up a small portion of a disposal room, which could allow greater horizontal compaction in another portion of a room. However, super compacted waste containers are not allowed to be located next to each other.<sup>1; 9</sup> Super compacted waste containers randomly distributed throughout the room would likely shield the weaker CCO containers; thus, CCO compaction would likely be less than observed in simulations here (e.g., Fig. 7 and Fig. 10).<sup>1; 11</sup>

## IV.D. CCO Concentration Measure

### IV.D.1. Concentration of CCOs at 1000 years

A more direct measure of the CCO compaction is a uniformly weighted CCO concentration ( $c_{uniform}$ ) defined as

$$c_{uniform} = n_{CCO} / V_{sphere} \quad (1)$$

where  $n_{CCO}$  is the number of CCO pipes in a sphere volume  $V_{sphere}$  calculated as  $4\pi(r_{sphere})^3 / 3$  based on a defined sphere radius  $r_{sphere}$ . The sphere radius relates to the distance neutrons interact between CCOs through the interstitial material, here modeled as a 1:1 mixture of salt and MgO. As explained in the next section, the neutron flux is reduced by 2 orders of magnitude in 7 cm from an ideal point source;<sup>12</sup> hence, the sphere radius was set at 75 cm. The concentration for the irregular array is calculated for periodic boundary conditions to avoid artificially increasing the concentration when a CCO is near a boundary.

At 1000 years, CCO concentration has a mean between 10.9 and 11.9 CCO/m<sup>3</sup> and maximum between 15.3 and 18.1 CCO/m<sup>3</sup>, where the variation is caused by the initial emplacement configuration, either hexagonal or triangular, and the stratigraphic variation is represented by the upper and lower repository horizons (Fig. 12). The corresponding mean fissile concentration with 0.38 kg/CCO is between 4.1 and 4.5 kg Pu/m<sup>3</sup> and the maximum is between 5.8 and 6.7 kg Pu/m<sup>3</sup>.

### IV.D.2. Relative Weighted Concentration

In salt, the neutron flux ( $\phi$ ) rapidly attenuates.<sup>f</sup> This rapid decrease in  $\phi$  is not captured well by a calculating a CCO concentration that uniformly weights all CCOs within a specified radius (e.g., 75 cm). Thus, an alternative weighted concentration ( $c_{weight}$ ) has been defined:<sup>12</sup>

$$c_{weight} = \frac{\sum_{n=1}^N w(r_n)}{\int_{V_{sphere}} w(r) dV} \quad (2)$$

where  $w(r)$  is the weighting function that varies with radial distance  $r$ , and  $r_n$  is the radial distance corresponding to CCO center  $n$ . Eq. (2) reduces to Eq. (1) if  $w(r)$  is a constant.

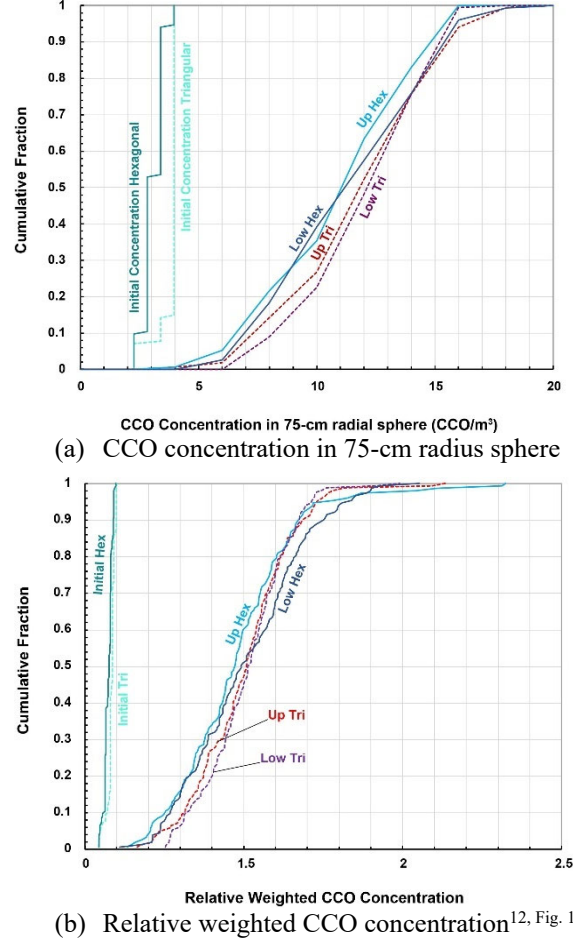


Fig. 12. Distribution of CCO concentration about each CCC center at 1000 years.

A reference weighted concentration for one CCO can also be defined as<sup>12</sup>

$$c_0 = \frac{\sum_{n=1}^N w(0)}{\int_{V_{sphere}} w(r) dV} \quad (3)$$

and a relative weighted concentration can be defined as

$$\hat{c} = \frac{c_{weight}}{c_0} = \sum_{n=1}^N \frac{w(r_n)}{w(0)} \quad (4)$$

To be consistent with the physics of the criticality analysis, the weighting function is chosen to resemble the attenuation of neutron flux from an ideal steady source, which can be approximated as a radial diffusion

<sup>f</sup>Neutron flux is the neutron density per unit volume multiplied by the neutron velocity. Neutron velocity varies over a wide spectrum. Neutrons released during fission of a fissile atom typically have high energy/high speed (average of 2 MeV). High energy/fast neutrons have a small probability of being absorbed by the nucleus of another fissile atom. In contrast, low

energy/slow neutrons (i.e., those with thermal energy ~0.025 eV) have a much greater probability of being absorbed by an atom and causing fission. Neutron interaction with other matter can moderate or reduce the neutron energy through inelastic impacts with heavy nuclei and elastic impacts with light nuclei.

process. The one-dimensional, steady-state diffusion equation for  $\phi$  emanating from a point source of strength  $S_0$  is

$$\frac{D_{\text{diff}}}{r^2} \frac{\partial}{\partial r} \left( r^2 \frac{\partial \phi}{\partial r} \right) - K_{\text{abs}} \phi = 0 \quad (5)$$

where  $D_{\text{diff}}$  and  $K_{\text{abs}}$  are the neutron diffusion and adsorption constants, respectively, of the salt/MgO mixture surrounding the point source. The solution to this equation with the boundary conditions of  $\lim_{r \rightarrow 0} (-4\pi r^2 D_{\text{diff}} d\phi / dr) = S_0$  and  $\lim_{r \rightarrow \infty} \phi = 0$  is

$$\phi = \frac{A}{r} \exp \left( \frac{-r}{r_{\text{char}}} \right) \quad (6)$$

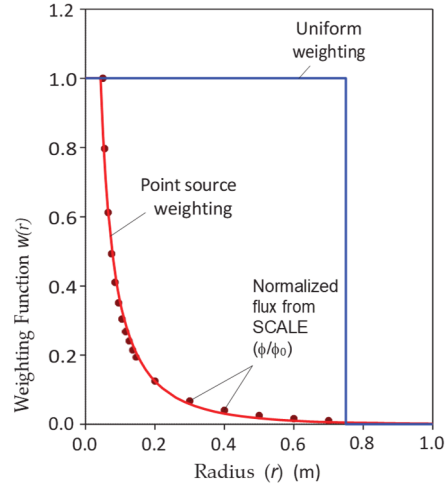
where the characteristic radius  $r_{\text{char}}$  is  $\sqrt{D_{\text{diff}} / K_{\text{abs}}}$  and the constant  $A$  is  $S_0 / (4\pi D_{\text{diff}})$ .

The weighting function  $w(r)$  is based on Eq. (6) but a limit is placed on  $w(r)$  for small  $r$  because at the source with  $r$  of zero, the neutron flux is infinite. Consequently,  $w(r)$  is set at unity for  $r < r_{\text{pt}}$ . A limit is also placed on  $w(r)$  for large  $r$  to avoid evaluating the weighting at infinite radii. With these constraints, the point source weighting function is

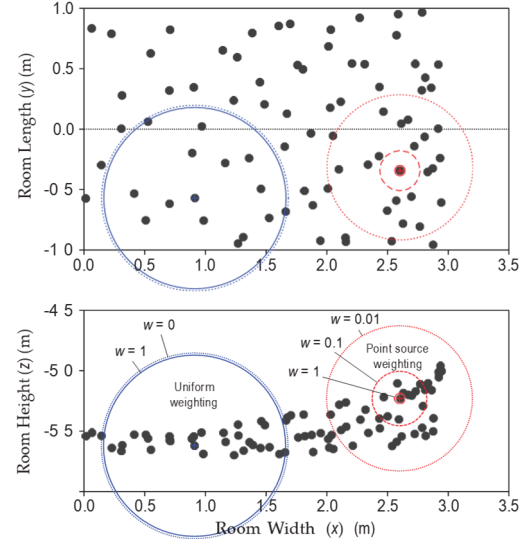
$$w(r) = \begin{cases} 1 & \text{for } 0 \leq r \leq r_{\text{pt}} \\ \frac{r_{\text{pt}}}{r} \exp \left( \frac{r_{\text{pt}} - r}{r_{\text{char}}} \right) & \text{for } r_{\text{pt}} < r \leq r_{\text{max}} \\ 0 & \text{for } r_{\text{max}} < r \end{cases} \quad (7)$$

This point source weighting function values of  $r_{\text{pt}}$ ,  $r_{\text{char}}$ , and  $r_{\text{max}}$  were calibrated against neutron flux results of a model built with waste set in a 0.05-m radius sphere surrounded by 50% WIPP salt and 50% MgO of infinite extent using the MAVERIC module in SCALE.<sup>12</sup> In general, the neutron flux drops two orders of magnitude in 0.7 m radial distance (i.e.,  $\phi / \phi_0 = 0.01$  for  $r > 0.7$  m) (Fig. 13).

Although the weighting of nearby CCO neighbors is different, the similarities in the distributions of the uniformly weighted (simple) and relative-weighted concentration measure after 1000-year room closure (Fig. 12), reinforces the earlier conclusion from the room closure measure (Fig. 9) that changing the repository horizon or the emplacement configuration does not have a dramatic impact on the final arrangement of CCOs in a compacted room.



(a) Difference in weighting function profiles

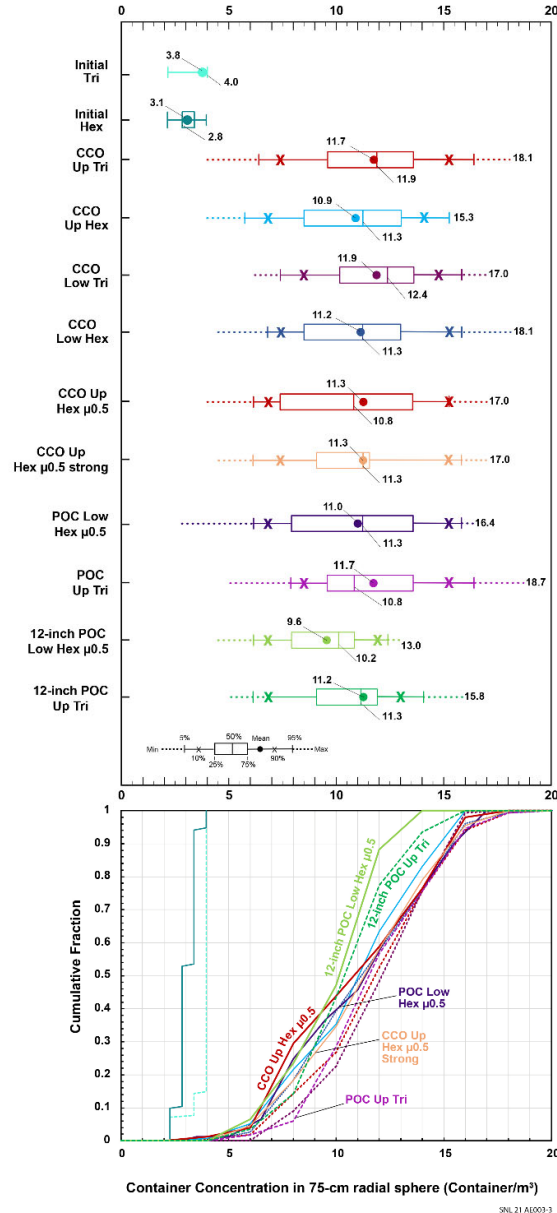


(b) Spheres of influence

Fig. 13. Weighting in sphere of influence for uniformly weighted (simple) and relative-weighted concentration<sup>12, Fig. 8</sup>

#### IV.D.3. Concentration at 1000 years for Containers with Different Strengths

The simple concentration distributions remain similar for CCOs with (1) high strength (4 times nominal) strength; (2) change to 6-inch POC with its different construction and, thus, compaction strength; and (3) 6-inch POCs in strata with clay friction coefficient ( $\mu$ ) of 0.5 (Fig. 14). In particular, the means of the simple concentration are similar. Furthermore, the distribution tails of the simple concentration are remarkably similar at high concentration values between 13 and 18.7 containers/m<sup>3</sup> (cumulative fraction above 0.75 in.

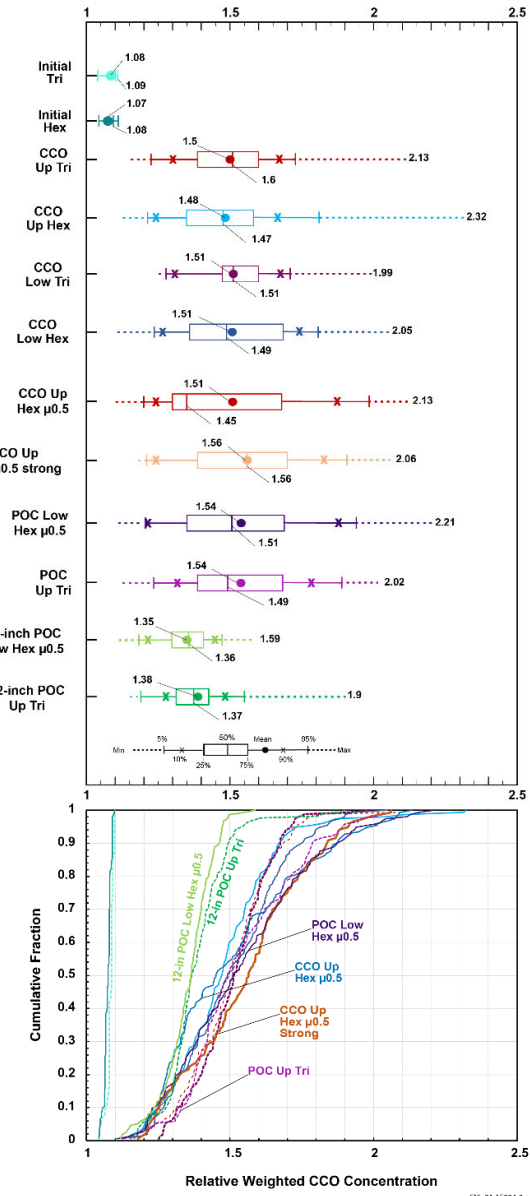


(a) Container concentration in 75-cm radial sphere

Fig. 14. Change in distribution of container concentration at 1000 years with change in clay friction coefficient ( $\mu$ ), change in CCC stainless-steel strength, and change in POC container; unlabeled curves same as Fig. 12.12, Fig. 19

The means of the relative-weighted concentration also remain similar for CCO with high strength and 6-inch POCs.<sup>g</sup> In contrast, however, the relative weighted concentration have increased variation at high values. That is, the relative weighted concentration is more discerning in identifying differences in the final arrangement of containers at the distribution tail of high concentrations.

<sup>g</sup> Although 6-inch POC arrays have a similar geometric concentration as CCO arrays (Fig. 14), the fissile concentration is less since POCs contain 0.2 kg/POC (e.g.,



(b) Relative-weighted container concentration<sup>12, Fig. 19</sup>

A room filled with 12-inch POCs has similar minimum concentration values (Fig. 14). However, the 12-inch POC with roughly twice the stainless-steel inner pipe mass and, thus, the structural strength significantly reduces the maximum and the mean concentration.

mean of 11.7 POC/m<sup>3</sup>—2.3 kg Pu/m<sup>3</sup> versus mean of 11.7 CCO/m<sup>3</sup>—4.4 Pu/m<sup>3</sup> when emplaced in triangular arrays).

#### IV.E. Room Closure and CCO Concentration Stability

The geomechanical compaction analysis evaluated the influence of changes in (1) repository horizon and, thereby, changes arrangement of clay strata; (2) clay friction coefficient; (3) emplacement configuration (triangular and hexagonal); (4) strength of CCC (a) directly through increase of yield strength by 4 times, and (b) indirectly through analysis of empty room and changing to 6-inch POC construction; and (5) change to 12-inch POC sizes and mass (i.e., twice the stainless steel mass) (Fig. 9, Fig. 11, Fig. 12, and Fig. 14). Except for 12-inch POC, these variations cause only minor changes in final room closure. Furthermore, the variations all produced a wide variety of deformed spacing between CCOs, as measured by the distribution of CCO concentration, but the distribution shape and range of the simple and more complicated relative weighted CCO concentration measures remain stable. Consequently, the coordinate positions of CCOs for the 4 cases of the irregular, non-uniformly compacted array reasonably represent conditions in the WIPP disposal for subsequent criticality calculations.

### V. CRITICALITY ANALYSIS OF COMPACTED ARRAYS WITHOUT BORON CARBIDE

#### V.A. Computational Tool

To evaluate the post-closure criticality potential of compacted rooms, a series of models were developed and analyzed with SCALE.<sup>15</sup> Version 6.2.3 was predominately used;<sup>14, §3</sup> however, version 6.2.4 was also used for validation analysis.<sup>14, App. H</sup> Within SCALE, the Monte Carlo module, KENO-VI (Criticality Safety Analysis Sequence Six—CSAS6), is used to calculate neutron multiplication factors ( $k_{\infty}$  or  $k_{eff}$ ).<sup>14, §3</sup> That is, the integral neutron and photon transport equations are solved with Monte Carlo techniques. The distance between interactions, the fissions that occur, and the neutron loss by capture or leakage are characterized by parameters such as, the mean free path lengths between interactions, the distribution describing scattering, the distribution of neutron energy, and the reaction cross-section of the atoms of each material. All analysis started

with the 252 group Evaluated Nuclear Data File/B Version 7.1 (ENDF/B-VII.1) criticality library of tabulated cross-sections, which is provided in the standard release of SCALE, and used CENTRM module to provide problem-dependent multigroup cross-sections.<sup>13; 14, §3</sup>

#### V.B. Upper Subcriticality Limit in Nuclear Criticality Modeling

The upper subcriticality limit (USL) at which a fissile configuration is considered critical is derived from the bias and uncertainties associated with SCALE, the underlying nuclear data, and the modeling fidelity. In an engineered system on the surface with humans present, great care is taken to conservatively define USL on the index of criticality ( $k_{eff}$ ).<sup>h</sup> For example, the USL is 0.9382 rather than unity for criticality analysis of WIPP TRU waste transport (e.g., TRUPACT-II package transporting CCOs).<sup>68, Ch. 6</sup> To elaborate, the approach for showing to the US Nuclear Regulatory Commission (NRC) that criticality is improbable during waste transport is rule-based (10 CFR §71.55 and §71.59).<sup>69, 70</sup> Benchmark experiments that are similar to the case under evaluation are used to determine the bias in the SCALE criticality model and the bias uncertainty. In addition, an administrative factor is often added (i.e., USL = 1 – (code bias + bias uncertainty + administrative factor) where only unfavorable code bias and bias uncertainty is considered, and the administrative factor is 0.05 when analyzing transportation events, which dominates the offset from unity).

Furthermore, bounding scenarios of assembling fissile material are developed for engineered systems with humans present. To elaborate, an engineered system for fissile material has a clearly specified design configuration. Hypothetical accident events disrupt this design and potentially lead to assembly of fissile material in a critical configuration. For transportation, for example, the contents of each payload container (i.e., Type A containers) must be assumed to assemble together after an accident and not go critical when optimally moderated or the payload container must maintain sufficient fissile separation with other payload containers in the transport cask (i.e., Type B packages).

Finally, very conservative assumptions are made to fashion worst-case final accident configurations for

<sup>h</sup>A fissile system is critical when a nuclear chain reaction is sustained, which is described by a neutron multiplication factor ( $k$ ) of unity. Traditionally,  $k_{\infty}$  denotes a homogenous system of infinite extent and  $k_{eff}$  denotes a multiplication factor for a system of finite extent.<sup>67, pp. 75-84</sup> We also speak generally about the system reactivity ( $\rho$ ), which is related to  $k_{eff}$  (i.e.,

$\rho = \ln(k_{eff}) \simeq (k_{eff} - 1) / k_{eff}$  at  $k_{eff}$  near unity). ANSI/ANS-8.1-2014 describes  $k_{eff}$  as “the ratio of the total number of neutrons produced during a time interval... to the total number of neutrons lost by absorption and leakage during the same interval.” This definition is conceptually useful here because neutron absorption and leakage plays an important role in explaining behavior of a deformed CCO array.

nuclear criticality analysis (where these worst-case scenarios may be the result of unrealistic combinations of imagined events such as optimal moderation with water, polyethylene, and beryllium when transport package is not allowed to leak as described below). Showing that the calculated  $k_{eff}$  from nuclear criticality analysis of worst-case scenarios plus any Monte Carlo calculation uncertainty ( $k_{eff} + 2\bar{\sigma}_{SCALE}$ ) is less than a conservatively defined USL demonstrates that scenario does not result in criticality and, thereby, ensures safety when humans may be nearby.

A similar rule-based standard is ANSI/ANS-8.1-2014 (*An American National Standard for Nuclear Criticality Safety in Operations with Fissionable Materials Outside Reactors*), major aspects of which WIPP implicitly follows when implementing DOE Orders on facility operations, but as the American National Standards Institute/American Nuclear Society (ANSI/ANS) title suggests, it describes rules for evaluating criticality safety during facility operations not after closure of a geologic disposal system.<sup>71</sup>

After closure of a geologic disposal system like WIPP, the EPA standard 40 CFR 191 and implementing regulation 40 CFR 197 apply. Phenomenological modeling, such as salt-creep modeling, is necessary to predict a range of reasonable fissile configurations as natural processes cause the disposal system to evolve. Much uncertainty exists as to the plausible configurations. The factors that determine the uncertainty in reasonable configurations, such as variation in initial conditions of waste, variation in host rock characteristics (e.g., porosity, saturation, and host rock composition), and arrangement of geologic layers (e.g., position of clay layers and influence on salt creep) have more influence on whether the system is critical than calculational biases and uncertainties in neutron/photon transport codes. (i.e., the uncertainty in specifying the physical state of the assembly after 1000 or more years, using Sierra/Solid Mechanics finite-element code system, is larger than the calculation uncertainty and bias in codes like SCALE). Furthermore, applicable criticality experiments are lacking.

EPA envisions in 40 CFR 191 and 40 CFR 197 an approach based on “reasonable expectation” using mean or representative values that considers both positive and negative uncertainty. Consequently, it is not necessary for the WIPP Project to develop worst case scenarios for evaluating the potential for post-closure criticality (as explained further in §VI.A). Furthermore, the  $2\bar{\sigma}_{SCALE}$  offset for  $k_{eff}$  is omitted. Only an administrative margin of 0.05 is included for USL to account for CCO configuration and geologic uncertainty. Hence, for post-closure criticality analysis at WIPP, postulated assembly

of fissile material in a geologic setting is subcritical when the criticality index  $k_{eff} \leq 0.95$ .

## V.C. Conceptual Model for Criticality

Whether a fissile region (or assembly of fissile regions) is critical depends upon the generation and interaction of neutrons with matter within and outside the assembly, which for a finite heterogenous system, depends upon four general categories of parameters (1) type, mass, and form of fissile material; (2) material mixed with the fissile material and its overall concentration; (3) nearby material and its concentration outside the fissile array, and (4) shape including individual and array configuration of fissile regions (and thereby neutron leakage). In the criticality analysis here, the parameters in the first category are fixed and parameters in the latter three categories varied to determine relative importance.

### V.C.1 Plutonium, Waste Form, Volume, and Mass

Here, we are most interested in  $^{239}\text{Pu}$  from atomic energy defense activities, in general, and surplus  $^{239}\text{Pu}$ , in particular. In general, the contact-handled TRU waste disposed at WIPP is only 90% enriched in  $^{239}\text{Pu}$  (and remote-handled TRU waste, 78% enriched).<sup>1</sup> Table IV; 72 However, some of the surplus Pu may have higher enrichment (e.g., >93%) and may dominate when disposed at WIPP. Other isotopes mixed with  $^{239}\text{Pu}$ , such as  $^{240}\text{Pu}$ , influence criticality. Thus, the transportation limit is set at 380 FGE of  $^{239}\text{Pu}$ , rather than  $^{239}\text{Pu}$ . The Pu FGE is the mass of  $^{239}\text{Pu}$  plus a factor for other fissionable masses:<sup>17</sup> specifically, 0.113- $^{238}\text{Pu}$ , 0.0225- $^{240}\text{Pu}$ , 2.25- $^{241}\text{Pu}$ , 0.00750- $^{242}\text{Pu}$ , 0.900- $^{233}\text{U}$ , 0.643- $^{235}\text{U}$ , 0.0150- $^{237}\text{Np}$ , 0.0187- $^{241}\text{Am}$ , 34.6- $^{242m}\text{Am}$ , 0.0129- $^{243}\text{Am}$ , 15.0- $^{245}\text{Cm}$ , 0.500- $^{247}\text{Cm}$ , 45.0- $^{245}\text{Cf}$ , and 90.0- $^{251}\text{Cf}$ . This approach for the fissile content bounds isotopic influences including changes with the decay over the 10 000-y regulatory period. Hence, for criticality analysis, the fissile content is modeled as 100%  $^{239}\text{Pu}$ . The Pu mass is set at the transportation maximum of 380  $^{239}\text{Pu}$  FGE per CCO. The volume of TRU waste disposed at WIPP in CCOs is the inner 0.0128-m<sup>3</sup> volume of the CCC.

For the surplus Pu that may come to WIPP, ~6.4 metric tons is already oxidized, the remainder will also be oxidized to plutonium dioxide ( $\text{PuO}_2$ ). Granted some generic Pu waste forms that use the CCO may be metallic Pu or Pu with water of hydration or hydroxyl groups (i.e.,  $\text{PuO}_2(\text{OH})_2 \cdot \text{H}_2\text{O}$  or  $\text{Pu}(\text{OH})_4$ ), but the mineral form only influences criticality limits when the mixture is severely under moderated for highly enriched  $^{239}\text{Pu}$ .<sup>45</sup> The CCO array must be fairly well moderated to be critical. The CCO array is far from critical when severely under moderated (see §V.B.1). Therefore, all Pu is modeled as  $\text{PuO}_2$ .

## V.C.2. Material Mixed with Pu Waste

### V.C.2.a. Hydrogenous Material

The POC analysis for CRA-2019 examined 3 hydrologic regimes: (1) dry conditions exterior to the container up to 1000 years, (2) a transitional phase with influx of some brine that partially saturates pores and initiates some container corrosion up to 2000 years; and (4) a final phase with influx of sufficient brine to saturate containers and complete container corrosion after 2000 years. The hydrologic regime of the fissile region (Region 1) and the reflector (Region 2) surrounding the fissile region changed to reflect the room evolution through the three regimes. The POC analysis clearly showed that introduction of brine into the disposal room reduced  $k_{eff}$  in the second regime, and greatly reduced  $k_{eff}$  in the third regime.<sup>1</sup>

Hence, the CCC criticality analysis here focuses on the first hydrologic regime with dry conditions outside the CCC in a disposal room (during initial salt compaction) with water and polyethylene only inside the CCC in the fissile region. However, brine (density of 1160 kg/m<sup>3</sup>) inside and outside the CCC is also considered in one case.

The criticality analysis examines up to 3 kg of 100% water or 100% polyethylene (CH<sub>2</sub>) moderator inside the fissile region for most simulations, but does examine up to 6 kg of moderator for a several simulations. Water is only present as adsorbed water because the WIPP WAC limits free water to  $\leq 1$  wt. % to prevent (a) spillage contaminating the repository during operations and (b) undue container corrosion prior to salt creep entombing the containers. Polyethylene (CH<sub>2</sub>) is generally only present in CCOs as thin bagging material for Pu and Pu-contaminated articles and cannot reasonably exceed 25% of the available volume. Polyethylene has a slightly higher hydrogen density than water and the carbon is a better moderator than oxygen except at highly over moderated conditions.<sup>73</sup> Other hydrocarbons and polymer compounds are usually bound by polyethylene, because the addition of other elements into hydrocarbon or polymer (such as oxygen, nitrogen, chlorine, fluorine, silicon, sulfur) decreases the reactivity.<sup>74</sup>

### V.C.2.b. Beryllium

Previous sensitivity studies with POCs showed only a small influence of beryllium (Be—density of 1848 kg/m<sup>3</sup>) or beryllium oxide (BeO) regardless of whether mixed with the fissile material or around the fissile assembly in geologic systems;<sup>1, 16</sup> however, Be/BeO may act a special moderator when the system is highly under moderated with hydrogenous material and so is included here. The contents of a CCO is not authorized to contain  $>1$  wt. % of Be/BeO,<sup>1, Table VI;</sup><sup>17</sup> which translates to 0.545 kg as follows: The CCO empty mass is 104.3 kg; the

maximum gross mass is 158.8 kg; thus, the maximum waste mass is 54.5 kg; hence, the maximum authorized Be/BeO content is 0.545 kg. For the criticality analysis, a slightly larger 0.585-kg per CCO is used (7% increase).

### V.C.2.c. Graphite/Carbon Filler

The criticality analysis examines the influence of other materials that might be mixed with a Pu-water-polyethylene mixture in CCCs. As a surrogate for other material, graphite (density of 2300 kg/m<sup>3</sup>) is included in the Pu fissile region in some studies. Other material present within the CCC often increases the minimum mass but adding graphite to the Pu-water-polyethylene mixture does not likely increase the minimum mass, based on a Pu-carbon ideal system.<sup>46, Fig. 11</sup>

### V.C.2.d. Cement-Like Filler Material

For surplus plutonium waste, a cement-like material has been used to bound the adulterant that will actually be mixed with Pu in the fissile region to prevent ready diversion of the Pu for nefarious purpose.<sup>44</sup> The cement-like filler material is composed of 58.5 wt. % SiO<sub>2</sub>, 19.8 wt. % MgO, 11.7 wt. % Al<sub>2</sub>O<sub>3</sub> and 10 wt. % H<sub>2</sub>O with density of 2400 kg/m<sup>3</sup>.<sup>44, App A; 46, Table 3</sup> In an ideal system, the cement-like filler increases the minimum mass and, thus, decreases the probability of criticality.<sup>46, Fig. 14b</sup>

## V.C.3. Material Surrounding Individual CCCs

Material in between individual CCCs and surrounding the fissile assembly may either reflect neutrons back into the fissile mass assembly or absorb neutrons and, thereby, promote or suppress criticality, respectively. In the criticality analysis, the fissile material (Region 1) inside the CCC is surrounded by reflecting/absorbing material (Region 2). A 10-m layer of salt (modeled as pure NaCl—density of 2165 kg/m<sup>3</sup>) is around the reflecting material (Region 3—Fig. 15).

One reflecting/absorbing material is 304L stainless steel (Schedule 40) of the CCC. Stainless-steel handling cans inside the CCC and the CCO carbon-steel overpack drum are not usually included with the discrete reflector of the CCC. The 4 end plates and 6 ring plates of  $\frac{3}{4}$ -inch plywood spacers are also not included ( $\sim 15.2$  kg plywood per CCO if plywood density is  $\sim 387$  kg/m<sup>3</sup>).

A second reflector material is magnesium oxide (MgO—density of 1450 kg/m<sup>3</sup>), which is placed on the top tier of containers in polypropylene bags. As the room closes, MgO filters down between the CCOs. MgO combines with any CO<sub>2</sub> formed during degradation of organic matter such that highly soluble Pu carbonate species are not formed. In the criticality analysis, MgO is usually mixed with salt in Region 2 in a volume ratio of 1:1 (with calculated density of 1737 kg/m<sup>3</sup>);<sup>14, §4</sup> however, sensitivity analysis with 100% salt shows that the influence of MgO to reactivity is not large.

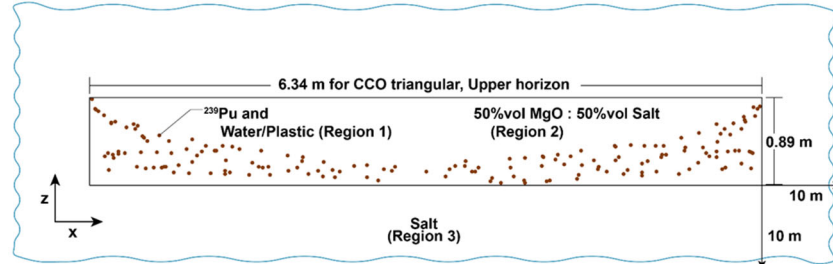


Fig. 15. Three material regions of criticality model where dimensions of Region 2 defined by maximum extent of the coordinates for CCO centers, which change somewhat per simulation (Region 2 dimensions shown for CCOs in upper horizon initially as triangular array).

#### V.C.4. Geometry: Irregular CCO Array Configuration

The coordinate positions of CCOs for the irregular, non-uniformly compacted array are used in the criticality analysis. The dimensions of Region 2 are defined by the maximum extent of the coordinate positions of the corresponding simulation (e.g., CCO emplaced in upper horizon as triangular array—Fig. 15). The ~2-m slice uses periodic boundary conditions to represent a room segment of infinite extent down its axis (y-direction), but also examines the influence of mirror boundary conditions.<sup>16</sup>, Table E-1

#### V.C.5. Geometry: Idealized Uniform Array

A criticality analysis of an idealized regular, uniformly compacted CCO array is also conducted to more fully explain behavior observed in the irregular, non-uniformly compacted array. This supporting uniform analysis assumes that the CCO array remains intact (i.e., CCOs remain vertical and in 3 tiers); only the spacing between the CCC decreases, similar to previous criticality analysis. The CCOs are placed in a triangular array with alternating 17 and 18 CCOs per row when uniformly spaced.

The uniform criticality analysis uses both a 25% and 50% reduction in uniform horizontal spacing. The latter value corresponds to the early ORNL criticality analysis using uniformly compacted CCO arrays.<sup>13, 44</sup> The 50% reduction bounds the observed range for the irregular array (i.e., between 39.0% and 42.4% horizontal closure (Fig. 17) and corresponds to 14.3-cm radius reduction of the 28.7-cm radius CCO (Fig. 1).

The reasonableness of the 25% lower bound of overall compaction observed at the center of the room is explained as follows. Although the decrease in vertical spacing could follow a similar idealized adjustment, the criticality analysis sets the CCC collapse to the height of the waste inside the CCC.

The width of the gap between the salt wall and CCOs is (Fig. 16)<sup>12</sup>

$$L_x^{gap} = L_x - L_x^{CCOs} \quad (8)$$

where

$$L_x^{CCOs} = n_x^{CCOs} L_x^{Drum}$$

and  $n_x^{CCOs}$  is 14 CCO/row.

The total room closure is the sum of the closure on the left and right, and where no closure occurs down the axis of the room segment (i.e., plane strain) (Fig. 16):

$$\delta_x = \delta_x^{left} + \delta_x^{right} \quad (9)$$

$$\delta_y = 0 \quad (10)$$

The corresponding compaction of the intact array of CCOs is

$$\delta_x^{CCOs} = \left( (\delta_x - L_x^{CCOs}) + |\delta_x - L_x^{CCOs}| \right) / 2L_x^{CCOs} \quad (11)$$

$$\delta_y^{CCOs} = 0 \quad (12)$$

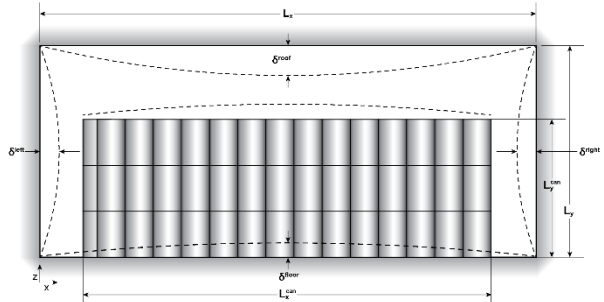


Fig. 16. Room closure of uniform array of CCOs.<sup>12</sup>

The average uniform horizontal compaction of CCCs of all four cases initially arranged in triangular and hexagonal arrays in the upper and lower horizons is 26.85% (Fig. 17) and corresponds to 7.7-cm radius reduction of the 28.7-cm radius CCO (Fig. 1). The percentage compaction includes the emplaced void space within the room, which shows as an offset in Fig. 17.

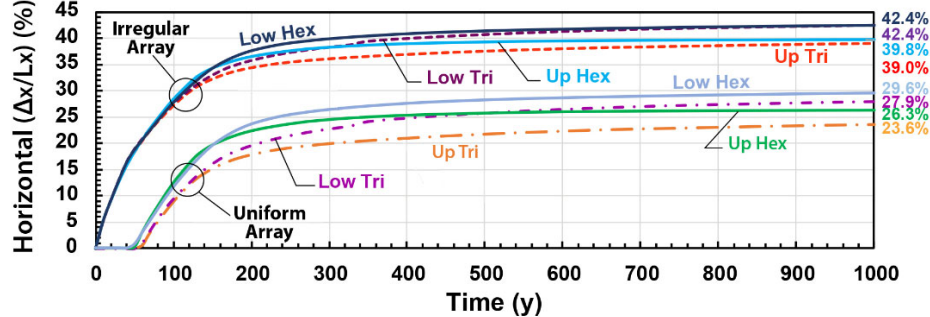


Fig. 17. Range of horizontal room closure in modeled irregular and idealized uniformly compacted CCO arrays initially emplaced as triangular and hexagonal arrays in upper and lower repository horizons.<sup>12</sup>, Fig. 10

#### V.C.6. Geometry: Fissile Shape

The criticality analysis places cylinders, bound by the original CCC diameter, or spheres of fissile material at the centers of the deformed CCO arrays. For the cylinders and spheres, the Pu waste form in any handling convenience containers is combined and centered in the CCC pipe, since a combined mass of fissile material is more applicable to a generic waste and concentrating the Pu mass is more conservative.

The diameter of the CCC, inside the CCO, constrains the fissile shape until the CCC corrodes. To be consistent with no gas generation and thereby maximum salt-creep compaction, no CCC corrosion is assumed. Yet, a sphere (usually the most reactive shape for criticality analysis) optimally moderated with hydrogenous material cannot fit inside a 7.7-cm radius CCC (inside radius). A sphere with insufficient hydrogenous material is often less reactive than a cylindrical shape. Hence, cylinders of three radii (4.80, 6.25, 7.70 cm) are used, where the cylinder height is determined by the amount of  $^{239}\text{Pu}$ , moderator, and filler in the fissile Region 1. For the criticality analysis with cylinders, the model uses the final orientation of the CCC.

An *unconstrained* spherical shape for the fissile Region 1 (where the radius is determined by the  $^{239}\text{Pu}$ , moderator, and filler in the CCC) is also examined because a spherical shape avoids making assumptions as to the initial distribution of Pu in generic waste forms and the compaction of that material within the CCC from salt creep.

#### V.D. Room Reactivity with and without Filler Material in Fissile Region

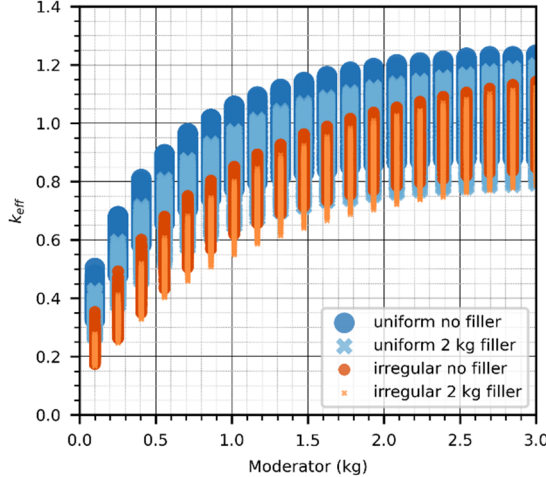
##### V.D.1. Generic and Carbon Filler

Without any filler homogeneously mixed in the fissile Region 1, the allowable hydrogenous moderator in the CCO at emplacement is  $\leq 1.69$  kg for the representative irregular, non-uniformly compacted array (Fig. 18 and Table II). For the more reactive bounding regular, uniformly compacted CCO array, the allowable hydrogenous moderator is  $\leq 0.82$  kg.

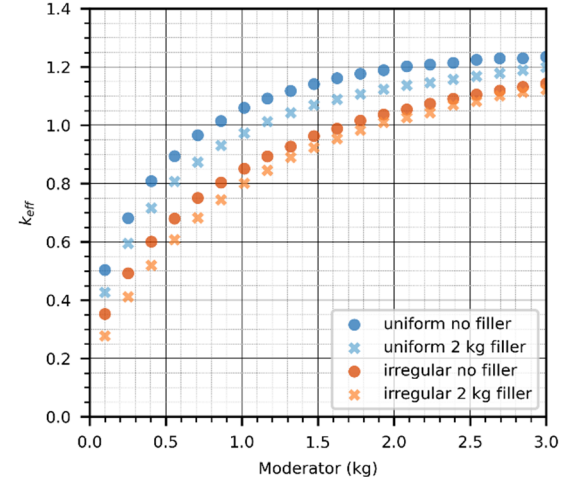
Including a non-hydrogenous homogeneous filler in the fissile region substantially reduces the reactivity of an irregular non-uniformly and regular, uniformly compacted CCO array, whether the filler material is conservatively modeled as graphite or a representative generic material (modeled here as cement-like silicon dioxide, magnesium oxide material).

For an irregular, nonuniformly compacted array, adding 2 kg of filler decreases  $k_{\text{eff}}$  by 0.03 near  $k_{\text{eff}}$  of unity and increases the maximum mass of allowed moderator by 11% from 1.69 kg to 1.88 kg (Fig. 18 and Table II). For a regular, uniformly compacted array, adding 2 kg of either graphite or cement-like material decreases  $k_{\text{eff}}$  by 0.08 and increases the maximum allowable moderator mass by 37% from 0.82 kg to 1.12 kg.

In Fig. 18a, the variation band at each discrete moderator mass is caused by the variation in all other parameters examined in the criticality analysis besides the presence or absence of 2 kg of filler. The maximums are more readily observed in Fig. 18b.



(a) Full range of variation



(b) Maximum values

Fig. 18. Adding 2 kg graphite or non-hydrogenous generic filler to fissile region moderately reduces reactivity of irregular, non-uniformly compacted CCO array; similar trend observed for more reactive regular, uniformly compacted CCO array.

For an irregular compacted array, adding 4 kg of filler increases the maximum mass of allowed moderator by 20% (factor of 1.20 greater) from 1.69 kg to 2.02 kg (Fig. 19 and Table II). For a uniformly compacted array,

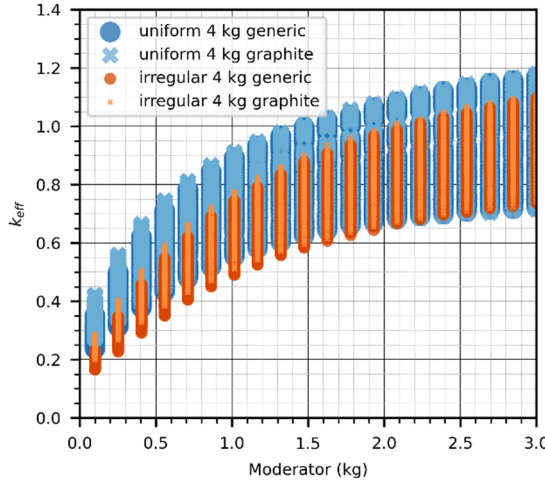
adding 4 kg graphite/cement-like material increases the maximum allowable moderator mass by 76% from 0.82 kg to 1.44 kg.

Table II. Allowable Moderator Mass per CCO with Non-Hydrogenous Filler and Metal Mixed in Fissile Region with Subcriticality Limit of Unity

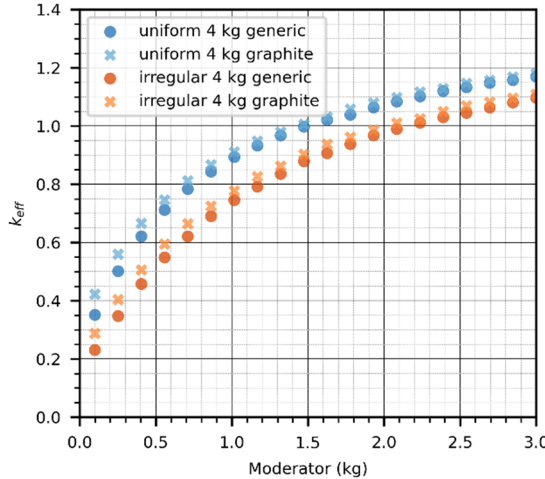
CCO Array	Allowable Moderator Mass per CCO in Upper Horizon (kg)						
	Non-Hydrogenous Graphite/Generic Filler					Stainless Steel Material	
	No Filler	2 kg Filler	Increase from No-Filler Case	4 kg Filler	Increase from No-Filler Case	1 kg Material	Increase from No Filler Case
Irregular with spheres	1.69	1.88	Δ0.19—11%	2.02	Δ0.33—20%	1.86	Δ0.17—10%
Uniform with cylinders	0.82	1.12	Δ0.30—37%	1.44	Δ0.62—76%	0.93	Δ0.11—13%
Δk <sub>eff</sub> from irregular <sup>a</sup>	0.225	0.15		0.10		0.20	

The maximum  $k_{eff}$  in the irregular array for either the 4 kg of generic/cement-like filler or 4 kg of graphite filler are similar (Fig. 19). The allowable moderator mass is 1.49 kg for generic/cement-like filler and 1.44 kg for graphite filler at  $k_{eff}$  of unity (3.4% difference). The same is true for the uniform array. The allowable moderator mass is 2.16 for generic/cement-like filler and 2.02 kg

for graphite filler at  $k_{eff}$  of unity (7% decrease). The influence of the two fillers is primarily the change in the volume of the fissile region and the corresponding change in neutron leakage. This geometric influence on leakage dominates over the difference in reflection or absorption of neutrons.



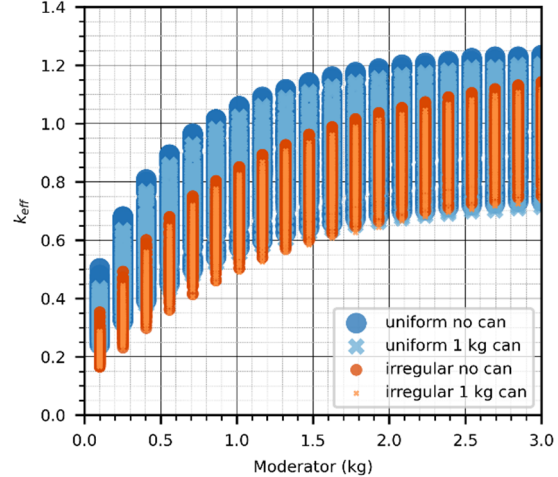
(a) Full range of variation



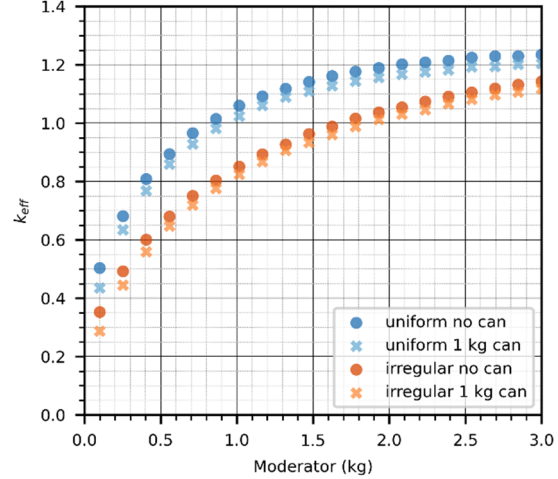
(b) Maximum values

Fig. 19. Adding 4 kg graphite and generic/cement-like filler have similar influence on maximum reactivity and allowable moderator for irregular, non-uniformly compacted and regular, uniformly compacted CCO arrays. V.D.2. Metallic Filler

The addition of metal homogeneously mixed in the fissile region is perhaps unrealistic in a practical sense but instructive for comparison to the non-hydrogenous graphite/generic filler, since some stainless steel from handling canisters may be present. For an irregular array, adding 1 kg of the metal components of stainless-steel filler to a mixture of Pu and polyethylene decreases  $k_{eff}$  by 0.025 near  $k_{eff}$  of unity and increases the allowable moderator mass by 10% from 1.69 g to 1.86 g (Fig. 20 and Table II.). The metal filler is about twice as effective as graphite/generic filler. For a uniformly compacted array, adding 1 kg of stainless-steel filler increases the allowable moderator mass by 13% from 0.82 kg to 0.93 kg



(a) Full range of variation



(b) Maximum values

Fig. 20. Stainless steel material from handling canisters in fissile region substantially reduces reactivity of uniform array and moderately reduces reactivity of irregular CCO array. V.D.3. Mixing of Pu, Moderator, and Filler

In most criticality analysis discussed here, Pu, moderator, and filler in the fissile region is modeled as a homogeneous mixture (with  $^{239}\text{Pu}$  mass fixed at 380 g). Homogeneous mixtures of Pu (and U) at *high* enrichments are usually more reactive than heterogeneous mixtures<sup>46</sup>, Fig. 31

#### V.D.4. Influence of Spherical and Cylindrical Fissile Region on Reactivity

For a fissile region *constrained* by the CCC with 7.7 cm maximum inside radius, a cylindrical representation is more reactive for both the irregular, non-uniformly compacted and the regular, uniformly compacted CCO array (Fig. 21). The cylindrical representation has a wide range of reactivity because both the radius and height vary.

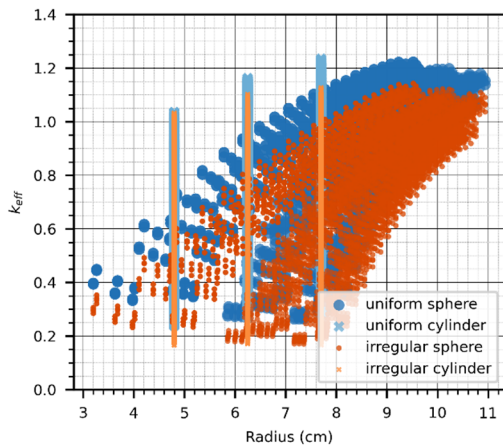
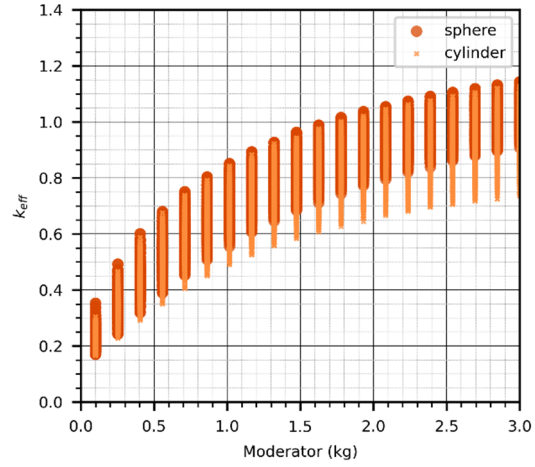


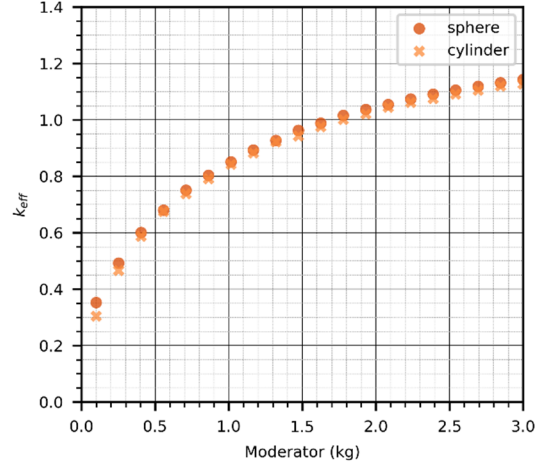
Fig. 21. Cylindrical representation most reactive if fissile region constrained by 7.7 cm radius of CCC in both irregular, non-uniformly compacted and regular, uniformly compacted CCO array.

However, an *unconstrained* spherical representation of the CCO fissile region is slightly more reactive than the cylindrical representation for the irregular CCO array (Fig. 22). Consequently, this analysis uses the unconstrained spherical representation for the irregular CCO array, as a convenient modeling conservatism, because the difference is small ( $\Delta k_{eff}$  of 0.025 near  $k_{eff}$  of unity, which translates into allowable moderator of 1.77 kg for cylinder versus 1.69 kg (5% difference) for unconstrained sphere representation).

For the uniformly compacted array, a cylindrical representation of the fissile region is more reactive than an unconstrained spherical representation ( $k_{eff}$  is 0.92 for unconstrained spherical representation versus unity for a cylindrical representation at allowable moderator mass of 0.82 kg—Fig. 23b).



(a) Full range of variation

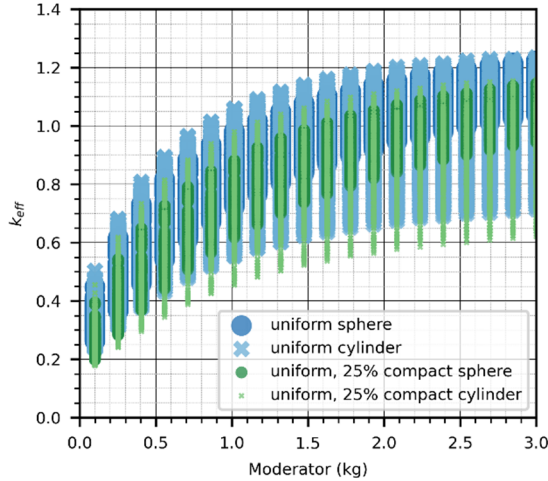


(b) Maximum values

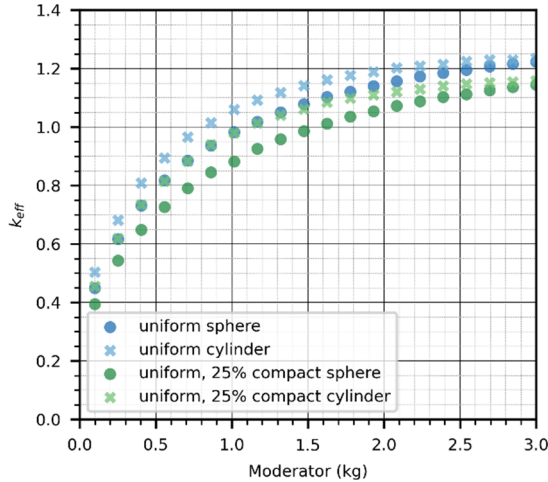
Fig. 22. Unconstrained spherical fissile region slightly more reactive than cylindrical fissile region for irregular, non-uniformly compacted CCO array.

In most analysis with the uniformly compacted array, a bounding horizontal compaction of 50% is used. However, as shown above (§V.C.5) the actual horizontal compaction of a uniformly compacted CCO array is much closer to 25% (Fig. 9), and the allowable moderation is 1.11 kg for cylindrical fissile region, an increase from 0.82 kg of 35% (Fig. 23).

For the uniformly compacted array, the most reactive cylindrical CCO array changes from the smallest 4.8-cm radial cylinder at low moderation to the largest 7.7-cm radial cylinder at high moderation (Fig. 24). The behavior is similar for irregular, non-uniformly compacted CCO array but the transition to the largest radius occurs at higher moderation.



(a) Full range of variation

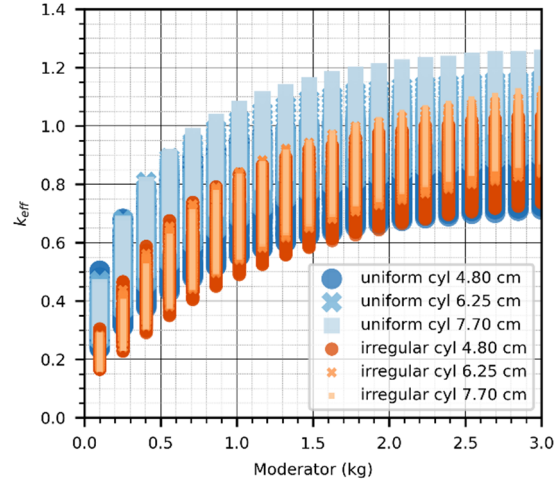


(b) Maximum values

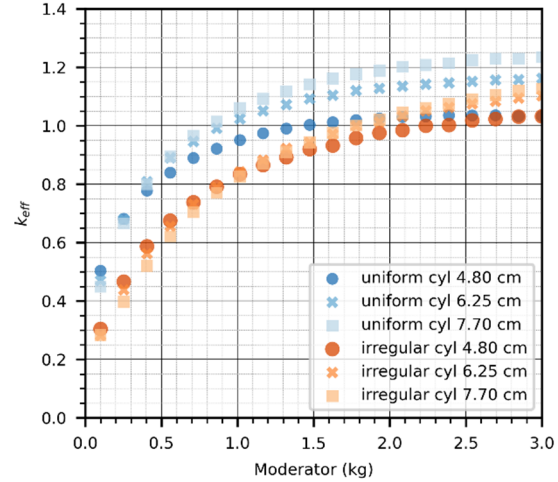
Fig. 23. Cylindrical representation of fissile region for 50% and 25% uniformly compacted array remains more reactive than unconstrained sphere.

The uniformly compacted array results suggest an allowable threshold of 0.82 kg moderator when no credit is taken for graphite/generic filler but a large benefit for accounting for the graphite/generic filler (76% increase in moderator mass) whereas the more representative irregular array has a high threshold of allowable 1.69 kg moderator when no credit is taken for graphite/generic filler and moderate benefit for accounting for either the graphite/generic filler (18%).

The reason for the different influence of the filler is that for the uniformly compacted array, the disk-like cylinders of the fissile region (which are most reactive) are stacked on top of each other to form essentially a single stub cylinder (with similar height to diameter ratio) that is very reactive with essentially the  $^{239}\text{Pu}$  mass of three CCOs.<sup>75, Fig. 1</sup>



(a) Full range of variation



(b) Maximum values

Fig. 24. Largest reactivity of irregular, non-uniformly compacted CCO array with cylindrical fissile region changes from smallest radius at low moderation to largest radius at high moderation; behavior is similar for uniformly compacted CCO array but the transition to the largest radius occurs at lower moderation.

The reactivity greatly decreases (leakage greatly increases) for the uniformly compacted array as the height of the cylinder is increased to include the graphite/generic filler. To elaborate, the cylindrical fissile region no longer has similar height to diameter ratio because the cylindrical fissile region elongates axially as filler is added since the cylinder cannot expand radially beyond the maximum CCC diameter.

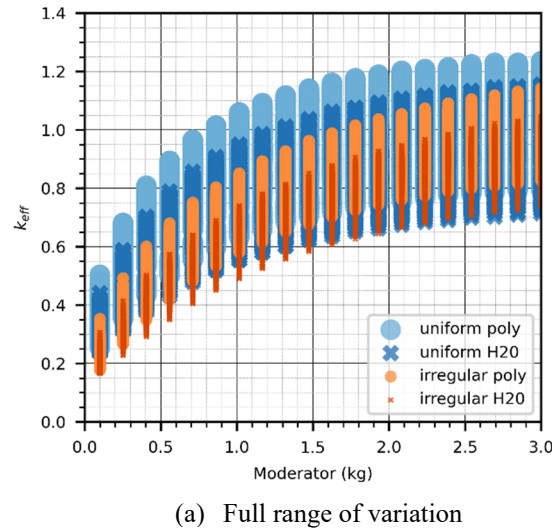
In contrast, the irregular non-uniformly compacted array with spheres are scattered about the room and the reactivity does not change much (i.e., leakage in the system does not greatly increase) as the fissile region radius increases to accommodate the filler.

## VI. INFLUENCE OF OTHER PARAMETERS ON ROOM REACTIVITY WITHOUT B<sub>4</sub>C

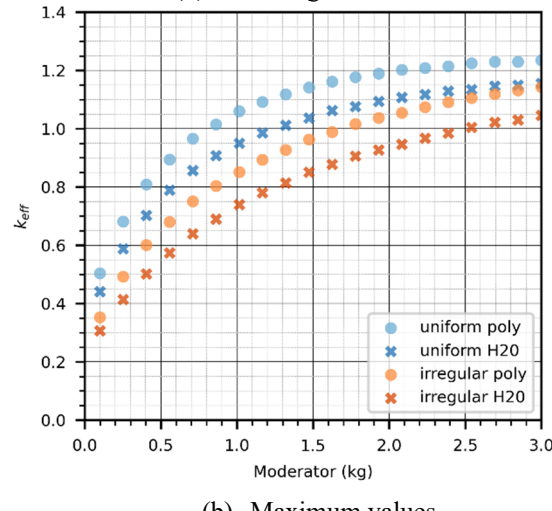
### VI.A. Room Reactivity with Material in Fissile Region

#### VI.A.1. Water and Polyethylene Moderator

As expected, water as the sole moderator in the fissile region is much less reactive than polyethylene as moderator (Fig. 25):  $k_{eff}$  is reduced by 0.125 near  $k_{eff}$  of unity and the allowable moderator mass increased by ~50% for both the irregular, non-uniformly compacted and regular, uniformly compacted CCO array.



(a) Full range of variation



(b) Maximum values

Fig. 25. CCO array with water moderator less reactive than polyethylene moderator for irregular array; the uniform array follows a similar trend.

Specifically, the allowable moderator mass substantially increases from 1.69 kg polyethylene moderator to 2.51 kg water moderator for the irregular CCO array (Fig. 25). For the uniformly compacted CCO array, the allowable moderator mass increases from 0.82 kg polyethylene moderator to 1.26 kg of water.

#### VI.A.2. Density and Salt/MgO Proportion

In the criticality analysis model, ~118 kg MgO per CCO is in a disposal room as follows: The volume of the reflector box at 1000 years when modeling 168 CCOs is ~12.4 m<sup>3</sup> (i.e., 6.05-m length, 0.95-m height, and 2.08-m model width—Fig. 15). For MgO with a grain density of 3600 kg/m<sup>3</sup>, the MgO mass in one-half of the reflector box is 19.8 metric tons at the final total room porosity of 0.08 in CCA-1996 (because MgO and salt is mixed in a 1:1 ratio).

The specific amount of MgO in an actual WIPP disposal room is determined by the container contents and is adjusted daily for the emplaced container batch.

The MgO mass emplaced in a disposal room ( $m^{MgO}$ ) is calculated based on the disposal room mass of cellulose ( $m^c$ ) rubber ( $m^r$ ), and plastics ( $m^p$ ) with a safety factor ( $f_{MgO}^{safety}$ ), and assumes a one-to-one correspondence between CO<sub>2</sub> produced and carbon in (a) cellulose (C<sub>6</sub>H<sub>10</sub>O<sub>5</sub>) waste, (b) rubber waste, and (c) factor of 1.7 for plastic waste:

$$m^{MgO} = [6f_{MgO}^{safety} (m^c + m^r + 1.7m^p) / 162 \text{ g /mole cellulose}] + m_{lost}^{MgO} [40.3 \text{ g /mole MgO}]$$

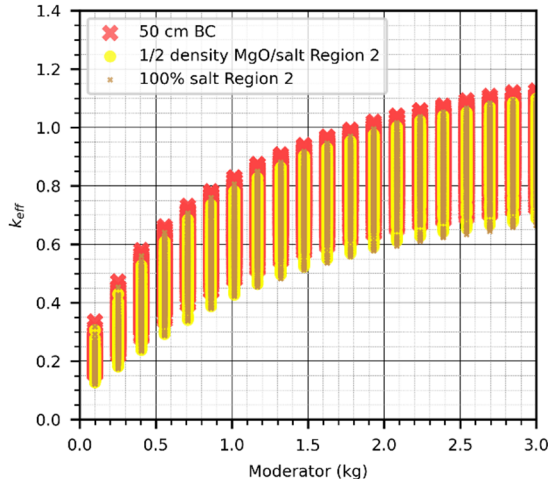
where  $m_{lost}^{MgO}$  is fixed mass of MgO lost to brine flow ( $6.9 \times 10^7$  moles MgO in entire repository or 90 moles MgO per 55-gallon drum assuming 76 356 drums per panel and 10 panels in the original WIPP repository). After May 2008, a safety factor of 1.2 must be maintained above the estimated amount necessary to react with the cellulose, plastic, and rubber contents in a container.

CCCs containing surplus Pu generally have only a small amount of plastic used to bag the handling cans (to reduce the possibility of Pu contamination in the packaging facility). For 0.40 kg polyethylene per CCO and 15.2 kg of plywood per CCO, 32 kg of MgO per CCO is required (or about one 1905-kg MgO sack on every third 7-pack column of CCOs). Hence, ~3.7 times more MgO is placed in a room segment in the model as necessary.

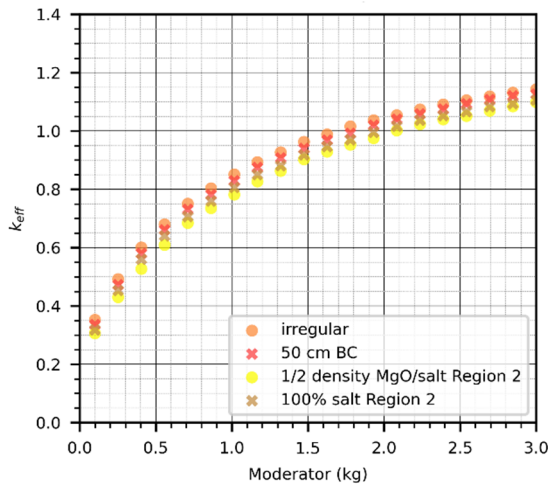
MgO reflects neutrons and thereby contributes to reactivity. MgO also dilutes the salt, which is the most important interstitial component in Region 2 for absorbing neutrons and isolating CCOs. Yet, the influence of the excess MgO is small since the reactivity with 100% salt is only slightly less (i.e.,  $k_{eff}$  decreases by

0.025 near  $k_{eff}$  of unity—Fig. 26). Reducing the density of MgO/Salt mixture by one-half, assuming salt consolidation is not complete, also has a small influence (i.e.,  $k_{eff}$  decreases by 0.08 near  $k_{eff}$  of unity—Fig. 26).

When examining the reactivity difference between salt and MgO, the boundary of Region 2 was enlarged by 50 cm to accommodate changes in material. The slight decrease in reactivity is displayed in Fig. 26 in addition to the decrease in reactivity from changing salt and MgO density and proportion.



(a) Full range of variation



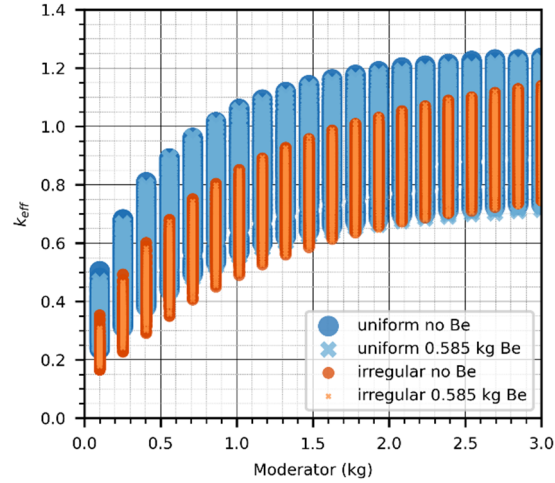
(b) Maximum values

Fig. 26. Influence of MgO in Region 2 on system reactivity is small.<sup>14, App. L</sup>

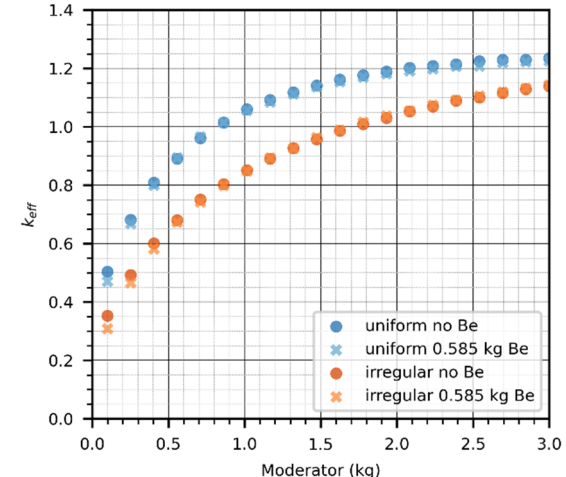
#### VI.A.3. Beryllium Influence

Excluding Be/BeO special reflector material from the fissile region has little influence on reactivity near  $k_{eff}$  of unity ( $k_{eff}$  decreases by <0.01 and allowable moderator increases  $\sim 0.03$  kg) for both the irregular and uniform CCO array (Fig. 27). However, the influence of Be/BeO

is stronger away from a  $k_{eff}$  of unity: Excluding Be/BeO slightly reduces reactivity at low and high moderation for the uniformly compacted array and reduces reactivity at low moderation for the irregular array.



(a) Full range of variation



(b) Maximum values

Fig. 27. Adding 0.585 kg Be/BeO has little influence on reactivity for  $k_{eff}$  near unity but does slightly reduce reactivity below and above  $k_{eff}$  of unity.

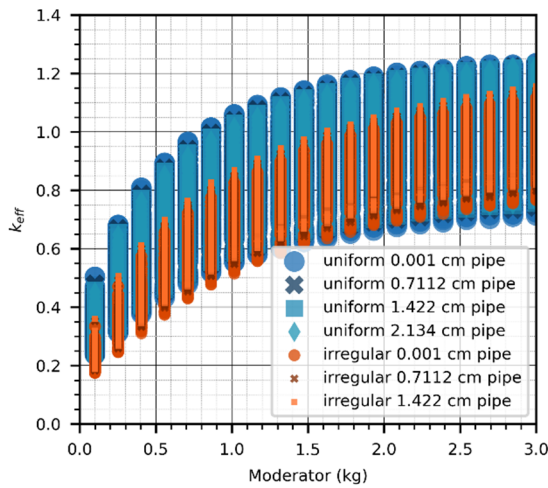
#### VI.B. CCC Stainless Steel Around Fissile Region

For the irregular array base case, a 0.71-cm discrete stainless-steel reflector is set around the fissile Region 1 (Fig. 15), which is the thickness of the CCC. The allowable moderator mass is 1.69 kg. A 1.41-cm thick discrete stainless-steel reflector around the fissile Region 1, which is twice the thickness of the CCC, slightly increases  $k_{eff}$  by 0.03 near  $k_{eff}$  of unity. The corresponding allowable moderator mass decreases 5% to 1.61 kg (Fig. 28).<sup>14, App. O</sup> If the stainless-steel reflector is removed,  $k_{eff}$  decreases by 0.05 and the allowable moderator mass

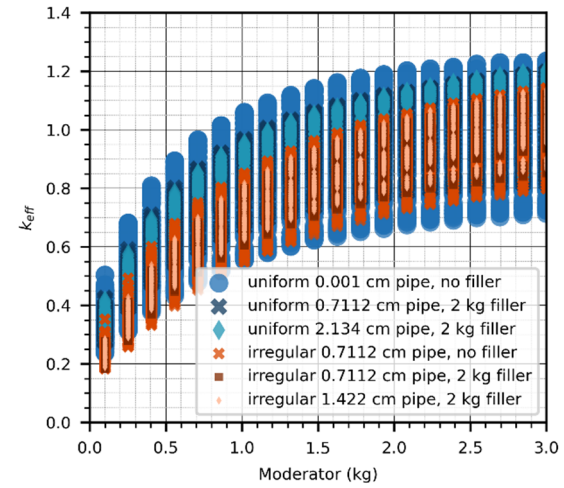
increases 11% to 1.87 kg. The stainless-steel reflector increases reactivity by reflecting neutrons back into the fissile region.

A reflective thickness twice the thickness of the 0.71-cm CCC considers the possibility of a handling can used inside the CCC. While the allowable moderator mass from 1.69 kg is reduced; recall, however, an unconstrained radial sphere was used for the irregular array that increases reactivity somewhat over a constrained cylinder and decreases allowable moderator from 1.77 kg to 1.69 kg (5% decrease—Fig. 23). Hence, the 1.69 kg limit has a 5% margin.

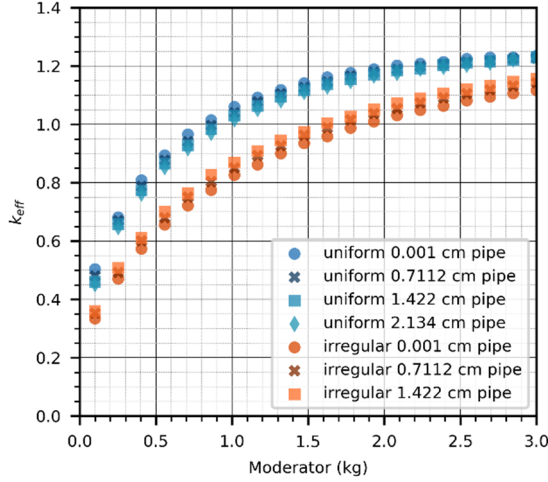
For the uniformly compacted array base case, no discrete reflector is set around the fissile Region 1.<sup>14, App. O</sup> The allowable moderator mass is 0.82 kg. A 0.71-cm thick stainless steel CCC around the fissile region slightly decreases  $k_{eff}$  by 0.020 at  $k_{eff}$  near unity and increases the allowable moderator mass 7% to 0.88 kg. A 1.42-cm thick reflector increases the allowable moderator mass 12% to 0.92 kg, and a 2.13-cm thick reflector further increases the allowable moderator mass 17% to 0.96 kg (Fig. 28b).



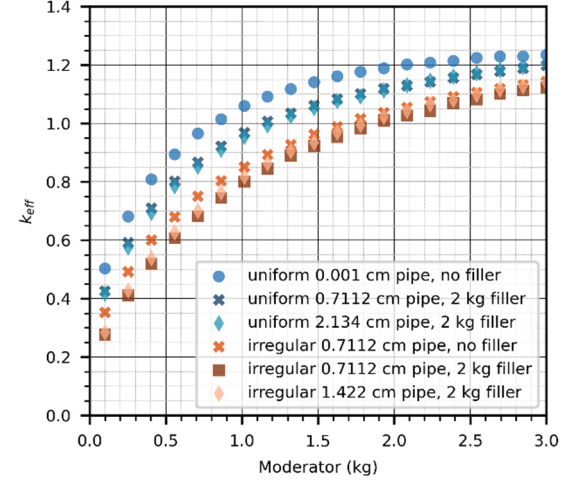
(a) Full range of variation without filler



(c) Full range of variation with filler



(b) Maximum values without filler



(d) Maximum values with filler

Fig. 28. Stainless-steel reflector, twice thickness of CCC, slightly changes the reactivity of irregular and uniformly compacted CCO arrays.

Although the stainless-steel CCC still increases neutron reflection in the uniform array, the competing increased isolation of the fissile regions from the stainless-steel CCC is more important and reduces the reactivity, because the close proximity of fissile regions in the uniformly compacted array benefit greatly from neutron interactions. In the comparison here, the cylindrical radius of the fissile Region 1 for the uniform array is defined by the inside CCC radius—7.7-cm—and, thus, the CCC thickness does not decrease the fissile Region 1 radius.

The reflector still decreases the allowable mass when 2 kg of filler is included in the fissile Region 1 for the irregular array; however, the 2 kg of filler dominates the behavior and so the allowable mass increases overall. As noted previously (§V.D.1), 1.69 kg of moderator mass is allowed for irregular array with 0.71-cm discrete reflector with no filler. With 2 kg filler the allowable moderator mass increases to 11% to 1.88 kg. Similarly, 1.61 kg of moderator mass is allowed for irregular array with 1.42-cm discrete reflector with no filler. With 2 kg filler, the allowable moderator mass increases 12% to 1.81 kg (Fig. 28d).

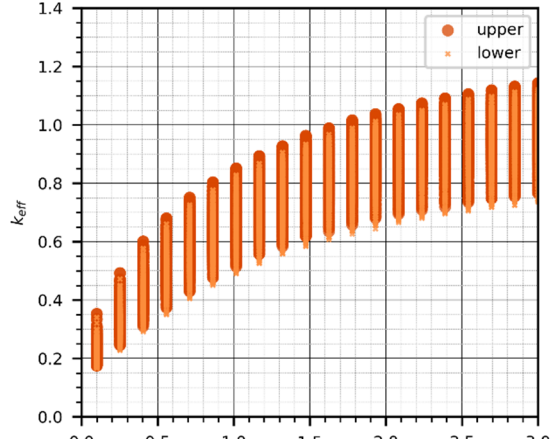
For the uniform array, the reflector increases isolation and so the allowable moderator mass increases with the increase in reflector thickness and filler mass. With no reflector, the allowable moderator mass increases 37% from 0.82 kg to 1.22 kg with 2-kg filler (Fig. 28d). With 0.71-cm discrete reflector, the allowable moderator mass increases 30% from 0.88 kg to 1.14 kg with 2-kg filler. With 2.13-cm discrete reflector, the allowable moderator mass increases 25% from 0.96 kg to 1.20 kg with 2-kg filler.

### VI.C. Uncertainty from Geologic Strata Arrangement

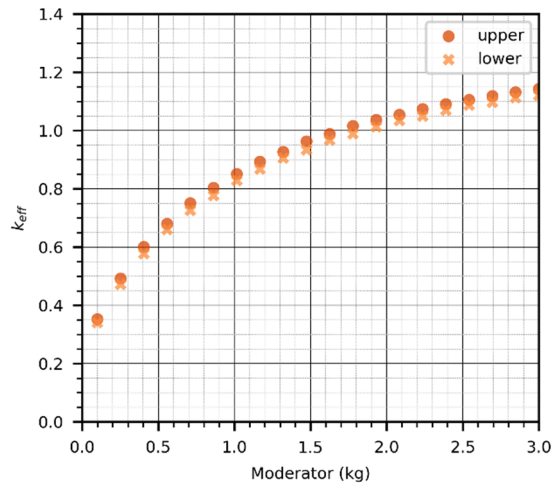
The CCO final configuration in upper horizon is more reactive;  $k_{eff}$  is ~0.025 larger in the upper horizon near  $k_{eff}$  of unity, which translates to an allowable moderator mass of 1.69 kg for CCOs placed in the upper horizon and 1.85 kg for CCOs in the lower horizon (9% increased moderator mass for lower horizon—Fig. 29 and Table II).

### VI.D. Minor Reactivity Differences between Hexagonal and Triangular Arrays

The slightly wider range in closure and concentration of CCOs initially emplaced in a hexagonal array translates into a slightly wider range of reactivity than CCOs initially emplaced in a triangular array (Fig. 30). In turn, the maximum moderator mass is 1.69 kg for a hexagonal array (§IV.D.1) and slightly increases to 1.74 kg for a triangular array without filler (3% increase).



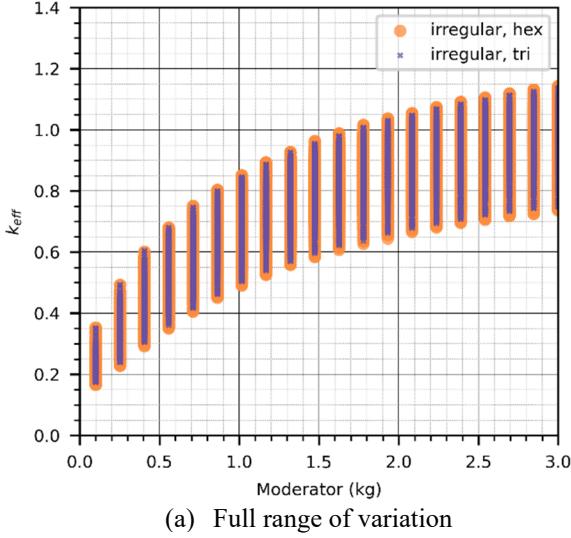
(a) Full range of variation



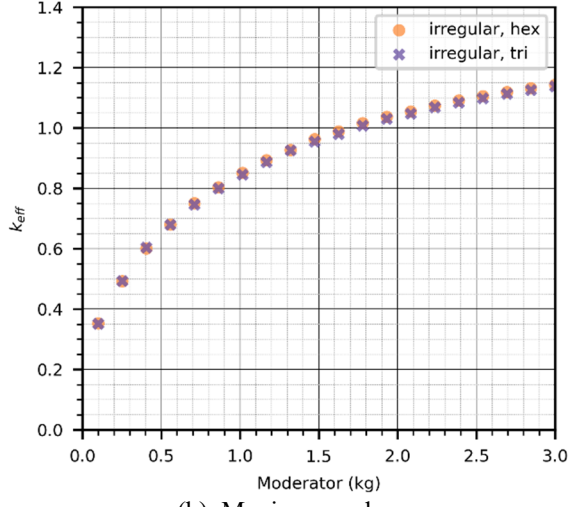
(b) Maximum values

Fig. 29. Reactivity of irregular CCO array in upper horizon greater than in lower horizon of repository when initially emplaced in hexagonal array

For the situation with filler the maximum moderator mass is 2.02 kg for a hexagonal array (§IV.D.1) and slightly increases to 2.08 kg for a triangular array with filler (3% increase). Thus, the room reactivity is only slightly influenced by the (1) initial CCO configuration (hexagonal versus triangular); (2) slight changes in fissile area mass (3.15 kg  $^{239}\text{Pu}/\text{m}^2$  for 153 CCOs initially in hexagonal array versus 3.57 kg  $^{239}\text{Pu}/\text{m}^2$  for 168 CCOs initially in triangular array); and (3) boundary conditions to represent room segment of infinite extend down its axis (mirror boundary conditions for hexagonal array versus periodic boundary conditions for triangular array).



(a) Full range of variation



(b) Maximum values

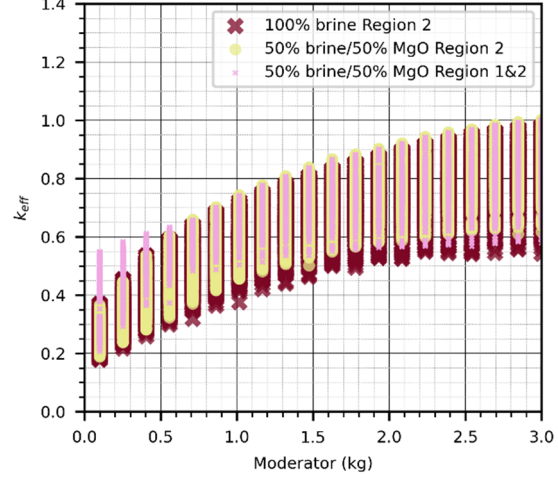
Fig. 30. Reactivity of irregular compacted array initially emplaced in a hexagonal configuration is similar to an irregular compacted array initially emplaced in a triangular configuration.

#### VI.E. Reduced Reactivity when Brine Enters Room

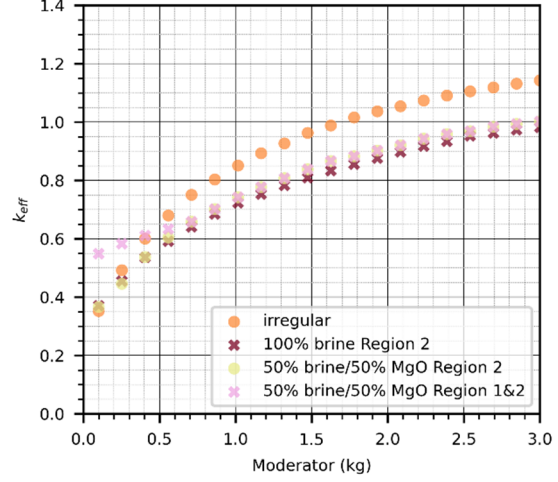
Some brine may enter a disposal room with creep closure, but on average little brine is present in the undisturbed scenario. However, much brine may enter a disposal with a hypothetical human intrusion. The presence of brine in Region 2 reduces the room  $k_{eff}$  by  $\sim 0.15$  to the point that 3 kg of moderator per CCO is allowable (Fig. 31).

Previous analysis with POCs also shows that the presence of brine greatly reduces the room reactivity.<sup>1</sup>, Fig. 28; <sup>16</sup> In contrast, however, brine present in fissile Region 1 (as could occur after extensive corrosion and brine inundation) does not reduce reactivity. In fact, the influx of brine provides some hydrogen and increases reactivity when the CCC has very low initial moderation

at emplacement. This influence is somewhat artificial, however, since the hydrogen in the brine is not included in the summed moderator mass on the horizontal axis of Fig. 31).



(a) Full range of variation



(b) Maximum values

Fig. 31. Presence of brine in Region 2 greatly reduces room reactivity filled with CCOs.

#### VI.F. Reactivity as Room Creeps Closed

Although more readily apparent for CCOs uniformly compacted, the reactivity of a room non-uniformly compacted into an irregular array also generally increases as a room creeps closed. That is, the maximum opportunity for criticality generally occurs at maximum room closure at 1000 years because spacing is so important to determining room reactivity (Fig. 32).

However, the reactivity can be driven by local conditions in the irregular array. Between a moderator mass of 1.3 kg and 1.5 kg in the CCC, the reactivity is slightly higher at 600, 800, and 900 years than at 1000 years. The maximum difference between  $k_{eff}$  at 1000 years and earlier times is 0.16%.

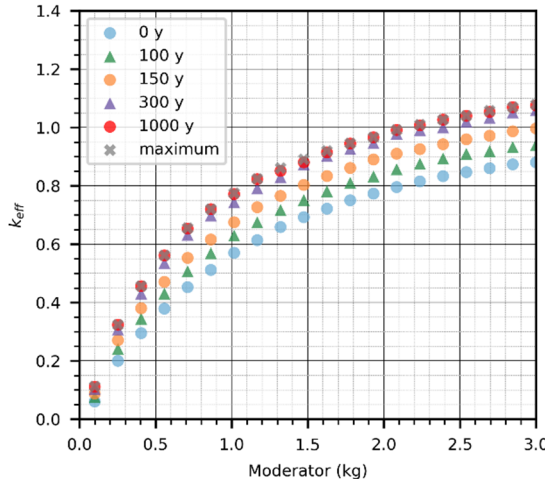


Fig. 32. General monotonic increase of reactivity as room creeps closed in upper repository horizon filled with CCOs using polyethylene CCC, 100% polyethylene moderator, and without any filler or beryllium.

### VI.G. Correlation of CCO Concentration with Neutron Flux

As noted above in §V.C, room reactivity depends upon (1) type, mass, and form of fissile material; (2) material mixed with the fissile material and its overall concentration; (3) nearby material and its concentration outside the fissile array, and (4) shape including individual spacing and array configuration of fissile regions. However, the individual spacing of fissile regions plays a primary role for a compacted room as described below.

The spatial distribution of the simple and relative weighted concentrations for CCOs initially placed in a hexagonal array in the lower and upper horizon show the highest simple and relative-weighted CCO concentrations are on either side of the room near the collapsed room wall (between 10% and 40% of the distance to the room center) (e.g., Fig. 33).

A neutron flux evaluation considered fluxes in the irregular array with periodic boundary conditions at 1000 years with 585 g Be/BeO. The analysis determined the high flux regions for CCO arrays with/without stainless steel reflector and with/without 2 kg or 4 kg of graphite filler for polyethylene moderator mass of 1.016 kg, 1.168 kg, 1.231 kg, 3.00 kg (twelve cases overall).

For the lower horizon, the neutron flux is dominated by an area on the left side of a room, which correlates with the maximum simple (Fig. 33) and relative-weighted CCO concentration (Fig. 34). In all cases, the highest flux occurred at CCO 117 ( $\{-2.315, 0.191, -5.406\}$  with large star symbol), which overlays the maximum relative-weight flux.<sup>14, App. M</sup> The second

highest fluxes were at either CCO 18 or 29 ( $\{-2.160, 0.230, -5.425\}$  or  $\{-2.207, 0.056, -5.459\}$ , respectively, with  $\times$ 's)—Fig. 33 or Fig. 34).

In solving for the reactivity of the room, generally SCALE focuses on an area with the highest flux and ignores other areas of the room (i.e., it does solve a reactivity and flux field). Hence, the flux analysis also forced SCALE to focus on the right side of the room. In all but 3 cases, the maximum flux on the right side in the lower horizon was at CCO 94 (point  $\{2.496, 0.154, -5.544\}$  with large plus symbol).<sup>14, App. M</sup> Three other points (80, 73, and 74 in rank order are also shown ( $\{1.855, -0.523, -5.631\}$ ,  $\{2.062, -0.607, -5.490\}$ , and  $\{2.048, -0.458, -5.628\}$  with plus symbols).

In the upper horizon, the simple concentrations are fairly symmetrical on both sides of the room (more so than for the lower horizon—Fig. 33 versus Fig. 35); but, the relative-weighted concentration is asymmetrical with the maximum on the right side (Fig. 36). In all but two cases, however, the highest neutron flux occurred on the opposite left side of the room at CCO 34 ( $\{-2.762, -0.384, -2.832\}$  with large star symbol—Fig. 36).<sup>14, App. M</sup> The second and third highest values on the left were frequently at CCO 7 and CCO 8 ( $\{-2.638, -0.283, -2.840\}$  and  $\{-2.825, -0.309, -3.038\}$ , respectively, with  $\times$ 's).

The forced analysis on the right side of the upper horizon did not have a dominant flux area but CCO 96 was the most frequent area in the 12 cases ( $\{2.800, 0.674, -2.882\}$  at large plus symbol). Three other areas in relative rank order were at CCO 88, 82, and 79 ( $\{2.929, 0.577, -2.872\}$ ,  $\{2.706, -0.906, -2.781\}$ , and  $\{2.301, -0.374, -2.977\}$ , respectively, with plus symbol). The later point coincides with the maximum relative-weighted concentration.

In summary, the simple concentration suggests general areas on the left and right sides of the room that may have high flux (e.g., general area with many magenta squares); however, the relative-weighted concentration identifies several specific areas on the left and right sides (e.g., red triangles) in this general area that are more likely to have high flux (i.e., the relative-weighted concentration is better at differentiating high concentrations in the distribution tail, as suggested by Fig. 14, that indeed correspond to high flux areas).

Although the maximum reactivity varied somewhat, the area of maximum flux usually did not change when (a) removing or adding filler, (b) removing or adding the CCC stainless steel reflector, and (c) changing the mass of polyethylene moderator since all CCOs were simultaneously changing. Consequently, the compacted spacing of CCOs plays a very important role in determining room reactivity, and reaffirms the decision to carefully develop representative, compacted CCO configurations with high-fidelity modeling.

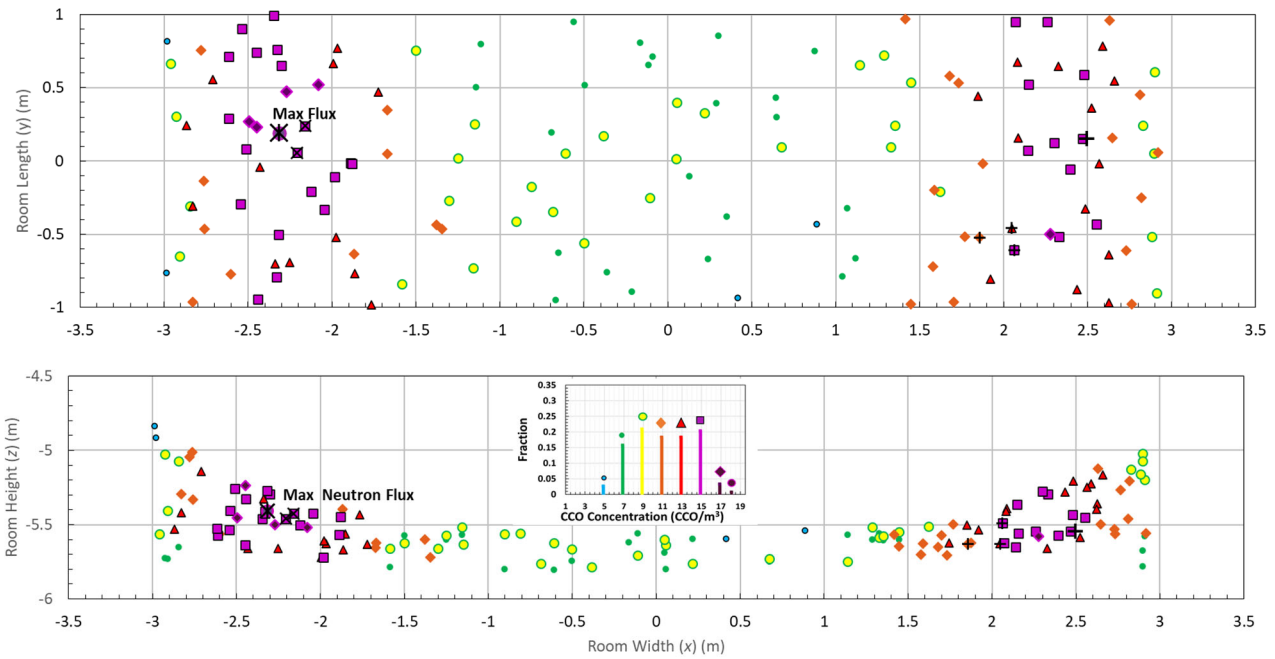


Fig. 33. Plan and side view of the spatial distribution of simple concentration at 1000 years for CCOs emplaced in a hexagonal array in the lower repository horizon; maximum neutron flux overlays maximum simple concentration.

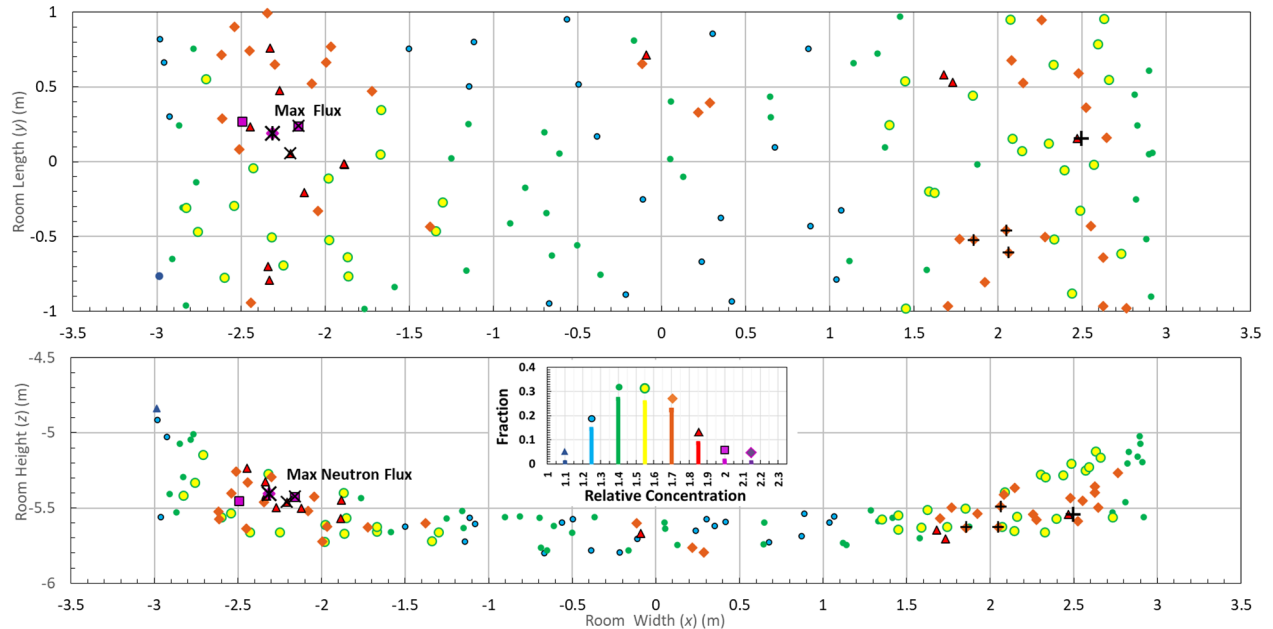


Fig. 34. Plan and side view of the spatial distribution of relative weighted concentration at 1000 years for CCOs emplaced in a hexagonal array in the lower repository horizon; maximum neutron flux overlays maximum relative weighted concentration.<sup>12, Fig. 29</sup>

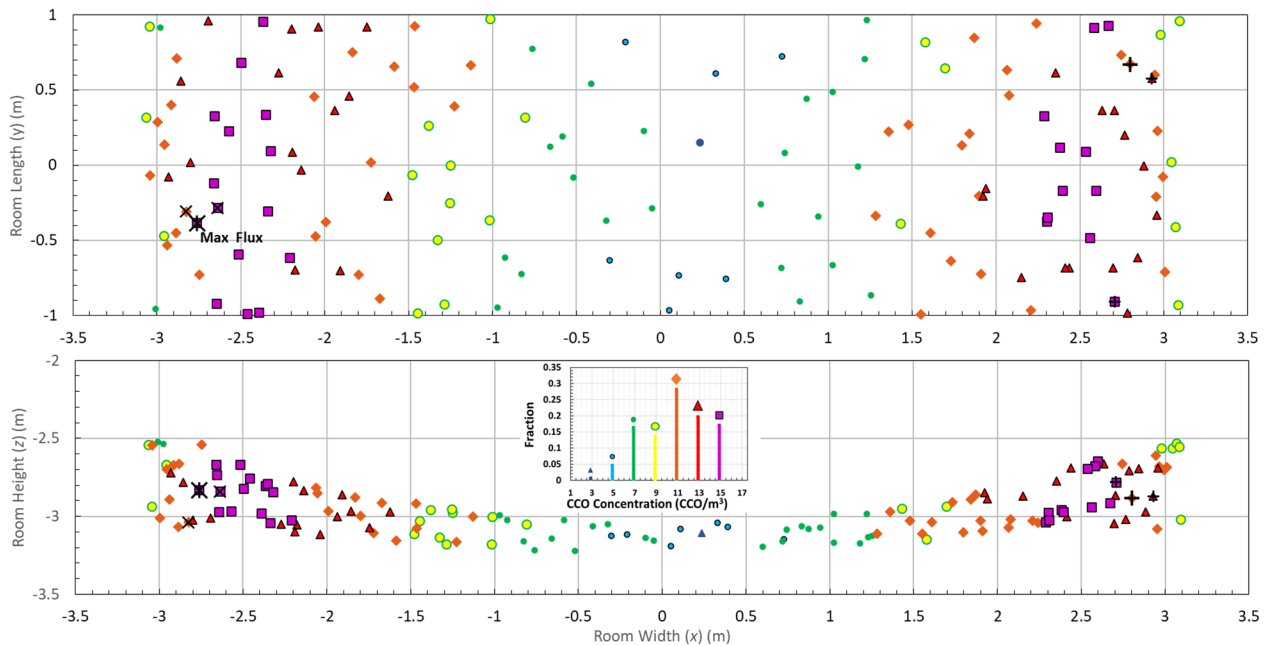


Fig. 35. Plan and side view of the spatial distribution of simple concentration at 1000 years for CCOs emplaced in a hexagonal array in the upper repository horizon; maximum neutron flux at edge of region with highest simple concentration.

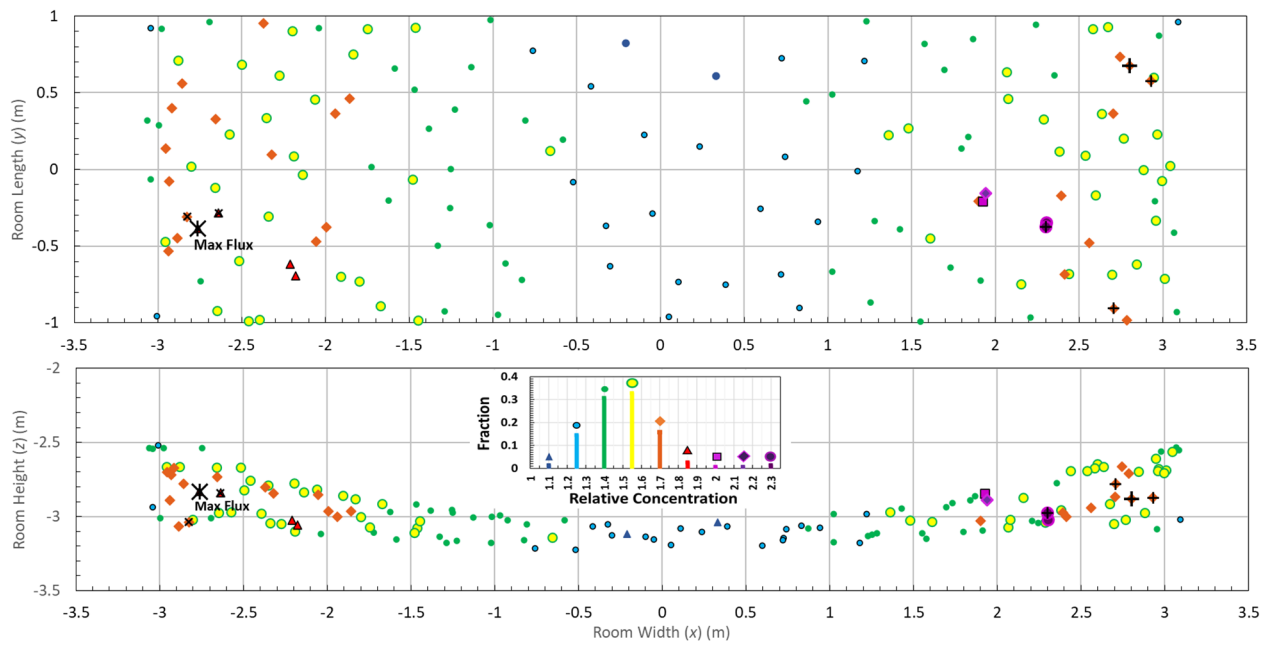


Fig. 36. Plan and side view of the spatial distribution of relative weighted concentration at 1000 years for CCOs emplaced in a hexagonal array in the upper repository horizon; maximum neutron flux at edge of region with high relative weighted concentration.<sup>12, Fig. 27</sup>

## VII. CRITICALITY ANALYSIS OF COMPACTED ARRAYS WITH BORON CARBIDE

The criticality analysis of compacted CCOs with B<sub>4</sub>C establishes the mass of B<sub>4</sub>C neutron poison necessary to prevent criticality. Other neutron poisons such as gadolinium, which forms insoluble compounds, would likely be acceptable but are not considered here.

### VII.A. Similar Conceptual Model of CCO Compaction with B<sub>4</sub>C.

The criticality analysis with B<sub>4</sub>C uses the same irregular array compaction, based on the salt-creep calculation, but includes B<sub>4</sub>C where natural boron is considered (19.9 wt. % <sup>10</sup>B and 80.1 wt. % <sup>11</sup>B).

Earlier criticality analysis with B<sub>4</sub>C, modeled a uniform array configuration rather than the irregular array configuration.<sup>13, 44</sup> Furthermore, (1) MgO was an unrealistic intact 63.5-cm MgO layer above the CCOs rather than uniformly mixed in reflector Region 2 (Fig. 15); and (2) the fissile Region 1 (Fig. 15) contained the generic filler of SiO<sub>2</sub>, MgO, Al<sub>2</sub>O<sub>3</sub> and H<sub>2</sub>O rather than the more reactive carbon/graphite filler (3.5% more reactive—§V.D.1).

### VII.B. Results with B<sub>4</sub>C

Between 10 g and 50 g of B<sub>4</sub>C and up to 6 kg of polyethylene moderator was added to the fissile Region 1 in the criticality analysis. Only 10 g of B<sub>4</sub>C is necessary to stay below  $k_{eff}$  of unity if the moderator mass is limited to 3.9 kg (Fig. 37).<sup>14, App. M</sup>

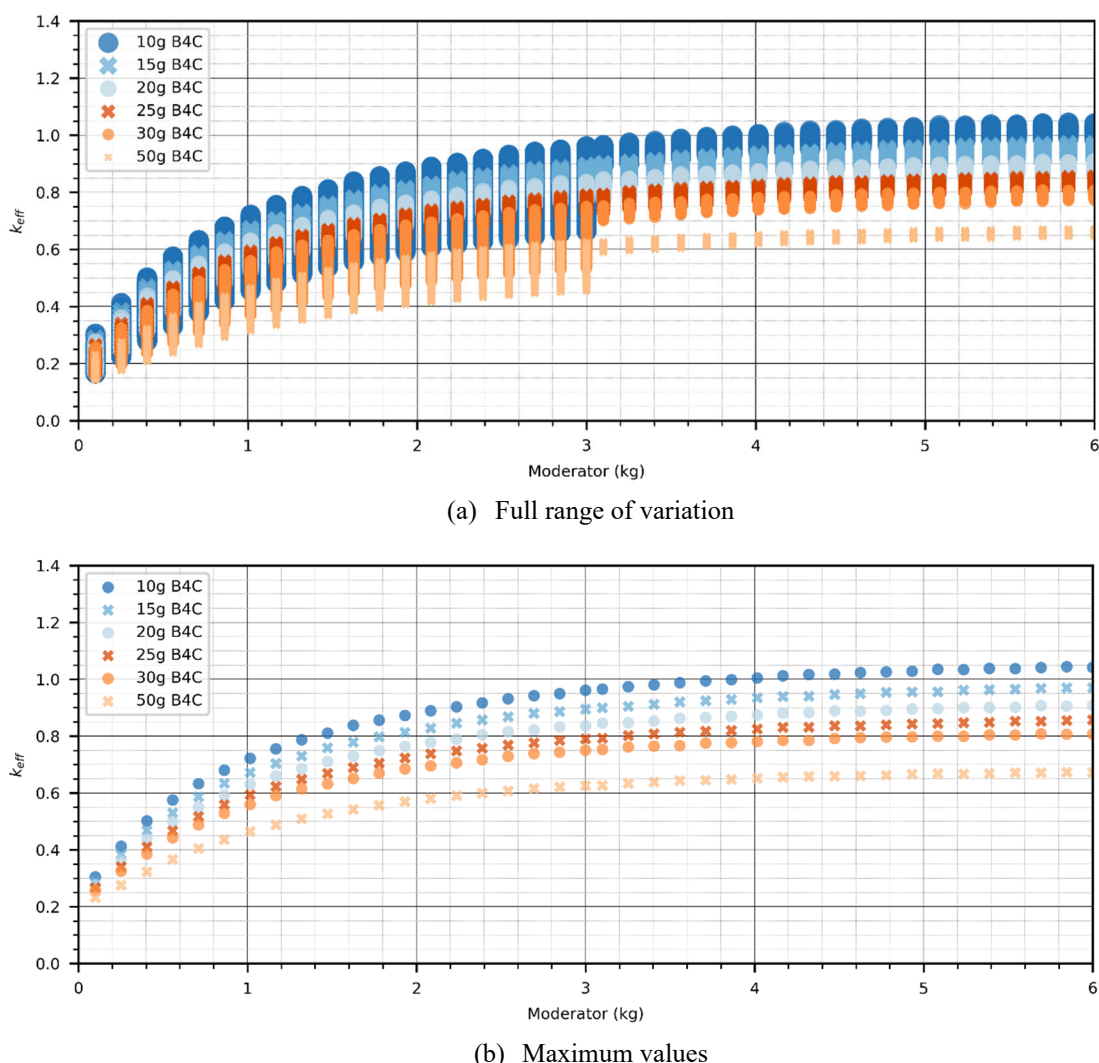


Fig. 37. Reactivity of irregular array with between 10 g and 50 g B<sub>4</sub>C and up to 6 kg moderator.

## VII.C. Longevity of B<sub>4</sub>C in Disposal Room

For B<sub>4</sub>C to remain effective as a neutron poison, it must remain in sufficient quantity in the CCO. The two feasible methods to deplete the B<sub>4</sub>C, dissolution and consumption in radiation field, will not reasonably occur within the WIPP repository.

### VII.C.1 Insolubility of B<sub>4</sub>C

B<sub>4</sub>C is third hardest material after boron nitride and diamond; it has a high absorption cross section of neutrons, without forming radioactive isotopes; and it is insoluble in water and acids.<sup>i</sup> If brine dissolved Pu in degraded CCOs, the B<sub>4</sub>C would be left behind as insoluble products of the CCO.

### VII.C.2. B<sub>4</sub>C Consumption in Radiation Field

Boron is used in the control rods of reactors where the boron is not significantly depleted even in the intense reactor neutron flux field. Because 10<sup>4</sup> years is long time; however, the following demonstrates that the minimal neutron flux from surplus Pu, where humans can be next to containers without shielding, is also not sufficient to deplete boron placed in the CCO.

Neutrons are potentially produced from three natural sources: (1) neutrons produced from cosmic rays (i.e., protons, alpha particles, heavy element nuclei, and free electrons) colliding with atmospheric matter; (2) spontaneous fission of Pu and U radioisotopes; and (3) alpha particles produced from decay of Pu and U colliding with Be. Within the repository, only the latter two sources are feasible since cosmic rays cannot penetrate beyond the top 10 m of the surface. Furthermore, the latter two sources would normally only produce a small flux of neutrons.

Here, we make widely conservative assumptions that (1) all Pu isotopes decay; (2) abundant Be is present to produce neutrons from every Pu isotope decay (thus dominating over the neutrons produced by spontaneous fission); (3) the production of neutrons from all Pu isotopic activity is 10<sup>7</sup> neutrons/(s-Ci), which bounds the neutron conversion for <sup>238</sup>Pu interacting with Be of 2 × 10<sup>6</sup> neutrons/(s-Ci); and (4) every neutron produced is absorbed by <sup>10</sup>B.

The 10<sup>7</sup> neutrons/(s-Ci) is equivalent to 2.7 × 10<sup>-4</sup> neutrons/decay from alpha particle or 3700 <sup>239</sup>Pu atom decays/neutron since 3.7 × 10<sup>10</sup> decays/(s-Ci). If every produced neutron is absorbed by <sup>10</sup>B, then 3700 <sup>239</sup>Pu atom decays for every <sup>10</sup>B atom absorption. Converting from atoms to grams of <sup>239</sup>Pu and <sup>10</sup>B through the Avogadro constant yields 88 389 g <sup>239</sup>Pu/g <sup>10</sup>B. For a CCO containing 380 g <sup>239</sup>Pu, 0.0043 g of <sup>10</sup>B would be

consumed. In 10-g B<sub>4</sub>C placed in a CCO are 7.8 g of B of which 19.75% is <sup>10</sup>B, or 1.53 g <sup>10</sup>B. Thus, only 0.28% of the 1.53 g <sup>10</sup>B is consumed even for exceedingly conservative assumptions (e.g., all Pu isotopes fully decay and all neutrons produced from abundant Be are absorbed by <sup>10</sup>B.)

## VIII. WIPP WASTE ACCEPTANCE CRITERIA

### VIII.A. Approximation of Mean Probability of Criticality

EPA guidance implies that the mean of the probability of criticality ( $\bar{\phi}\{\mathcal{A}_C\}$ ) provides an adequate estimate for screening; thus, the WIPP Project does not present a distribution for the probability of criticality. To elaborate, EPA invoked “reasonable expectation” as the standard of proof for compliance with the Containment Requirements specified in 40 CFR §191.13(a)). Reasonable expectation connotes a flexible standard of proof and use of central estimates when encountering unknowns. Specifically, for the containment requirements EPA noted:<sup>26</sup> §191.13 (b)

... Proof of the future performance of a disposal system is not to be had in the ordinary sense of the word in situations that deal with much shorter time frames. Instead, what is required is a reasonable expectation, on the basis of the record before the implementing agency, that compliance with 191.13 (a) will be achieved.

Also, EPA noted in the guidance to 40 CFR 191:<sup>5, App. C</sup>

*Compliance with Section 191.13.* The Agency assumes that, whenever practicable, the implementing agency will assemble all of the results of the performance assessments to determine compliance with §191.13 into a “complementary cumulative distribution function [CCDF]” ...

In the implementing regulations, EPA stated “Finally, the CCA must demonstrate that the mean of the population of CCDFs meets the containment requirements of §191.13...”

Reasonable expectation and the use of mean results from stochastic/probabilistic calculations to evaluate compliance with its regulations, implies a mean estimate of the probability provides an adequate estimate for screening a FEP such as criticality.<sup>j</sup> Consequently, EPA does not expect nor does the WIPP Project provide worse-case scenarios that may combine unrealistic combinations of imagined events to assemble fissile material in order to estimate the probability of criticality

<sup>i</sup> <https://m.chemicalbook.com/CASDataBase> accessed 12/15/2021

<sup>j</sup> The use of the mean probability for screening FEPs is emphasized by Nuclear Regulatory Commission in the Yucca

Mountain Review Plan: <sup>76, 2.2-14</sup> “...the mean of the distribution range is to be used to screen an event from the performance assessment...”

after WIPP closure.<sup>k</sup> This use of mean or representative values for evaluating the probability of criticality after disposal and closure of the repository when personnel are absent, and the nearest humans are separated by 654 m of geologic strata such that consequences are minimal, differs substantially to screening criticality during TRU waste transportation and WIPP operations when humans may be nearby and consequences severe.<sup>22, 77</sup>

While the mean is formally evaluated in PA, the mean is usually approximated in screening FEPs and scenarios. Although we occasionally use bounding values or conditions in the supporting calculations, the purpose is not to produce a worse case but rather to ensure that the conditions will indeed bound a reasonable estimate of mean behavior or to show behavior does not change substantially at extreme conditions. For example, herein, we use a salt-creep analysis to estimate a reasonable configuration of compacted CCOs for disposal options, not the worst imaginable condition. Conservative estimates of some parameters are used, and conservative initial and boundary conditions are set, but these parameters are not set at extremes.

We also use conservative estimates for parameters related to criticality analysis, such as the maximum 380  $^{239}\text{Pu}$  FGE content of a CCO. Furthermore, we do not use extreme conditions of criticality from the uniformly compacted array for evaluating the criticality potential after closure of WIPP facility. Rather the conditions modeled using the uniformly compacted arrays provide assurance that the trends observed for representative behavior do not dramatically change at extremes.

### VIII.B. Supplemental WAC Limits for CCOs

The representative geomechanical analysis of salt creep closure of rooms and subsequent compaction of CCOs and the corresponding criticality analysis of the irregular array are used to define three supplement options for WIPP WAC (Table III) and screen the criticality scenario for TRU waste disposal in CCOs. Providing three options provides flexibility in using CCO with different waste forms.

A subcriticality limit of 0.95 rather 1.0 is used for the representative criticality results (Table II) to account for geometric uncertainty beyond that analyzed (e.g., uncertainty in geologic strata and configuration of reflective metals in CCC such as a convenience can). The conservative bias drops the allowable moderator to 1300 g per CCO without filler and to 1500 g per CCO when the miscellaneous, non-hydrogenous filler mass is at least 2000 g per CCO (Table II).<sup>1</sup> The filler mass is expressed as 6 times the amount of  $^{239}\text{Pu}$  FGE (Table III)

to facilitate spreading the filler between several inner convenience cans (i.e., internal handling container) that contain a portion of the maximum 380 g of Pu in a CCC.

Table III. Supplemental WIPP Waste Acceptance Criteria for a CCO

Option <sup>(1)</sup>	Boron Carbide (B <sub>4</sub> C) <sup>(2)</sup> (g)	Hydrogenous Content <sup>(3)</sup> (g)	Miscellaneous Filler <sup>(4)</sup> (g)
A	≥10	≤2800	—
B	—	≤1300	—
C	—	≤1500	≥6×FGE

- (1) Waste packaged in each CCO shall adhere to limits in Table 1 of WIPP Waste Acceptance Criteria in addition to limits specified under Options A, B, or C.
- (2) The B<sub>4</sub>C shall be well mixed with the  $^{239}\text{Pu}$  fissile gram equivalent (FGE) and remain so during transportation, storage, and handling operations. The B<sub>4</sub>C mass is based on the natural abundance of  $^{10}\text{B}$  (i.e., 19.9 wt. %  $^{10}\text{B}$ ). The B<sub>4</sub>C mass requirement shall apply to (a) each CCC that contains directly loaded TRU waste with  $^{239}\text{Pu}$  FGE, or (b) any convenience containers used to load a CCC that contain  $^{239}\text{Pu}$  FGE. For example, if a CCC is directly loaded with TRU waste containing  $^{239}\text{Pu}$  FGE and also loaded with two cans containing  $^{239}\text{Pu}$  FGE, the directly-loaded TRU waste in the CCC and each can in the CCC shall include at least 10-g of well mixed B<sub>4</sub>C.
- (3) Mass of hydrogenous content shall include mass of any organic material (e.g., mass of plastic, cellulose, foam) and mass of water associated with any inorganic material (e.g., mass of adsorbed water on zeolite, water of hydration in concrete and clay, or water in hydrate such as hydrated metal ion).
- (4) Only the non-hydrogenous portion of miscellaneous filler mass well mixed with  $^{239}\text{Pu}$  fissile gram equivalent (FGE) shall meet the miscellaneous filler mass requirement. The miscellaneous filler shall remain well mixed with  $^{239}\text{Pu}$  FGE during transportation, storage, and handling operations. If several convenience containers are used to load a CCC, then each convenience container shall independently meet the miscellaneous filler criteria. For example, if a CCC is loaded with two convenience containers, where the first contains 100  $^{239}\text{Pu}$  FGE and the second contains 280  $^{239}\text{Pu}$  FGE, at least 600 g and 1680 g of miscellaneous filler shall be present within each respective convenience container.

The general conditions of waste packaged in a CCO are as follows: (1) waste shall adhere to criteria in Table 1 of WIPP WAC (e.g., ≤ 380  $^{239}\text{Pu}$  FGE and ≤ 1 wt. % Be/BeO); (2) optional B<sub>4</sub>C shall be well mixed with the  $^{239}\text{Pu}$  FGE and shall include placing ≥ 10-g B<sub>4</sub>C in each convenience container in the CCC that contains  $^{239}\text{Pu}$  FGE; (3) the mass of hydrogenous material in CCC shall

<sup>k</sup> We avoid referring to this screening approach as a credibility argument herein because in nuclear criticality safety analysis for operating engineered systems the term connotes a rule-

based approach with worst-case scenarios to demonstrate that the scenario does not result in criticality.

<sup>1</sup> Limits are reported in grams to match the specification used in the WIPP WAC.

include the mass of all organic material (e.g., mass of polyethylene plastic wrap) and the mass of water associated with all inorganic material (e.g., adsorbed moisture on zeolite, water of hydration in clay, or water in hydrated metal ion such as  $\text{CoCl}_2 \cdot 6\text{H}_2\text{O}$ ); and (4) optionally credited miscellaneous, non-hydrogenous filler shall be well mixed with  $^{239}\text{Pu}$  FGE, which may be divided between any convenience containers inside the CCC in proportion to their  $^{239}\text{Pu}$  FGE contents.<sup>m</sup> The three option requirements are for an individual CCO; any combination of CCOs using different options may be placed in a room.

The only neutron poison considered in this analysis is  $\text{B}_4\text{C}$ ; however, other neutron poisons, such as gadolinium that forms insoluble compounds, would likely be acceptable provided a technical justification is developed and the WAC revised.

The requirement for well-mixed  $\text{B}_4\text{C}$  for Option A and well-mixed miscellaneous filler for Option C is not equivalent to requiring a homogeneous or uniform mixture. Rather, what is implied is that the  $\text{B}_4\text{C}$  or the credited miscellaneous filler have particle sizes relative to the fissile material such that (1) the  $\text{B}_4\text{C}$  or the miscellaneous filler may occupy interstitial spaces between the fissile material, and (2) separate regions of  $\text{B}_4\text{C}$  or credited miscellaneous filler do not form.<sup>n</sup>

The hydrogenous limits are based on 100% polyethylene ( $\text{CH}_2$ ), which bounds most material potentially present in TRU waste (e.g., organic material and water associated with other contents).<sup>74</sup> This approach has been used for including the effects of compaction in other payload containers. Nonetheless, less stringent requirements are possible for most other hydrogenous material. For example, the allowable moderator mass substantially increases from 1600 g polyethylene moderator to 2500 g water moderator for the each CCO in an irregular array, a 50% increase (§VI.A.1). However, establishing increased limits for specific moderator materials requires the CCO user to provide technical justification for the hydrogen equivalence to  $\text{CH}_2$ .

### VIII.C. Use of Acceptable Knowledge

Acceptable knowledge can be used to determine presence of  $\text{B}_4\text{C}$ , graphite/generic filler, and allowable hydrogenous material (primarily water and plastic) present in CCCs to determine compliance with Table III. Compliance with WAC limits for many TRU waste stream characteristics are established via acceptable

knowledge, where the WAC defines acceptable knowledge as follows:<sup>78</sup>

Acceptable knowledge –Any information about the process used to generate waste, material inputs to the process, and the time period during which the waste was generated, as well as data resulting from the analysis of waste, conducted prior to or separate from the waste certification process authorized by the EPA’s Certification Decision, to show compliance with Condition 3 of the certification decision (Appendix A of this part) (40 CFR §194.2 and §194.67).

Option A in Table III (placing 10 g of  $\text{B}_4\text{C}$  in each CCC) may be useful for TRU waste that can be well mixed with  $\text{B}_4\text{C}$  and has high plastic and water content, or contains hydroscopic salts that may theoretically increase water content. In the latter case, a technical evaluation of the water adsorbed by a hydroscopic material might be used, if necessary, to show that greater than 2800 g requires free water.

Option B assesses only the mass of hydrogenous material in a CCC (usually water and plastic), which may be useful for TRU waste that cannot be well mixed with  $\text{B}_4\text{C}$  (or miscellaneous filler material in Option C) and/or has existing limits on water and plastic content, such as planned surplus Pu disposal at WIPP.

For surplus Pu disposal, for example, the starting content of the stabilized plutonium-bearing oxide or other fissile material used as feedstock have a known moisture content based on process controls. The adulterant filler used to dilute  $^{239}\text{PuO}_2$  is either non-hydroscopic or has defined moisture based on process controls. The plastic content may be assessed through procurement and process controls on mass of plastic bags used for packaging and contamination control. Thus, the total moderator can be evaluated as the sum of plastic packaging and total estimate of moisture contents. Adherence to process controls (i.e., verification of packaging configuration) could be verified by routine radiography, if required.

Option C assesses both the mass of non-hydrogenous, well-mixed filler and mass of hydrogenous material in a CCC. Option C may be useful for waste forms with defined amounts of miscellaneous filler that could benefit from the marginal increase in allowable moderator.

<sup>m</sup> A generator site could properly apportion  $\text{B}_4\text{C}$  between handling/convenience containers, but ensuring well mixing of such small amounts of  $\text{B}_4\text{C}$  with  $^{239}\text{Pu}$  FGE might not be able to rely upon acceptable knowledge. Thus, this approach is not considered here.

<sup>n</sup>The term well-mixed is as used for soils: a well-mixed soil has a distribution of particle sizes such that interstitial spaces are readily filled. In soils engineering, however, well mixing is specified to improve soil compaction density. Here, well mixing is specified to ensure adequate neutron interaction with the  $\text{B}_4\text{C}$  or miscellaneous filler.

## IX. RATIONALE OF LOW-PROBABILITY OF CRITICALITY IN CCO AT WIPP

The approach here develops a qualitative low-probability rationale that room closure from rock fall and salt creep cannot sufficiently compact emplaced criticality container overpacks (CCOs) containing up to 380 fissile gram equivalent  $^{239}\text{Pu}$  to form a critical assembly provided (a) sufficient boron carbide ( $\text{B}_4\text{C}$ ) neutron poison is mixed with the fissile material, or (b) a constraint is placed on the mass of hydrogenous material present in CCOs (primarily water and plastics), which, in turn, depends upon the mass of non-hydrogenous filler mixed with the fissile material (Table IV).

The criticality scenario class has been screened out from consideration in performance assessments for WIPP compliance certification applications based on combining this finding with the rationale that (1) drums, boxes, and POCs are also insufficiently compacted within WIPP disposal rooms, and (2) hydrologic and geochemical conditions cannot sufficiently concentrate  $^{239}\text{Pu}$  and  $^{235}\text{U}$  elsewhere within the WIPP disposal system, as presented in companion papers.<sup>1;47</sup>

Support for a low-probability rationale in the closed WIPP repository depends upon constraints developed from (1) geomechanical phenomenological modeling of rock fall and salt creep, and (2) criticality modeling of neutron transport. Geomechanical modeling establishes a reasonable configuration of CCOs during two representative repository phases: (1) early large salt block fall onto CCOs, and (2) later gradual salt compaction of a room filled with CCOs.

Because of the importance of fissile spacing, high-fidelity geomechanical modeling is used to simulate rockfall and room closure by salt creep and the subsequent configuration of CCOs. The rockfall and room closure models represent a segment in disposal Room 4 (middle of a panel of 7 rooms) halfway down the 91-m room axis where the ratio of horizontal to vertical compaction is likely the greatest.

### IX.A. Rock Fall in Room Filled with CCOs

Two models of rock fall are developed (§III). In the first roof-fall simulation, the entire length of a large, trapezoidal salt block detaches from the roof, similar in size and shape to the largest rock fall observed at WIPP that separated at a clay seam in the lower repository horizon. Although the shape imparts some rotation, the salt block lands almost flat, bounces slightly, and settles on top of the drum ensemble. The internal CCCs mostly return to the disposed configuration, without noticeable deformation or clustering.

In the second roof-fall simulation, the salt block progressively detaches from the roof, to impart more rotation. The CCCs are jostled more, but still no clustering or collapse of CCCs occurs.

Because of the bounding conditions selected for the rock fall, salt block falls shortly after WIPP closure are not likely to cause extensive deformation, collapse, or clustering and, thereby, produce a critical assembly of CCOs prior to later gradual room closure from salt creep.

### IX.B. Compaction of CCOs from Salt Creep

Although salt creep beneficially encapsulates the TRU waste the emplaced array of CCOs is severely disrupted. The geomechanical analysis sought to establish a reasonable, representation of the disrupted CCO array for subsequent criticality analysis. Care is taken to demonstrate that the disrupted CCO array is reasonable and representative, by examining the influence of four cases on the final configuration based on the combination of two situations: horizon of the room in the salt strata, and the initial configuration of the emplaced CCO array.

The room is modeled at both horizons of the bedded salt repository (designated simply as upper and lower horizons) to consider the influence of differing arrangements of geologic strata, particularly the interspersed clay seams where slippage occurs, which subtly influence room closure.

The salt compaction analysis includes results both where the CCOs start as a hexagonal array and where the CCOs start as a more compact triangular array. Although a room full of 7-packs of CCOs would initially be placed in a hexagon configuration, the 7-packs are held together with plastic wrapping that will allow CCOs to readily shift once the walls contact the emplaced containers.

To expand the pool of situations modeled, past geomechanical analyses are reevaluated using conditions consistent with the current analysis to examine room closure with different clay friction coefficients, CCOs with different strengths, and rooms filled with different containers (6-inch and 12-inch POCs—§ ).<sup>8;9;11;12</sup>

Finally, several conservative assumptions are employed that promote more compaction: (a) any gas pressure from cellulose degradation and metal corrosion that would normally arrest compaction is not included; (b) container elements are deleted from the analysis once they become severely distorted or the material fractured thereby reducing material volume in room (e.g., plywood quickly splintered and thus not much of the plywood elements remain at 1000 years); (c) plywood failure strength is reduced 80%; (d) the stainless steel CCCs are empty; thus, structural stiffening from TRU waste is omitted; and (e) magnesium oxide ( $\text{MgO}$ ) bags are omitted thereby reducing material volume in a room by ~5%.

Shortly after the room ceiling contacts the CCO drums (in the room center by ~40 years and along the entire length after ~60 years), the outer CCO shell crumples and the plywood spacers rapidly fail. By 100 years, the inner CCCs have begun to topple over on their

sides, and by 200 years, most CCOs are on their side. By 300 years, most room closure has occurred. Yet, the room closure asymptotically approaches a maximum at 1000 years. The greater closure at the room center displaces much of the top tier of CCOs toward the room sides. The center is mostly a single layer, which consists primarily of the bottom tier of CCOs. CCOs are not clumped or bunched together down the axis of the room in the  $y$ -direction.

The CCO concentration measure of the container spacing shows that the geomechanical simulations produce a wide range in the distribution, but the concentration distributions remained similar both in terms of range and shape in the upper and lower horizon and when starting with either a triangular or hexagonal array even when varying clay friction coefficients, CCO strength, and changing to 6-inch POC construction. Only the 12-inch POC, is noticeably different. Consequently, the coordinate positions of CCOs for the irregular, non-uniformly compacted array reasonably represent conditions in the WIPP disposal room for subsequent criticality calculations. The coordinate positions of the CCO centers from the four geomechanical cases are subsequently used in the criticality analysis.

### IX.C. Criticality Analysis of Compacted Arrays without Boron Carbide

Two general types of criticality analysis are performed: (1) criticality analysis without boron carbide ( $B_4C$ ) mixed with CCO contents (discussed here),<sup>13</sup> and (2) analysis with  $B_4C$ , (discussed below in §IX.D).<sup>14</sup> In both cases, the analysis examines the potential for criticality in CCOs with generic waste forms to avoid specifying specific waste forms, and, thereby, expands the usefulness of CCOs beyond the currently anticipated surplus Pu waste.

Whether a fissile region (or assembly of fissile regions) is critical depends upon the generation and interaction of neutrons with matter within and outside the assembly, which for a finite heterogenous system, depends upon four general categories of parameters (1) type, mass, and form of fissile material (i.e., 380 g FGE  $^{239}Pu$  as  $PuO_2$ ); (2) material mixed with the fissile material and its overall concentration (e.g., special reflector  $Be/BeO$ , moderating hydrogenous material such as water and plastics, non-hydrogenous filler modeled as graphite, cement-like material, and stainless steel components); (3) nearby material and its concentration outside the fissile array (e.g., reflecting stainless steel,  $MgO$ , salt, and brine); and (4) shape of individual CCOs and array configuration of fissile regions and, thereby, neutron leakage (e.g., spherical and cylindrical fissile region, uniform CCO array, and four geomechanical simulation cases for irregular array—upper/lower horizon and hexagonal/triangular emplacement). In the criticality analysis here, the

parameters in the first category are fixed and parameters in the latter three categories are varied to determine relative importance.

#### IX.C.1. Allowable Hydrogenous Moderator with and without Filler in Fissile Region

The modeled system remains subcritical (i.e.,  $k_{eff} \leq 0.95$ —§VIII.B) when the allowable hydrogenous moderator in the CCO is  $\leq 1.3$  kg/CCO for the representative irregular, non-uniformly compacted array without  $B_4C$  (Table IV). Including  $\geq 2$  kg of a non-hydrogenous filler material in the fissile region reduces the reactivity of the CCO array, whether the filler material is conservatively modeled as graphite or represented as a cement-like mixture of silicon dioxide, magnesium oxide, and aluminum oxide (i.e.,  $SiO_2$ ,  $MgO$ , and  $Al_2O_3$ , respectively).

#### IX.C.2. Other Material in Fissile Region

Based on varying other parameters, additional factors are not necessary to control to ensure improbability of post-closure criticality. As expected, using water as the sole moderator in the fissile region is much less reactive than polyethylene:  $k_{eff}$  is reduced by 0.125 and the allowable the allowable moderator mass increases by  $\sim 50\%$  for the irregular, non-uniformly compacted CCOs (§VI.A.1).

The influence of excess  $MgO$  surrounding individual CCOs (which may act as a reflector) is small. The model includes  $\sim 3.7$  times the amount of  $MgO$  that would be necessary in the room full of CCOs, yet, the reactivity with 100% salt is only slightly less ( $k_{eff}$  decreases by 0.025) (§VI.A.2).

Finally, including 585-g beryllium ( $Be$ ) or beryllium oxide ( $BeO$ ) special reflector material in the fissile region (7% more than allowed in WIPP Waste Acceptance Criteria—WAC) has little influence on reactivity ( $k_{eff}$  decreases by  $<0.01$  near  $k_{eff}$  of unity) for irregular array (§VI.A.3).<sup>14</sup>

#### IX.C.3. CCC Stainless Steel Around Fissile Region

For the irregular array base case, a 0.71-cm discrete stainless-steel reflector is set around the fissile region, which is the thickness of the CCC (§VI.B). The stainless-steel reflector increases reactivity by reflecting neutrons back into the fissile region. The allowable moderator mass is 1.3 kg ( $k_{eff} \leq 0.95$ —§VIII.B). A 1.41-cm thick discrete stainless-steel reflector around the fissile region of the CCC, which is twice the thickness of the CCC, slightly increases  $k_{eff}$  by 0.03 near  $k_{eff}$  of unity. The corresponding allowable moderator mass decreases 5%.<sup>14, App. O</sup> If the stainless-steel reflector is removed,  $k_{eff}$  decreases by 0.05 and the allowable moderator mass increases 11%.

A reflective thickness twice the thickness of the 0.71-cm CCC considers the possibility of reflective metal inside the CCC. While the allowable moderator is

reduced 5%, it is not excessive. Furthermore, a sphere with unconstrained diameter was used for the irregular array that increases moderator mass ~5% over the more realistic sphere constrained by the CCC diameter. Furthermore, the administrative margin on  $k_{eff}$  of 0.05 adds another ~12% margin.

#### *IX.C.4 Uncertainty from Geologic Strata*

The CCO compacted configuration of CCOs in upper repository horizon is slightly more reactive (§VI.C);  $\Delta k_{eff}$  is ~0.025 larger a  $k_{eff}$  near unity, which translates to an allowable moderator mass of 1.3 kg per CCO. In the less reactive lower horizon, the allowable moderator mass is 1.4 kg per CCOs (9% increase in allowable moderator mass for lower horizon).

#### *IX.C.5. Minor Influence of Initial CCO Configuration and Boundary Conditions*

The slightly wider range in closure and concentration of CCOs initially emplaced in a hexagonal array translates into a slightly wider range of reactivity than CCOs initially emplaced in a triangular array (Fig. 30). In turn, the maximum moderator mass is 1.69 kg per CCO for a hexagonal array with mirror boundary conditions and increases 3% to 1.74 kg for a triangular array with periodic boundary conditions. For the situation with filler the maximum moderator mass is 2.02 kg per CCO for a hexagonal array and increases 3% to 2.08 kg for a triangular array with filler (§VI.D).

#### *IX.C.6. Reduced Reactivity from Brine around Fissile Region*

The introduction of brine around the fissile region reduces reactivity as occurred previously when analyzing the behavior of pipe overpack containers. The presence of brine about the CCOs reduces the room  $k_{eff}$  by 0.15 to the point that 3 kg of moderator per CCO is allowable (§VI.E).

### **IX.D. Criticality Analysis of Compacted Arrays with Boron Carbide**

A criticality analysis of compacted CCOs containing B<sub>4</sub>C neutron poison establishes the fact that 10 g of B<sub>4</sub>C mixed with the contents prevents criticality provided the moderator mass is 2.8 kg ( $k_{eff} \leq 0.95$ ), as controlled by the WIPP WAC (§VIII.B). The criticality analysis uses the previous assumptions and the same irregular array configuration, based on the salt-creep calculation, but includes B<sub>4</sub>C where natural boron is considered (19.9 wt. % <sup>10</sup>B and 80.1 wt. % <sup>11</sup>B).

### **IX.E. Uniform Array Analysis Provides Additional Understanding**

Criticality analysis of a regular, uniformly compacted array is also conducted to more fully explain behavior observed in the irregular, non-uniformly

compacted array. The supporting uniform analysis assumes that the CCO array remains intact (i.e., CCOs remain vertical and in 3 tiers); only the spacing between the CCC decreases. The uniform criticality analysis uses a 25% and 50% reduction in a uniform horizontal spacing (§V.C.5). The latter value corresponds to early criticality analysis using uniformly compacted CCO arrays.<sup>13, 44</sup>

The reactivity of the uniformly array always bounds the reactivity of the irregular array, and in many cases the trends observed in the uniformly compacted follows those of the irregular compacted array. For example, behavior for a bounding regular, uniformly compacted array follows the trend of the irregular, non-uniformly compacted array: (1) when water is the sole moderator the allowable moderator mass increases by 50% for the both the irregular and uniform array; (2) influence of beryllium special reflector is small near  $k_{eff}$  of unity; and (3) both a graphite and cement-like filler increases the maximum allowable moderator mass.

When differences in behavior occur, the differences in neutron leakage and reflection in the configuration explain the different behavior. Two specific differences are as follows.

First, adding 2-kg filler to the fissile region of the CCC for uniformly compacted array provides a large benefit (37% increase in allowable moderator mass), but only provides a modest benefit for the irregular compacted array (18% increase in allowable moderator mass). For the uniformly compacted array, the disk-like cylinders of the fissile region (which are most reactive) are stacked on top of each other to form essentially a single stub cylinder (with similar height to diameter ratio) that is very reactive with essentially the <sup>239</sup>Pu mass of three CCOs. The reactivity greatly decreases (leakage greatly increases) for the uniformly compacted array as the height of the cylinder is increased to include the graphite/generic filler. In contrast, the irregular non-uniformly compacted array with spheres (or cylinders) are scattered about the room and the reactivity does not change much (i.e., leakage in the system does not greatly increase) as the fissile region size increases to accommodate the filler.

Second, adding a discrete reflector in around the CCC, decreases the reactivity of a uniformly compacted array but increases the reactivity of the irregular compacted array. Because the fissile regions are spread out in the irregular array, the stainless-steel CCC increases reactivity by reflecting neutrons back into the fissile region. Although the stainless-steel CCC still increases neutron reflection in the uniform array, the increased isolation of the fissile regions provided by the stainless-steel CCC is more important, because the close proximity of fissile regions in the uniformly compacted array promote neutron interactions.

Table IV. Low Probability of Criticality Caused by Salt Creep Compacting CCOs in WIPP Repository

Process Event	Rationale for Rock Fall and Salt-Creep Not Promoting Criticality in CCOs
<b>Rock Fall Undisturbed</b>	<b>Spacing Sufficient to Prevent Criticality in CCOs when TRU Waste Emplaced in Disposal Room</b>  A large, rigid trapezoidal shaped salt block that either separates suddenly or progressively along the salt block length from the roof jostles the emplaced CCO array but does not cause collapse or clustering and, thereby, produce a critical assembly prior to later salt creep (§III).
<b>Salt Creep Undisturbed</b>	<b>Limiting Hydrogenous Material to <math>\leq 1.3</math> kg Sufficient to Prevent Criticality after Compaction</b>  CCO concentration measure shows that the geomechanical simulations produce a wide range in CCO spacing, but the resulting concentration distributions remain similar. Consequently, the coordinate positions of CCOs in the irregular, non-uniformly compacted array reasonably represent conditions in the WIPP disposal room (§IV.E)  The representative irregular, non-uniformly compacted array at 1000 years with $\leq 1.3$ kg of plastics (bounded by polyethylene) mixed with 380 $^{239}\text{Pu}$ FGE as spheres of unconstrained diameter at center of CCO centerline emplaced in most reactive upper repository horizon is subcritical ( $k_{eff} \leq 0.95$ —§VIII.B) 1. Room reactivity and moderator mass of $\leq 1.3$ kg (as controlled in supplemental criteria in the WIPP Waste Acceptance Criteria) are not noticeably influenced by (a) excess magnesium oxide (MgO) (§VI.A.2), or (b) presence of beryllium (Be or BeO) (§VI.A.3). A more reactive bounding uniformly compacted array follows these trends. 2. Adding additional reflective material around the fissile region beyond the 0.71-cm thick CCC somewhat increases reactivity and decreases the moderator limit 5% but the assumed spherical fissile region with unconstrained diameter (~5% effect) and administrative margin of 0.05 on $k_{eff}$ (~11% effect) easily compensate (§VI.B). 3. Different arrangements of clay seams in geologic strata have only minor influence (§VI.C) 4. Initial CCO configuration (hexagonal versus triangular, including mirror or periodic boundary conditions down room axis to represent room of infinite extend (§VI.D) 5. Room reactivity generally increases monotonically as room creeps closed (§VI.F).  <b>Accounting for <math>\geq 2</math> kg Miscellaneous Non-Hydrogenous Filler and Limiting Hydrogenous Material to <math>\leq 1.5</math> kg Sufficient to Prevent Criticality in CCOs after Salt-Creep Compaction</b>  Representative irregular, non-uniformly compacted array with $\geq 2$ kg of non-hydrogenous carbon or generic ( $\text{SiO}_2$ , $\text{MgO}$ , and $\text{Al}_2\text{O}_3$ ) filler material and $\leq 1.5$ kg plastics mixed with 380 g of $^{239}\text{Pu}$ as spheres at center of CCO centerline in most reactive upper horizon is subcritical ( $k_{eff} \leq 0.95$ —§VIII.B). A more reactive bounding uniformly compacted array follows this trend: reactivity decreases when adding non-hydrogenous filler (§VI.A.1)  <b>10-g B<sub>4</sub>C Sufficient to Prevent Criticality in CCOs after Salt-Creep Compaction</b>  Only 10 g of B <sub>4</sub> C is necessary to remain subcritical if the moderator mass is limited to $\leq 2.8$ kg ( $k_{eff} \leq 0.95$ —§VIII.B)
<b>Salt Creep Human Intrusion</b>	Influx of brine into reflector region reduces $k_{eff}$ by 0.15 and increases allowable moderator mass by 78% (§VI.E)



## REFERENCES

1. R. P. RECHARD, "Improbability of Transuranic Waste Compaction by Salt Creep Causing Criticality in Bedded Salt Repository; Memorandum to Paul E. Shoemaker, 8880; Todd Zeitler, 8863; Ross Kirkes, 8883; November 2019," Sandia National Laboratories (2019).
2. AREVA, "Criticality Control Overpack Criticality Analysis for TRUPACT-II and HalfPACT," 01937.01.M009-1, Revision O, AREVA Federal Services (2012).
3. PUB. L. 102-579, "Waste Isolation Pilot Plant Land Withdrawal Act." 106 Stat. 4777, (1992).
4. EPA (US ENVIRONMENTAL PROTECTION AGENCY), "40 CFR Part 191: Environmental Standards for the Management and Disposal of Spent Nuclear Fuel, High-Level and Transuranic Radioactive Wastes: Final Rule," *Federal Register*, **50**(182), 38066-38089 (1985).
5. EPA (US ENVIRONMENTAL PROTECTION AGENCY), "40 CFR Part 191: Environmental Radiation Protection Standards for the Management and Disposal of Spent Nuclear Fuel, High-Level and Transuranic Radioactive Wastes, Final Rule," *Federal Register*, **58**(242), 66398-66416 (1993).
6. EPA (US ENVIRONMENTAL PROTECTION AGENCY), "40 CFR Part 194: Criteria for the Certification and Re-Certification of the Waste Isolation Pilot Plant's Compliance with the 40 CFR Part 191 Disposal Regulations; Final Rule," *Federal Register*, **61**(28), 5224-5245 (1996).
7. R. P. RECHARD, "Historical Background on Performance Assessment for the Waste Isolation Pilot Plant," *Reliability Engineering and System Safety*, **69**(1-3), 5-46 (2000).
8. B. REEDLUNN, J. E. BEAN, JR., J. WILKES and J. BIGNELL, "Simulations of Criticality Control Overpack Container Compaction at the Waste Isolation Pilot Plant," SAND2019-3106 O, Sandia National Laboratories (2019).
9. B. REEDLUNN and J. E. BEAN, JR., "Further Simulations of Criticality Control Overpack Container Compaction at the Waste Isolation Pilot Plant, Memorandum," SAND2020-5105 CTF, Sandia National Laboratories (2020).
10. SNL (SANDIA NATIONAL LABORATORIES), "Sierra/Solid Mechanics User's Guide. 4.50," SAND2018-10673, Sandia National Laboratories (2018).
11. B. REEDLUNN and J. E. BEAN, JR, "Simulations of Pipe Overpack Container Compaction at the Waste Isolation Pilot Plant,," SAND2019-12111, Sandia National Laboratories (2019).
12. B. REEDLUNN and J. E. BEAN, JR., "Additional Simulations of Criticality Control Overpack and Pipe Overpack Container Compaction at the Waste Isolation Pilot Plant" SAND2021-11268 CTF, Sandia National Laboratories (2021).
13. E. M. SAYLOR, "Nuclear Criticality Safety Assessment of Criticality Control Containers without Moderation Control at Waste Isolation Pilot Plant," ORNL/TM-2020/1713, Oak Ridge National Laboratory (2020).
14. B. D. BRICKNER, R. CUMBERLAND and R. REED, "Post-Closure Nuclear Criticality Safety Evaluations for Disposition of Criticality Control Overpacks at the Waste Isolation Pilot Plant," ORNL/TM-2021/2046, Oak Ridge National Laboratory (2022).
15. ORNL (OAK RIDGE NATIONAL LABORATORY), "SCALE Code System," ORNL/TM-2005/39, Version 6.2.3, Oak Ridge National Laboratory. Most recent version available from Radiation Safety Information Computational Center as CCC-834 (2018).
16. B. D. BRICKNER, "Post-Closure Nuclear Criticality Evaluations Involving 6- and 12-Inch Pipe Overpack TRU Waste Containers at the Waste Isolation Pilot Plant," ORNL/TM-2019/1222, Oak Ridge National Laboratory (2019).
17. DOE (US DEPARTMENT OF ENERGY), "CCPcp Transuranic Authorized Methods for Payload Control (CCP-CH-TRAMPACT)," CCP-PO-003, Rev. 13, Carlsbad Field Office, US Department of Energy (2013).
18. R. P. RECHARD, L. C. SANCHEZ, H. R. TRELLUE and C. T. STOCKMAN, "Unfavorable Conditions for Nuclear Criticality Following Disposal of Transuranic Waste at the Waste Isolation Pilot Plant," *Nuclear Technology*, **136**(1), 99-129 (2001).
19. R. P. RECHARD, "Probability and Consequences of Nuclear Criticality at a Geologic Repository--I: Conceptual Overview for Screening," *Nuclear Technology*, **190**(2), 97-126 (2015).
20. DOE (US DEPARTMENT OF ENERGY), "Surplus Plutonium Disposition, Record of Decision," *Federal Register*, **81**(65), 19588-19594 (2016).
21. DOE (US DEPARTMENT OF ENERGY), "Notice of Intent to Prepare an Environmental Impact Statement for the Surplus Plutonium Disposition Program," *Federal Register*, **85**(242), 81460-81462 (2020).
22. NWP (NUCLEAR WASTE PARTNERSHIP), "Nuclear Criticality Safety Evaluation for Contact-Handled Transuranic Waste Containers

at the Waste Isolation Pilot Plant," WIPP-016, Revision 6, Nuclear Waste Partnership (2021).

23. B. A. DAY, "Calculation of CH and RH Payload Container Waste Volumes," PLD-CAL-0001, Nuclear Waste Partnership (2009).
24. NWP (NUCLEAR WASTE PARTNERSHIP), "CH Waste Downloading and Emplacement Technical Procedure," WP 05-WH1025, Rev. 25-FR3, Nuclear Waste Partnership (2019).
25. PUB. L. 97-425, "Nuclear Waste Policy Act of 1982," 96 Stat. 2201; 42 U.S.C. 10101 et seq. (1983).
26. EPA (US ENVIRONMENTAL PROTECTION AGENCY), "Background Information Document: Final Rule for High-Level and Transuranic Radioactive Wastes," EPA 520/1-85-023, US Environmental Protection Agency, Office of Radiation Programs (1985).
27. S. KAPLAN and B. J. GARRICK, "On the Quantitative Definition of Risk," *Risk Analysis*, 1(1), 11-27 (1981).
28. EPA (US ENVIRONMENTAL PROTECTION AGENCY), "40 CFR Part 197: Public Health and Environmental Radiation Protection Standards for Yucca Mountain, Nevada; Proposed Rule," *Federal Register*, 70(161), 49014 (2005).
29. EPA (US ENVIRONMENTAL PROTECTION AGENCY), "40 CFR Part 197: Public Health and Environmental Radiation Protection Standards for Yucca Mountain, Nevada; Final Rule," *Federal Register*, 73(200), 61256:61289 (2008).
30. F. W. BINGHAM and G. E. BARR, "Scenarios for the Long-Term Release of Radionuclides from a Nuclear-Waste Repository in the Los Medanos Region of New Mexico," SAND78-1730, Sandia National Laboratories (1979).
31. F. W. BINGHAM and G. E. BARR, "Development of Scenarios for the Long-Term Release of Radionuclides from the Proposed Waste Isolation Pilot Plant in Southeastern New Mexico," *Scientific Basis for Nuclear Waste Management, Proceedings of the International Symposium, Boston, MA, November 27-30, 1979*, C.J.M. NORTHRUP JR. ed., Vol. 2, , 771-778, New York, NY: Plenum Press (1980).
32. D. G. BROOKINS, "Geochemical Constraints on Accumulation of Actinide Critical Masses from Stored Nuclear Waste in Natural Rock Repositories," ONWI-17, Office of Nuclear Waste Isolation, Battelle Memorial Institute (1978).
33. R. L. HUNTER, "Events and Processes for Constructing Scenarios for the Release of Transuranic Waste from the Waste Isolation Pilot Plant, Southeastern New Mexico," SAND89-2546, Sandia National Laboratories (1989).
34. D. A. GALSON and P. N. SWIFT, "Recent Progress in Scenario Development for the WIPP," *High-Level Radioactive Waste Management 1995. Proceedings of the Sixth Annual International Conference, Las Vegas, NV, April 30-May 5, 1995*, 391-396, American Nuclear Society (1995).
35. D. A. GALSON, P. N. SWIFT, D. R. ANDERSON, D. G. BENNETT, M. B. GRAWFORD, T. W. HICKS and R. D. WILMOT, "Scenario Development for the Waste Isolation Pilot Plant Compliance Certification Application," *Reliability Engineering and System Safety*, 69 (1-3), 129-149 (2000).
36. R. P. RECHARD, L. C. SANCHEZ, C. T. STOCKMAN and H. R. TRELLUE, "Consideration of Nuclear Criticality When Disposing of Transuranic Waste at the Waste Isolation Pilot Plant," SAND99-2898, Sandia National Laboratories (2000).
37. GAO (GOVERNMENT ACCOUNTABILITY OFFICE), "Surplus Plutonium Disposition: NNSA's Long-Term Plutonium Oxide Production Plans Are Uncertain," GAO-20-166, US Government Accountability Office (2019).
38. DOE (US DEPARTMENT OF ENERGY), "Report of the Plutonium Disposition Working Group: Analysis of Surplus Weapon-Grade Plutonium Disposition Options," US Department of Energy (2014).
39. DOE (US DEPARTMENT OF ENERGY), "Draft Surplus Plutonium Disposition Supplemental Environmental Impact Statement," DOE/EIS-0283-S2, Office of Environmental Management, US Department of Energy (2012).
40. DOE (US DEPARTMENT OF ENERGY), "Final Surplus Plutonium Disposition Supplemental Environmental Impact Statement--Summary," EIS-0283-S2, US Department of Energy (2015).
41. GAO (GOVERNMENT ACCOUNTABILITY OFFICE), "Plutonium Disposition: Proposed Dilute and Dispose Approach Highlights Need for More Work at the Waste Isolation Pilot Plant," GAO-17-390, US Government Accountability Office (2017).
42. SAVANNAH RIVER NUCLEAR SOLUTIONS, "Surplus Plutonium Disposition Program Dilute and Dispose Approach: Life Cycle Cost Estimate Summary Report," SRNS-RP-2018-00570, Savannah River Nuclear Solutions (2018).
43. NA/NRC (NATIONAL ACADEMIES/NATIONAL RESEARCH COUNCIL), "Review of the Department of Energy's Plans for Disposal of Surplus Plutonium in the Waste Isolation Pilot Plant," The National Academies Press (2020).

44. E. M. SAYLOR and J. M. SCAGLIONE, "Nuclear Criticality Safety Assessment of Potential Plutonium Disposition at the Waste Isolation Pilot Plant," ORNL/TM-2017/751/R1, Oak Ridge National Laboratory (2018).

45. R. P. RECHARD, L. C. SANCHEZ, P. K. MCDANIEL, J. HUNT and G. BROADOUS, "Fissile Mass and Concentration Criteria in Geologic Media near Bedded Salt Repository" *International High-Level Radioactive Waste Management Conference, April 14-18, 2019, Knoxville, TN*, La Grange Park, IL: American Nuclear Society (2019).

46. R. P. RECHARD, L. C. SANCHEZ, M. OLVUN and G. RYBA, "Fissile Mass and Concentration Necessary for Criticality in Geologic Media near Bedded Salt Repository, Memorandum to Paul E. Shoemaker, 8880; Todd Zeitler, 8862; Ross Kirkes, 8883; November 2019," Sandia National Laboratory (2019).

47. R. P. RECHARD and E. STEIN, "Hydrologic and Geochemical Constraints on Criticality in Geologic Media near Bedded Salt Repository; Memorandum to Paul E. Shoemaker, 8880; Todd Zeitler, 8863; Ross Kirkes, 8883; November 2019," Sandia National Laboratories (2019).

48. R. D. CARTER, "Appendix N, Criticality Calculations. Nuclear Reactivity Evaluations of 216-Z-9 Enclosed Trench," ARH-2915, Atlantic Richfield Hanford Company (1973).

49. M. H. LIPNER and J. M. RAVETS, "Nuclear Criticality Safety Analyses for the Waste Isolation Pilot Plant Project," WAES-TME-3025, Advance Energy Systems Division, Westinghouse Electric Corporation (1980).

50. W. A. BLYCKERT and R. D. CARTER, "Criticality Parameters of 55-Gallon Waste Drum Arrays," RHO-SA-183; CONF 801107-58, Rockwell Hanford Operations, Rockwell International Corporation (1980).

51. W. R. STRATTON, "The Myth of Nuclear Explosions at Waste Disposal Sites," LA-9360, Los Alamos National Laboratory (1983).

52. C. D. BOWMAN and F. VENNERI, "Underground Supercriticality from Plutonium and Other Fissile Material," *Science and Global Security*, **5**(3), 279-302 (1996).

53. G. TAUBES, "News & Comment: Blowup at Yucca Mountain," *Science* **268**(5219), 1826-1839 (1995).

54. W. E. KASTENBERG, P. F. PETERSON, J. AHN, J. BURCH, G. CASHER, P. L. CHAMBRÉ, E. GREENSPAN, D. R. OLANDER, J. L. VUJIC, B. BESSINGER, N. G. W. COOK, F. M. DOYLE and L. B. HILBERT, "Considerations of Autocatalytic Criticality of Fissile Materials in Geologic Repositories," *Nuclear Technology* **115**(3), 298-310 (1996).

55. R. A. VAN KONYNENBURG, "Comments on the Draft Paper 'Underground Supercriticality from Plutonium and Other Fissile Material,'" *Science and Global Security*, **5**(3), 303-322 (1996).

56. W. L. MEYERS, W. R. STRATTON, R. H. KIMPLAND, R. G. SANCHEZ and R. E. ANDERSON, "The Myth of an Exploding Excess Nuclear Material Repository," *Transactions American Nuclear Society* **75**(214) (1996).

57. G. H. CANAVAN, S. A. COLGATE, O. P. JUDD, G. H. MCCALL, A. G. PETSCHEK, J. C. SOLEM, T. F. STRATTON, W. R. STRATTON and P. P. WHALEN, "Comments on 'Nuclear Excursions' and 'Criticality Issues,'" LA-UR-95-0851, Los Alamos National Laboratory (1995).

58. R. P. RECHARD, M. S. TIERNEY, L. C. SANCHEZ and M.-A. MARTELL, "Bounding Estimates for Critical Events When Directly Disposing Highly Enriched Spent Nuclear Fuel in Unsaturated Tuff," *Risk Analysis* **17**(1), 19-35 (1997).

59. R. P. RECHARD and M. S. TIERNEY, "Assignment of Probability Distributions for Parameters in the 1996 Performance Assessment for the Waste Isolation Pilot Plant, Part 1: Description of Process," *Reliability Engineering and System Safety* **88**(1), 1-32 (2005).

60. B. Y. PARK and F. D. HANSEN, "Determination of the Porosity Surfaces of the Disposal Room Containing Various Waste Inventories for WIPP PA," SAND2005-4236, Sandia National Laboratories (2005).

61. B. REEDLUNN, "Enhancements to the Munson-Dawson Model for Rock Salt," SAND2018-12601, Sandia National Laboratories (2018).

62. B. REEDLUNN, G. MOUTSANIDIS, J. BAEK, T.-H. HUANG, J. KOESTER, E. MATTEO, X. HE, K. TANEJA, H. WEI, Y. BAZILEVS, J.-S. CHEN, C. MITCHELL, R. LANDER and T. DEWERS, "Initial Simulations of Empty Room Collapse and Reconsolidation at the Waste Isolation Pilot Plant," SAND2019-15351, Sandia National Laboratories (2019).

63. B. REEDLUNN, J. G. ARGUELLO and F. D. HANSEN, "A Reinvestigation into Munson's Model for Room Closure in Bedded Rock Salt," *International Journal of Rock Mechanics and Mining Sciences*, **151**, (2022). doi.org/10.1016/j.ijmms.2021.105007

64. D. E. MUNSON, A. F. FOSSUM and P. E. SENSENY, "Advances in Resolution of Discrepancies between Predicted and Measured

in Situ WIPP Room Closures," SAND88-2948, Sandia National Laboratories (1989).

65. B. REEDLUNN, G. MOUTSANIDIS, J. BAEK, T.-H. HUANG, J. KOESTER, X. HE, H. WEI, K. TANEJA, Y. BAZILEVS and J.-S. CHEN, "Initial Simulations of Empty Room Collapse and Reconsolidation at the Waste Isolation Pilot Plant," *54th US Rock Mechanics/Geomechanics Symposium 28 June-1 July, Golden, Colorado*, American Rock Mechanics Association (2020).

66. B. REEDLUNN and J. BEAN JAMES E, "Impact of Properly Specifying the Clay F and Clay G Friction Coefficients in Disposal Room Closure Simulations at the Waste Isolation Pilot Plant. Memorandum," SAND2020-3537 CTF, Sandia National Laboratories (2020).

67. J. J. DUDERSTADT and L. J. HAMILTON, *Nuclear Ractor Analysis*, John Wiley & Sons, (1976).

68. DOE (US DEPARTMENT OF ENERGY), "TRUPACT-II Safety Analysis Report," Revision 23, US Department of Energy, Carlsbad Field Office (2013).

69. NRC (US NUCLEAR REGULATORY COMMISSION), "Certificate of Compilience for Radioactive Material Packages, TRUPACT-II," Certificate 9218, Rev 25, Docket 71-9218, US Nuclear Regulatory Commission (2020).

70. NRC (US NUCLEAR REGULATORY COMMISSION), "Packaging and Transporation of Radioactive Material," *Title 10 Code of Federal Regulations, Part 71*

71. ANSI (AMERICAN NATIONAL STANDARDS INSTITUTE), "An American National Standard for Nuclear Criticality Safety in Operations with Fissionable Materials Outside Reactors," ANSI/ANS-8.1-2014, American National Standards Institute (2014).

72. G. D. VAN SOEST, "Performance Assessment Inventory Report--2018," INV-PA-18, Revision 0, Los Alamos National Laboratory (2018).

73. J. K. THOMPSON, "Minimum Critical Mass of Plutonium-Polyethylene System Found to Be Significantly Lower Than Plutonium-Water System," *Nuclear Technology*, 33(2), 235-236 (1977).

74. G. W. NEELEY, D. L. NEWELL, S. L. LARSON and R. J. GREEN, "Reactivity Effects of Moderator and Reflector Materials on a Finite Plutonium System," SAIC-1322-001 Rev. 1, Science Applications International Corporation (2004).

75. H. C. PAXTON, J. T. THOMAS, D. CALLIHAN and E. B. JOHNSON, "Critical Dimensions of Systems Containing  $^{235}\text{U}$ ,  $^{239}\text{Pu}$  and  $^{233}\text{U}$ ," TID-7028, Los Alamos National Laboratory; Oak Ridge National Laboratory (1964).

76. NRC (US NUCLEAR REGULATORY COMMISSION), "Yucca Mountain Review Plan, Final Report," NUREG-1804, REV 2, Office of Nuclear Material Safety and Safeguards, US Nuclear Regulatory Commission (2003).

77. DOE (US DEPARTMENT OF ENERGY), "Waste Isolation Pilot Plant Documented Safety Analysis," DOE/WIPP 07-3372, US Department of Energy, Carlsbad Field Office (2016).

78. DOE (US DEPARTMENT OF ENERGY), "Transuranic Waste Acceptance Criteria for the Waste Isolation Pilot Plant," DOE/WIPP-02-3122, Rev 8, Carlsbad Field Office, US Department of Energy (2016).

## DISTRIBUTION

### E-mail—Internal

James Bean	01554	jebean@sandia.gov
Benjamin Reedlunn	01558	breedlu@sandia.gov
R. Chris Camphouse	08842	<a href="mailto:rccamph@sandia.gov">rccamph@sandia.gov</a>
Paul E. Shoemaker	08880	<a href="mailto:peshoem@sandia.gov">peshoem@sandia.gov</a>
G. Ross Kirkes	08883	grkirke@sandia.gov
Technical Library	01977	sanddocs@sandia.gov

### E-mail—External

Bret D. Brickner	<a href="mailto:bricknerbd@ornl.gov">bricknerbd@ornl.gov</a>	Oak Ridge National Laboratory
Riley M. Cumberland	<a href="mailto:cumberlandrm@ornl.gov">cumberlandrm@ornl.gov</a>	Oak Ridge National Laboratory
Brad A. Day	<a href="mailto:Brad.Day@wipp.ws">Brad.Day@wipp.ws</a>	Nuclear Waste Partnership LLC
Ron Livingston	ronald.livingston@srs.gov	Omega Technical Services







**Sandia  
National  
Laboratories**

Sandia National Laboratories is a multimission laboratory managed and operated by National Technology & Engineering Solutions of Sandia LLC, a wholly owned subsidiary of Honeywell International Inc. for the U.S. Department of Energy's National Nuclear Security Administration under contract DE-NA0003525.